

**NASA  
Technical  
Memorandum**

NASA TM - 100363

**SPACE STATION ECLSS SIMPLIFIED INTEGRATED  
TEST FINAL REPORT**

By Richard G. Schunk, Robert M. Bagdigian, Robyn L. Carrasquillo,  
Kathryn Y. Ogle, and Paul O. Wieland

Structures and Dynamics Laboratory  
Science and Engineering Directorate

March 1989

(NASA-TM-100363) SPACE STATION ECLSS  
SIMPLIFIED INTEGRATED TEST Final Report  
(NASA. Marshall Space Flight Center) 42 p  
CSCL 06K

N89-24044

Unclas  
G3/54 0211706



National Aeronautics and  
Space Administration

George C. Marshall Space Flight Center

1. REPORT NO. NASA TM-100363	2. GOVERNMENT ACCESSION NO.	3. RECIPIENT'S CATALOG NO.	
4. TITLE AND SUBTITLE Space Station ECLSS Simplified Integrated Test Final Report		5. REPORT DATE March 1989	
		6. PERFORMING ORGANIZATION CODE	
7. AUTHOR(S) Richard G. Schunk, Robert M. Bagdikian, Robyn L. Carrasquillo, Kathryn Y. Ogle, and Paul O. Wieland		8. PERFORMING ORGANIZATION REPORT #	
9. PERFORMING ORGANIZATION NAME AND ADDRESS  George C. Marshall Space Flight Center Marshall Space Flight Center, Alabama 35812		10. WORK UNIT NO.	
		11. CONTRACT OR GRANT NO.	
12. SPONSORING AGENCY NAME AND ADDRESS  National Aeronautics and Space Administration Washington, D.C. 20546		13. TYPE OF REPORT & PERIOD COVERED  Technical Memorandum	
		14. SPONSORING AGENCY CODE	
15. SUPPLEMENTARY NOTES  Prepared by Structures and Dynamics Laboratory, Science and Engineering Directorate.			
16. ABSTRACT  This report contains a discussion of the Space Station Simplified Integrated Test (SIT) which was conducted at the MSFC Core Module Integration Facility in June of 1987. The first in a series of three integrated ECLS system tests, the primary objectives of the SIT were to verify proper operation of ECLS subsystems functioning in an integrated fashion as well as to gather preliminary performance data for the partial ECLS system used in the test. Included in the report is a description of the SIT configuration, a summary of events, a discussion of anomalies that occurred during the test, and detailed results and analysis from individual measurements and water and gas samples taken during the test. The report also details the preprototype ECLS hardware used in the test, providing an overall process description and theory of operation for each hardware item.			
17. KEY WORDS  Environmental Control and Life Support Regenerative Life Support Water Reclamation Air Revitalization		18. DISTRIBUTION STATEMENT  Unclassified — Unlimited	
19. SECURITY CLASSIF. (of this report)  Unclassified	20. SECURITY CLASSIF. (of this page)  Unclassified	21. NO. OF PAGES  142	22. PRICE  NTIS

# TABLE OF CONTENTS

	Page
1.0 INTRODUCTION .....	1
2.0 TEST CONFIGURATION AND SCOPE .....	1
2.1 General .....	1
2.2 Subsystem Interfaces .....	3
2.2.1 TIMES .....	3
2.2.2 Static Feed Electrolysis .....	8
2.2.3 Sabatier .....	8
2.2.4 Four Bed Molecular Sieve .....	8
2.2.5 Trace Contaminant Control Subsystem .....	11
2.3 Temperature and Humidity Control System and Metabolic Simulator .....	11
2.4 Test Scope .....	11
3.0 TEST SUMMARY .....	14
4.0 TEST ANOMALIES .....	15
4.1 SFE Communication to PDU Failure .....	15
4.2 TIMES Manual Shutdown .....	15
4.3 First Sabatier Shutdown .....	16
4.4 External Flow Sensor for Sabatier Product Gas Vent .....	16
4.5 Weight Scales .....	16
4.6 DCC Console Fault Indicator .....	16
4.7 Second Sabatier Shutdown .....	17
4.8 SFE High Voltage Warning .....	17
4.9 O <sub>2</sub> in Molecular Sieve CO <sub>2</sub> Output .....	17
5.0 SUBSYSTEM DISCUSSION OF RESULTS .....	17
5.1 TIMES .....	18
5.1.1 Subsystem Description .....	18
5.1.2 Post Treatment Module Description .....	20
5.1.3 Discussion of Results .....	20
5.1.4 Recommendations/Lessons Learned .....	34
5.2 Sabatier .....	38
5.2.1 Subsystem Description .....	38
5.2.2 Discussion of Results .....	40
5.2.3 Recommendations/Lessons Learned .....	60
5.3 Static Feed Electrolysis .....	60
5.3.1 Subsystem Description .....	60
5.3.2 Discussion of Results .....	63
5.3.3 Recommendations/Lessons Learned .....	73

## TABLE OF CONTENTS (Concluded)

	Page
5.4 Four Bed Molecular Sieve .....	73
5.4.1 Subsystem Description .....	73
5.4.2 Discussion of Results .....	80
5.4.3 Recommendations/Lessons Learned .....	108
5.5 Trace Contaminant Control Subsystem .....	113
5.5.1 Subsystem Description .....	113
5.5.2 Discussion of Results .....	115
6.0 AIR AND WATER SAMPLING RESULTS .....	115
6.1 Introduction.....	115
6.2 Quality Control.....	115
6.3 Sampling Technique.....	124
6.4 Discussion of Results.....	124
7.0 CONCLUSIONS.....	125
APPENDIX.....	125



## LIST OF ILLUSTRATIONS

Figure	Title	Page
1.	Integrated ECLS test configuration.....	2
2.	Core module simulator .....	4
3.	Physical layout of ECLS subsystems.....	5
4.	TIMES.....	6
5.	TER/evaporator assembly .....	7
6.	SFE .....	9
7.	Sabatier.....	10
8.	4-bed molecular sieve .....	12
9.	TCCS .....	13
10.	TIMES schematic .....	19
11.	TIMES facility wastewater weight .....	22
12.	TIMES evaporator temperature TT01 .....	26
13.	TIMES evaporator temperature TT02.....	27
14.	TIMES evaporator temperature TT03.....	28
15.	TIMES evaporator temperature TT04.....	29
16.	TIMES steam pressure TP01 .....	30
17.	TIMES steam pressure TP02 .....	31
18.	TIMES brine conductivity TC01.....	33
19.	TIMES TER voltage TV02 .....	35
20.	TIMES TER current TI01.....	36
21.	TIMES TER current TI02.....	37
22.	Sabatier subsystem schematic .....	39
23.	Sabatier inlet H <sub>2</sub> flow FF02.....	41
24.	Sabatier inlet H <sub>2</sub> pressure FP02 .....	43
25.	Sabatier inlet H <sub>2</sub> temperature FT02.....	44
26.	Sabatier inlet CO <sub>2</sub> flow FF01 .....	45
27.	Sabatier inlet CO <sub>2</sub> pressure FP01 .....	46
28.	Sabatier inlet CO <sub>2</sub> temperature FT01 .....	48
29.	Sabatier inlet CO <sub>2</sub> oxygen content FO03 .....	49
30.	Sabatier reactor inlet temperature ST01.....	50
31.	Sabatier reactor inlet pressure SP01 .....	51
32.	Sabatier reactor bed temperature 1 ST03 .....	52
33.	Sabatier reactor bed temperature 2 ST04 .....	54

## LIST OF ILLUSTRATIONS (Continued)

Figure	Title	Page
34.	Sabatier condenser exit temperature ST02.....	55
35.	Sabatier water outlet pressure SP03 .....	56
36.	Sabatier gas outlet pressure SP02 .....	57
37.	Sabatier outlet vent flowrate FF03 .....	58
38.	Sabatier outlet vent temperature FT03 .....	59
39.	SFE subsystem schematic.....	61
40.	SFE subsystem cell current WI01 .....	64
41.	SFE subsystem cell voltage WV13 .....	66
42.	SFE subsystem operating pressure WP01 .....	67
43.	SFE subsystem delta press WP02.....	68
44.	SFE subsystem H <sub>2</sub> O tank pressure WP04 .....	69
45.	SFE subsystem operating temperature WT01 .....	70
46.	SFE subsystem H <sub>2</sub> flow FF04 .....	71
47.	SFE subsystem O <sub>2</sub> flow FF05 .....	72
48.	SFE subsystem H <sub>2</sub> outlet pressure FP03 .....	74
49.	SFE subsystem O <sub>2</sub> outlet pressure FP04 .....	75
50.	Molecular sieve subsystem schematic.....	76
51.	Molecular sieve subsystem operational schematic .....	78
52.	Molecular sieve subsystem bed 1 inlet air temperature MT03 .....	81
53.	Molecular sieve subsystem bed 3 inlet air temperature MT04 .....	82
54.	Molecular sieve subsystem blower outlet temperature MT02.....	84
55.	Molecular sieve subsystem HX air outlet temperature MT01 .....	85
56.	Molecular sieve subsystem bed 2 inlet air temperature MT06 .....	86
57.	Molecular sieve subsystem bed 4 inlet air temperature MT07 .....	87
58.	Molecular sieve subsystem sorbent bed 2 temperature MT10 .....	88
59.	Molecular sieve subsystem sorbent bed 4 temperature MT11 .....	89
60.	Molecular sieve subsystem desiccant bed 1 in temperature MT05 .....	91
61.	Molecular sieve subsystem desiccant bed 3 in temperature MT08 .....	92
62.	Molecular sieve subsystem desorption flow temperature MT09.....	93
63.	Molecular sieve subsystem inlet air dewpoint MDP1 .....	94
64.	Molecular sieve subsystem desiccant bed dewpoint outlet MDP2 .....	95
65.	Molecular sieve subsystem coolant inlet temperature FT04.....	97
66.	Molecular sieve subsystem coolant outlet temperature FT05 .....	98

## LIST OF ILLUSTRATIONS (Concluded)

Figure	Title	Page
67.	Molecular sieve subsystem coolant flowrate FF08 .....	99
68.	Molecular sieve subsystem inlet air flowrate FF13 .....	100
69.	Molecular sieve subsystem inlet CO <sub>2</sub> flowrate FF12 .....	101
70.	Molecular sieve subsystem outlet CO <sub>2</sub> flowrate FF01 .....	102
71.	Molecular sieve subsystem O <sub>2</sub> percentage FO03 .....	104
72.	Molecular sieve subsystem inlet CO <sub>2</sub> partial pressure FP12 .....	105
73.	Molecular sieve subsystem outlet CO <sub>2</sub> partial pressure FP13 .....	106
74.	Molecular sieve subsystem fan outlet pressure MP01 .....	107
75.	Molecular sieve subsystem sorbent bed outlet pressure MP08 .....	109
76.	Molecular sieve subsystem CO <sub>2</sub> accumulator pressure MP09 .....	110
77.	Molecular sieve subsystem bed 2 heater voltage MV01 .....	111
78.	Molecular sieve subsystem bed 4 heater voltage MV02 .....	112
79.	Trace contaminant control subsystem schematic .....	114

## LIST OF TABLES

Table	Title	Page
1.	Pretreated Urine Composition .....	20
2.	Comparison of Post Treated Distillate to Hygiene Water Quality Specification.....	24
3.	Results of TIMES Product Water .....	116
4.	Results of TIMES Brine Solution .....	118
5.	Results of Sabatier Water.....	120
6.	Results of Gas Analyses .....	121
7.	Microbial Analysis of TIMES Post Treated Distillate .....	122
8.	Microbial Analysis of TIMES Raw Distillate .....	123

## LIST OF ACRONYMS AND ABBREVIATIONS

CCA	Coolant Control Assembly (Static Feed Electrolysis)
CEU	Central Electronics Unit (Static Feed Electrolysis)
cfm	Cubic feet per minute
cm	Centimeter
CMIF	Core Module Integration Facility
CST	Central Standard Time
DCC	Display and Control Console (TIMES and Sabatier)
ECLSS	Environmental Control and Life Support System
FCA	Fluids Control Assembly (Static Feed Electrolysis)
4BMS	Four Bed Molecular Sieve
ft	Feet
HFM	Hollow Fiber Membrane (TIMES)
hr	Hour
HX	Heat Exchanger
JSC	Johnson Space Center
KOH	Potassium Hydroxide
lb	Pound
MCT	Metabolic Control Test
mmHg	Millimeters of Mercury (pressure)
MSFC	Marshall Space Flight Center
nom	Nominal
OD	Outside Diameter
PC	Personal Computer
PCA	Pressure Control Assembly (Static Feed Electrolysis)
pCO <sub>2</sub>	Pressure of carbon dioxide
PDU	Performance Diagnostic Unit (Static Feed Electrolysis)
ppm	Parts per million
psia	Pounds per square inch absolute
psid	Pounds per square inch difference
psig	Pounds per square inch gauge
REV	Revision
SFES	Static Feed Electrolysis Subsystem
SIT	Simplified Integrated Test
SLPM	Standard liters per minute

TCCS	Trace Contaminant Control Subsystem
TED	Thermoelectric Device (TIMES)
TER	Thermoelectric Regenerator (TIMES)
TGA	Trace Gas Analyzer
THCS	Temperature and Humidity Control System
TOC	Total Organic Content
TSA	Test Support Accessory (Static Feed Electrolysis)
umho	Micro Mhos (conductivity)
UPM	Urine Pretreat Mixer
Vdc	Volts direct current

## TECHNICAL MEMORANDUM

# SPACE STATION ECLSS SIMPLIFIED INTEGRATED TEST FINAL REPORT

## 1.0 INTRODUCTION

This report describes the space station Environmental Control and Life Support System (ECLSS) Simplified Integrated Test (SIT) that was conducted at the Core Module Integration Facility (CMIF) located in building 4755 of the Marshall Space Flight Center (MSFC). The test, which began on June 9, 1987, was 52 hr in duration with approximately 42 hr of integrated system operation. The primary objectives of this test were to verify proper operation of ECLS subsystems functioning together in an integrated fashion as well as to gather preliminary performance data for the partial ECLS system used in the test. The test was conducted inside an open module simulator with nominal three-man metabolic design loads imposed.

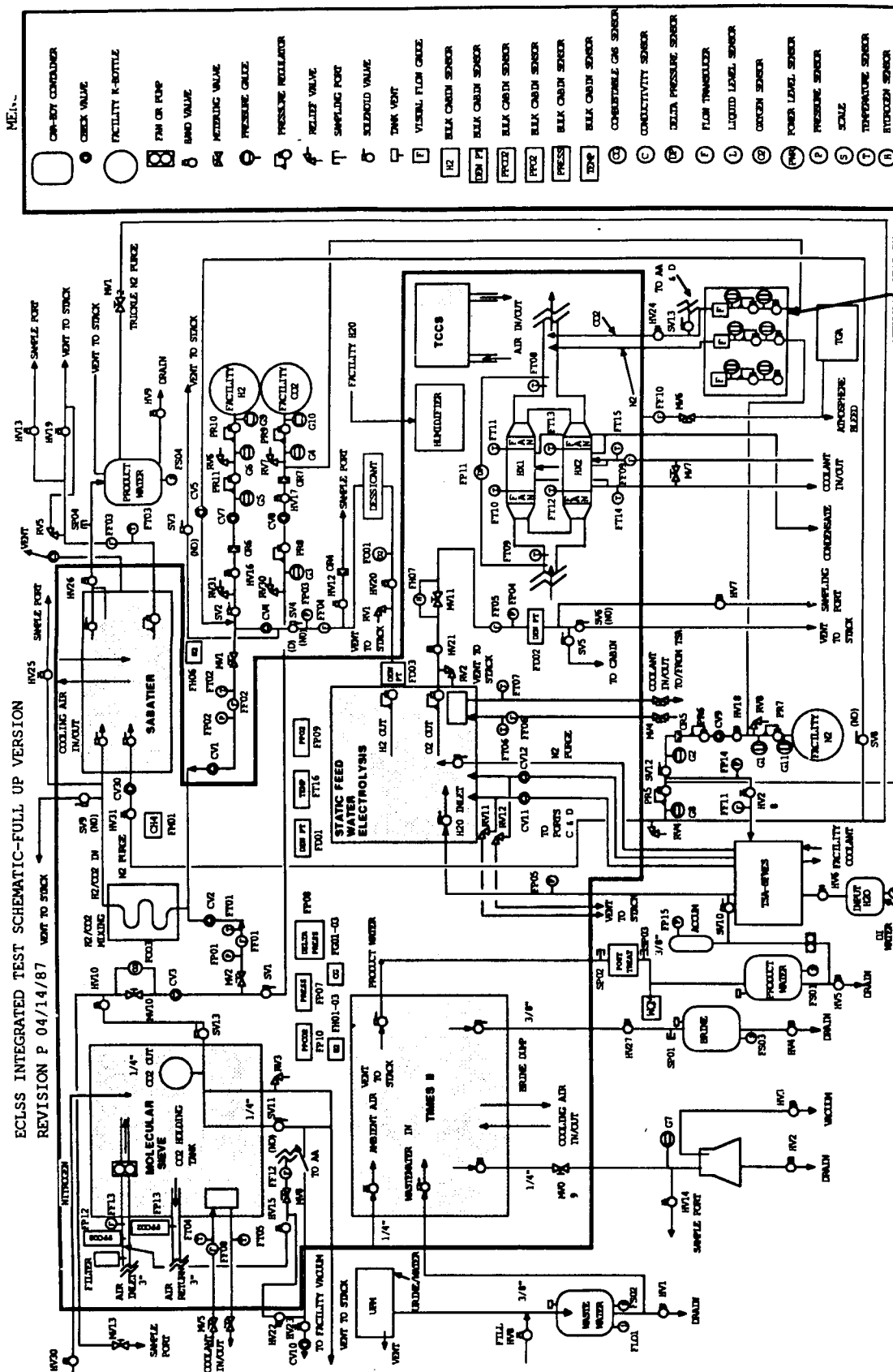
In order to verify proper performance of the ECLS system, 250 measurements were monitored continuously by on-site personnel and archived for later recovery by an automated data acquisition system. Additionally, water and gas samples were taken during the test to aid in verifying proper subsystem performance. All 250 measurements were reviewed, with analyses of over 60 of these measurements and the water and gas samples selected for inclusion in this report.

## 2.0 TEST CONFIGURATION AND SCOPE

### 2.1 General

The SIT configuration utilized five regenerative ECLS subsystems located inside the MSFC Core Module Simulator. The subsystems used were the Thermoelectric Integrated Membrane Evaporation System (TIMES) water reclamation subsystem, the Static Feed Electrolysis (SFE) oxygen generation subsystem, the Sabatier carbon dioxide reduction subsystem, the 4-Bed Molecular Sieve (4BMS) carbon dioxide removal subsystem, and the Trace Contaminant Control Subsystem (TCCS). Also internal to the simulator, a temperature and humidity control system provided sensible heat removal and ventilation for the open simulator environment. A number of support hardware items were located outside the simulator, including a metabolic simulator, a Performance Diagnostic Unit (PDU), a Test Support Accessory (TSA) for the SFE subsystem, and a Display and Control Console (DCC) for the TIMES and the Sabatier subsystems. Facility-provided services included a System and Components Automated Test System (SCATS) computer for data acquisition/management, bottled gases for metabolic simulations and system and subsystem purges, and necessary electrical power service.

Figure 1 shows the integrated phase II ECLS system test configuration in schematic detail. The five ECLS subsystems are denoted as shaded areas while the bold lines represent the boundary of the simulator. A number of components, including the metabolic simulator and supply and





product water tanks, were located outside the simulator. Additionally, much of the SFE/Sabatier hydrogen interface line was routed externally to the simulator for safety reasons. The Urine Pretreat Mixer (UPM) and the Trace Gas Analyzer (TGA), which are shown in the schematic, were not utilized during the SIT. The basic subsystem interfaces include the TIMES reclaimed water output to the SFE, the Sabatier mixed  $\text{CO}_2$  and  $\text{H}_2$  input, the Sabatier product gas vent, the TIMES waste water input and brine outputs, and the Molecular Sieve  $\text{CO}_2$  input. Referring to the schematic, the TIMES reclaimed water was delivered to a product water tank. This water was then pumped to the SFE through a TSA which was used as the SFE interface to facility services and other subsystems. The water was electrolyzed by the SFE into hydrogen and oxygen. The oxygen could be vented either internally or externally to the simulator as shown. Since the SIT was "open door," all generated oxygen was vented externally to the simulator. Hydrogen produced by the SFE was mixed with carbon dioxide concentrated by the Molecular Sieve in a mixing coil at the inlet to the Sabatier. As shown on the schematic, the Molecular Sieve utilized an accumulator to dampen the effects of the adsorption/desorption cycle. The  $\text{H}_2/\text{CO}_2$  mixture is reduced to methane and water by the Sabatier. The methane, along with the excess constituent from the  $\text{H}_2/\text{CO}_2$  reaction, was vented externally to the simulator. Water from the reaction was collected in an external tank. Aside from the basic subsystem interfaces, much of the complexity of the system was dedicated to supporting sampling of interconnecting process streams, nitrogen purging of subsystems and gas lines, and a design philosophy that required all subsystems be capable of stand-alone operation solely from facility-provided services.

A photograph of the core module simulator and the physical layout of the subsystems inside the simulator are shown in Figures 2 and 3. The mechanical interfaces for each of the major components are described in the sections that follow.

## **2.2 Subsystem Interfaces**

### **2.2.1 TIMES**

The TIMES achieves the reclamation of waste water through a distillation process. During the test, pretreated urine was input to the TIMES from an elevated tank located outside the simulator. This tank was positioned on a weighing scale with an analog output to the TIMES. After processing, the reclaimed water was collected in a product water tank which was located on a similar scale. The reclaimed water was pumped from the product tank to the SFE subsystem after passing through a post-treatment bed. Recycle of the TIMES output was activated by an internal conductivity sensor. Other facility interfaces for the TIMES included an overboard dump line for brine and a vent source to vacuum purge noncondensable gases from the TIMES. All internal TIMES measurements were recorded by the facility data management system through an RS-232 data-link located on the TIMES controller. The DCC was utilized by the TIMES and the Sabatier subsystem for real time data display and evaluation and manual subsystem control. Figure 4 is a photograph of the TIMES installed inside the simulator. Figure 5 is a cross-sectional drawing of the TIMES internal thermoelectric regenerator/evaporator assembly.

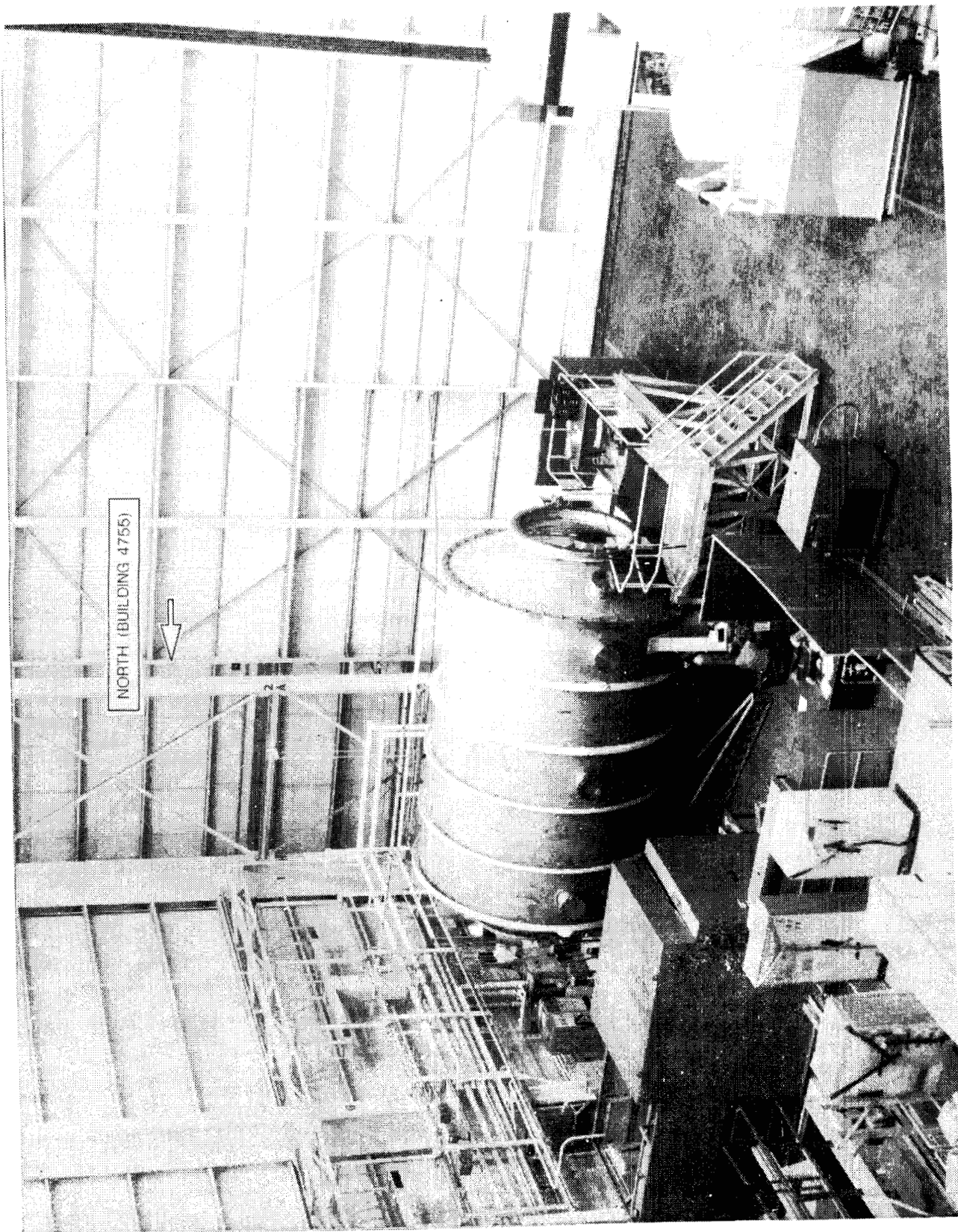


Figure 2. Core module simulator.

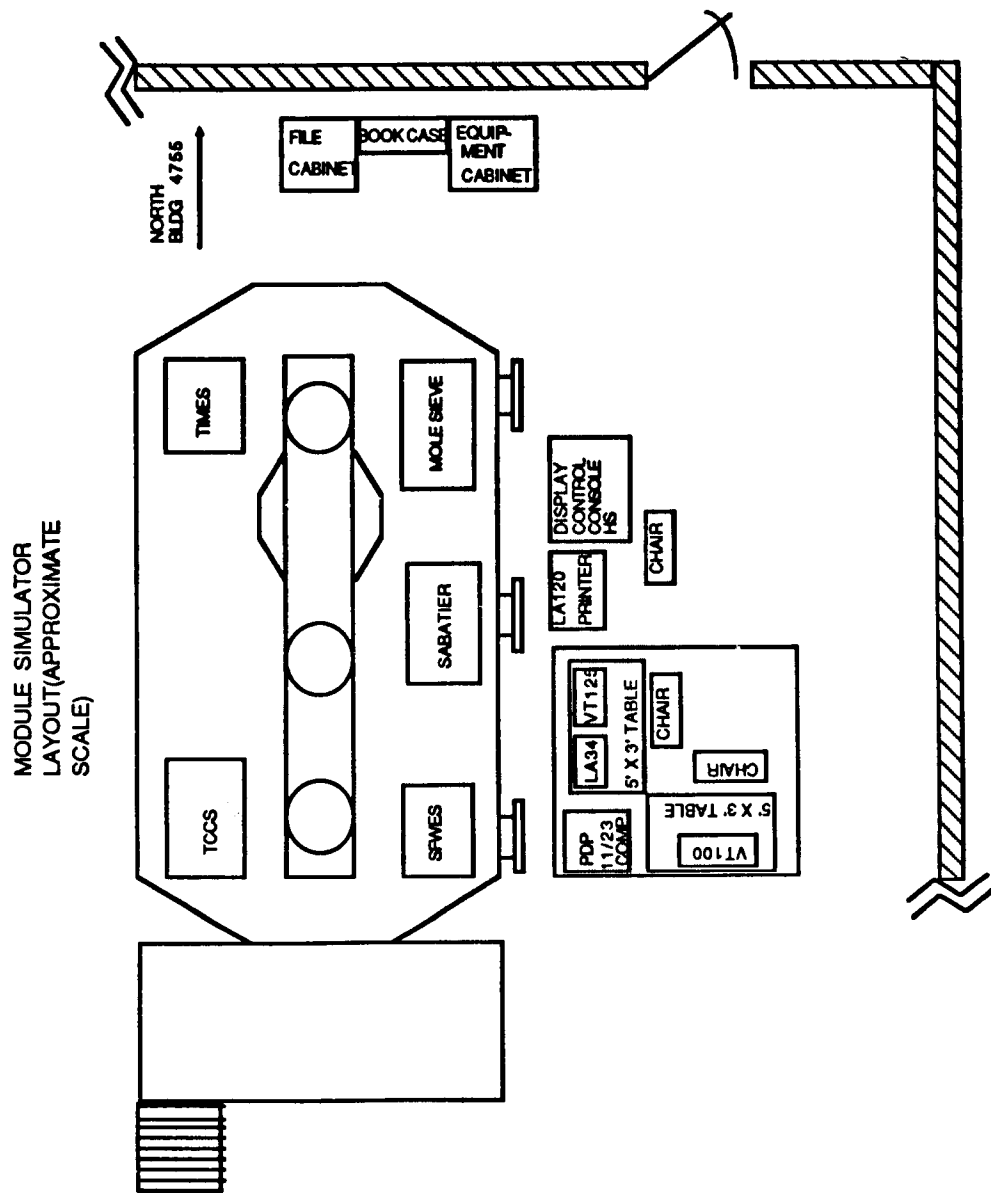


Figure 3. Physical layout of ECLS subsystems.

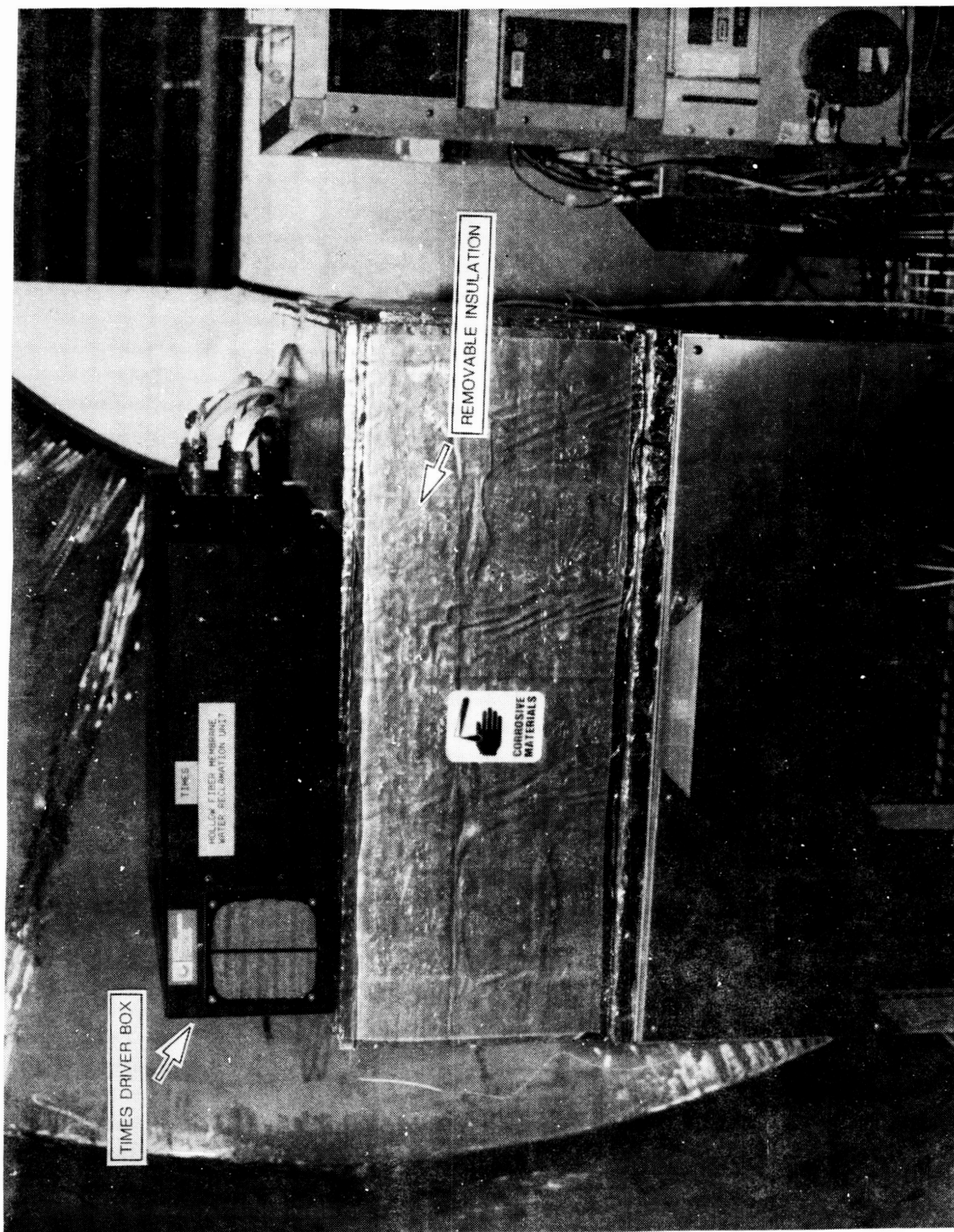


Figure 4. TIMES.

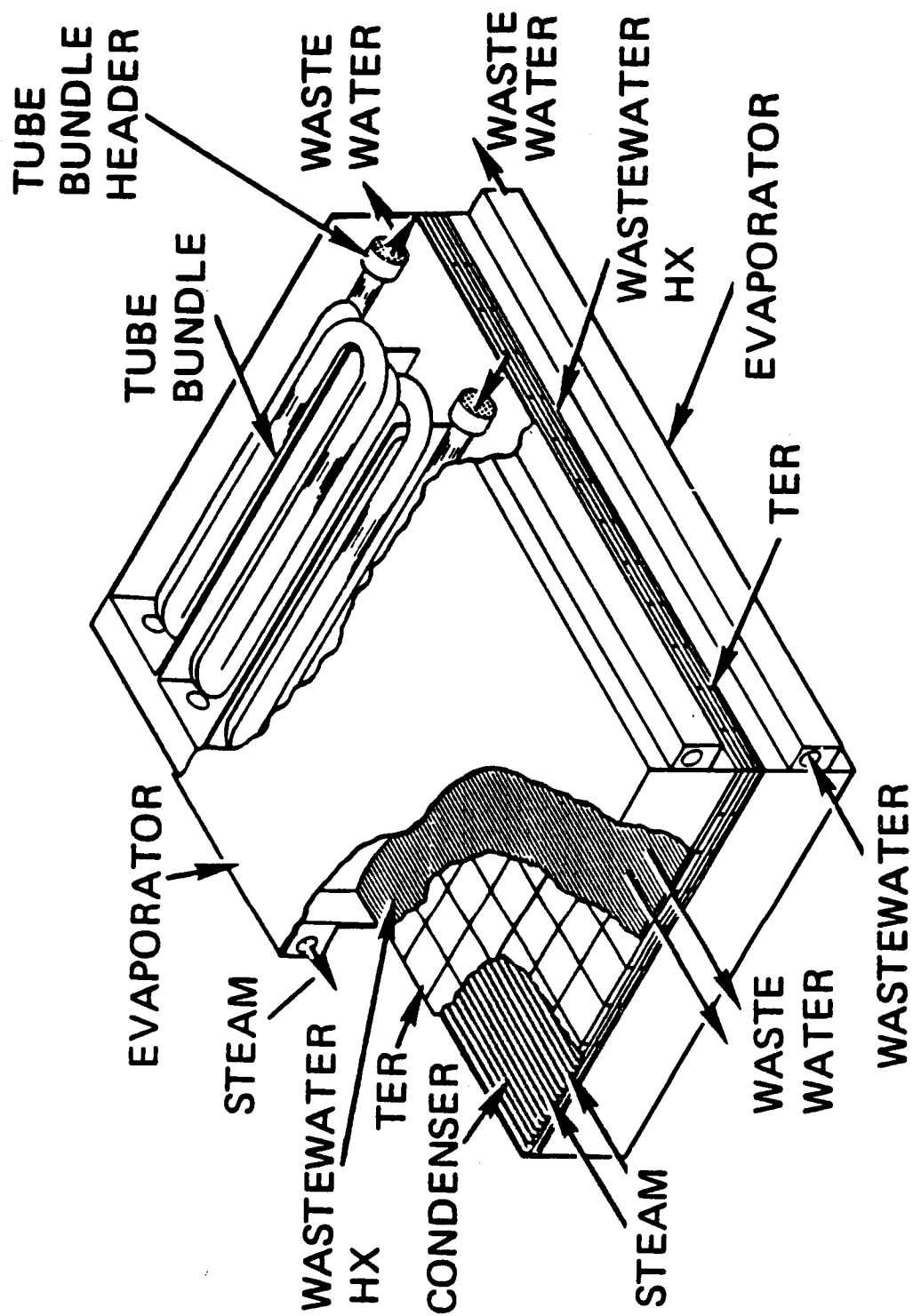


Figure 5. TER/evaporator assembly.

### **2.2.2 Static Feed Electrolysis**

The SFE subsystem was designed to electrolyze water into hydrogen and oxygen. In the test, input water could be provided as either reclaimed water from the TIMES or deionized water from the facility. The SFE was initially charged with facility deionized water and thereafter was operated from a mixture of TIMES product water and the original deionized water. Except during sampling periods, the SFE subsystem's total oxygen output was directed into the open simulator environment. The oxygen output stream contained instrumentation to measure temperature, flow, and pressure as well as to detect the presence of hydrogen in the oxygen output stream. Similarly, the SFE subsystem's total hydrogen output was directed to the Sabatier carbon dioxide reduction subsystem except during sampling. A moisture trap was located in the hydrogen output stream to prevent moisture passage to downstream components. Instrumentation on the hydrogen output stream was available to measure temperature, flow, and pressure as well as to detect the presence of oxygen. The SFE subsystem also used nitrogen for purging and facility water for cell stack temperature control. All inputs to the SFE subsystem were interfaced through the TSA. Internal measurements from the SFE were first processed by the PDU, which was used for subsystem control and real time data evaluation, before being sent to the facility data management system on a serial data bus. A photograph of the SFE mounted inside the simulator is shown in Figure 6.

### **2.2.3 Sabatier**

The Sabatier carbon dioxide reduction subsystem reacts a hydrogen/carbon dioxide mixture in the presence of a catalyst to form methane and water. If the hydrogen/carbon dioxide mixture is not balanced stoichiometrically, the excess constituent will pass unreacted into the gaseous output stream. During the test, hydrogen generated by the SFE and carbon dioxide concentrated by the Molecular Sieve were input to the Sabatier after passing through a mixing chamber and moisture trap external to the unit. Instrumentation was available upstream of the mixing chamber to measure pressure, temperature, and flow of each input stream. The gaseous output from the Sabatier was vented outside the building while product water, generated in the reaction, was collected in a tank which was located on a scale similar to the ones used to weigh the TIMES input and output water. Instrumentation was available to measure temperature and flow of the gaseous output stream although no real time measurement was available to determine the composition of the exit stream. Both the gaseous input and output streams on the Sabatier subsystem, as well as the product water tank, had provisions for sampling. Nitrogen was used as a purge gas for the unit. A "trickle" purge of nitrogen was also placed on the product water tank to prevent the possibility of dissolved methane from accumulating in the tank. Like the TIMES, internal measurements were sent simultaneously to the DCC and to the facility data management system (SCATS) in the form of a serial data stream. The Sabatier subsystem is shown in Figure 7.

### **2.2.4 Four-Bed Molecular Sieve (4BMS)**

The 4BMS subsystem removes and concentrates carbon dioxide from air via an adsorption/desorption process. During the test, air was pulled in from the module simulator by an internal fan and returned minus the removed carbon dioxide. The concentrated carbon dioxide was first collected in an accumulator before being mixed with hydrogen from the SFE subsystem in a mixing



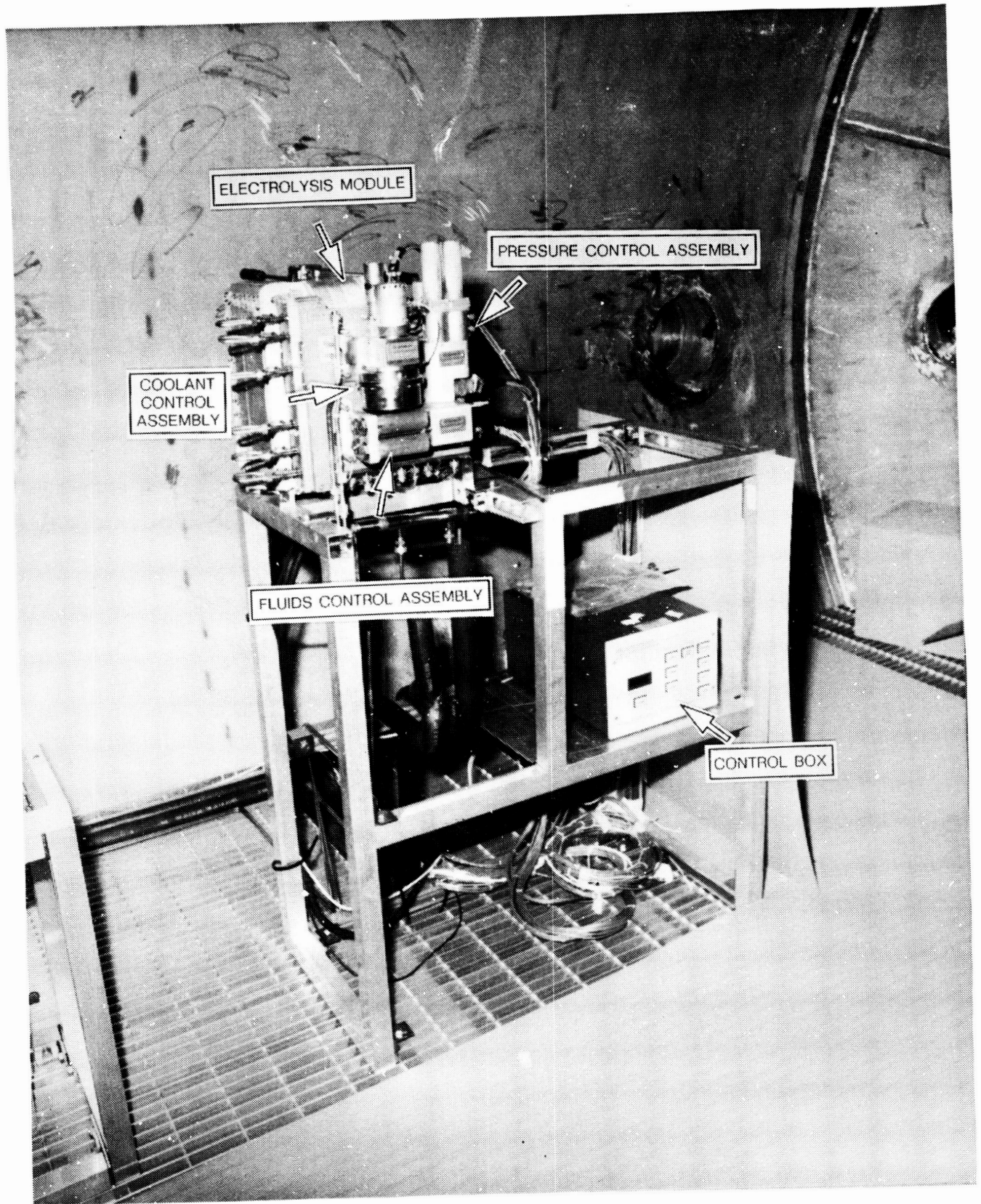


Figure 6. SFE.

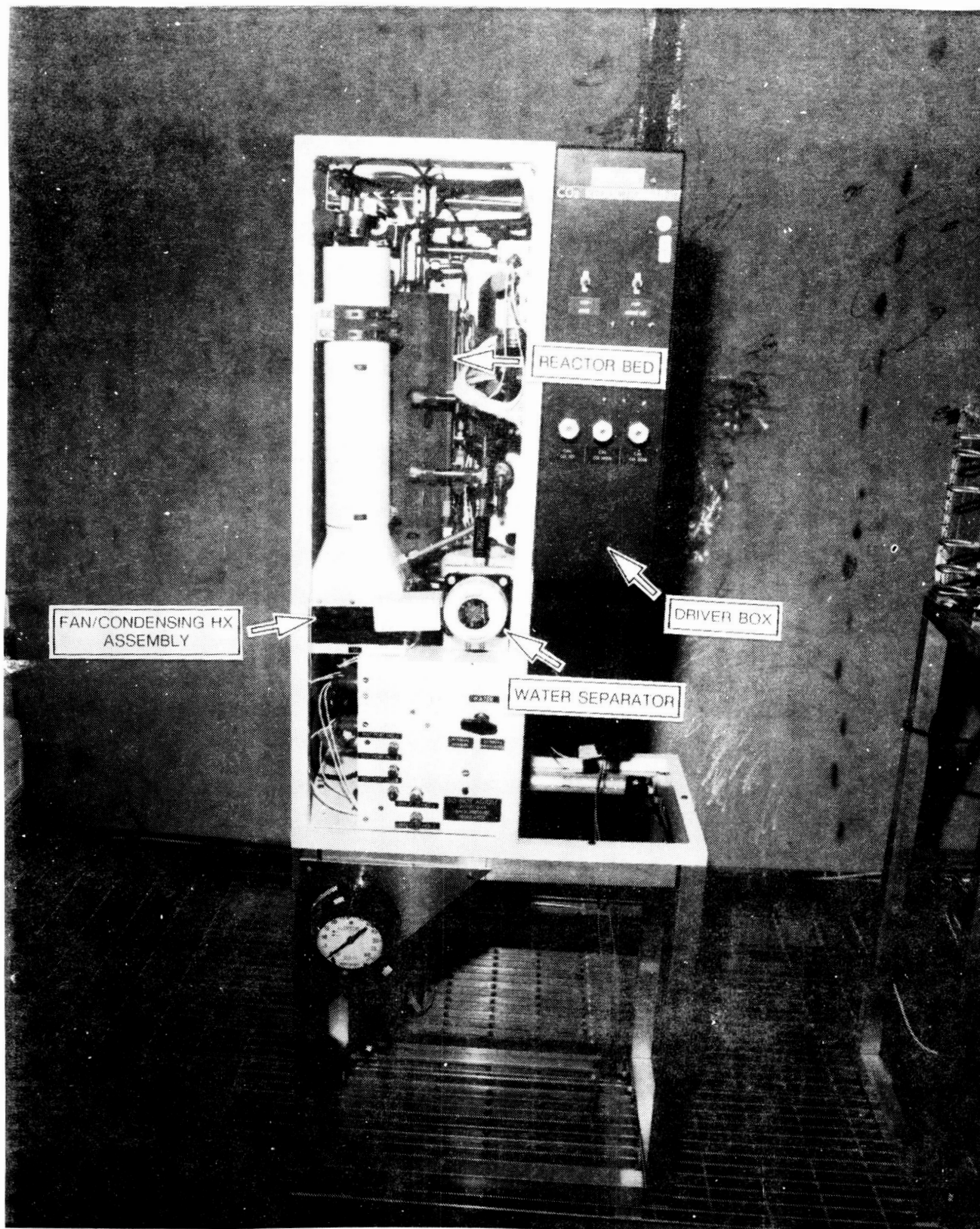


Figure 7. Sabatier.



coil and later reduction by the Sabatier subsystem. Other interfaces for the 4BMS included cooling water for thermal conditioning of desiccant bed outlet air, nitrogen for the operation of internal valves, and a vacuum source used to evacuate the CO<sub>2</sub> holding tank before filling with CO<sub>2</sub> prior to operation. Instrumentation external to the unit was used to measure inlet air flow, inlet and return air carbon dioxide partial pressure, and the concentrated carbon dioxide pressure, temperature, and flow. A sensor was also located in the carbon dioxide output stream to detect the presence of oxygen prior to hydrogen mixing. All measurements internal to the 4BMS were sent to the facility data management system through an instrumentation scanner. An IBM PC was used to display this information in a graphical format by interfacing with the facility data management system through a serial bus. The 4BMS and associated CO<sub>2</sub> accumulator is shown in Figure 8.

### **2.2.5 Trace Contaminant Control Subsystem (TCCS)**

The TCCS is designed to remove contaminants from the atmosphere. The system is composed of a catalytic oxidizer with pre- and post-sorbent canisters. During the test, the TCCS drew in air from the simulator and returned the purified air through a duct connected to the ventilation system. All instrumentation on the unit interfaced with the data management system through a facility scanner. A photograph of the system is shown in Figure 9.

### **2.3 Temperature and Humidity Control System (THCS) and Metabolic Simulator**

The internal THCS was built from commercial "off-the-shelf" components and was designed to provide sensible and latent heat removal from the module simulator internal environment as well as ventilation flow. Due to the open door simulation in the SIT, the THCS was utilized only for ventilation. All THCS components were located in the subfloor of the module simulator. An air supply duct was located at one end of the simulator with the return duct at the opposite end. Condensate was collected in a drip pan located on the bottom of each of the heat exchangers where it was sent to the facility drain.

The metabolic simulator was designed to allow for the introduction of various gases, namely carbon dioxide and nitrogen, into the module simulator. The metabolic simulator was constructed in the form of a panel with all components such as gauges, regulators, and valves mounted into the panel. During the SIT, carbon dioxide was bled into the Molecular Sieve inlet air duct at a three-man metabolic rate. No nitrogen was used although it will be required as a make-up gas in future "closed door" testing.

### **2.4 Test Scope**

Since the ECLS subsystems utilized in this test were at a "preprototype" level, no effort was made to simulate many of the higher system management functions as well as interactions with other space station elements such as thermal control and data management. In an actual flight system, many services such as O<sub>2</sub>/N<sub>2</sub> supply and control, air distribution and handling, integrated data management and control, hygiene/potable water processing and supply, and thermal control would be present. In the current test scheme, these functions, if provided at all, are available only as a non-flight-like facility service. Data from this and subsequent tests should provide valuable insight to the evolution of the ECLS system simulations at MSFC to flight type configurations.



Figure 8. 4-bed molecular sieve.

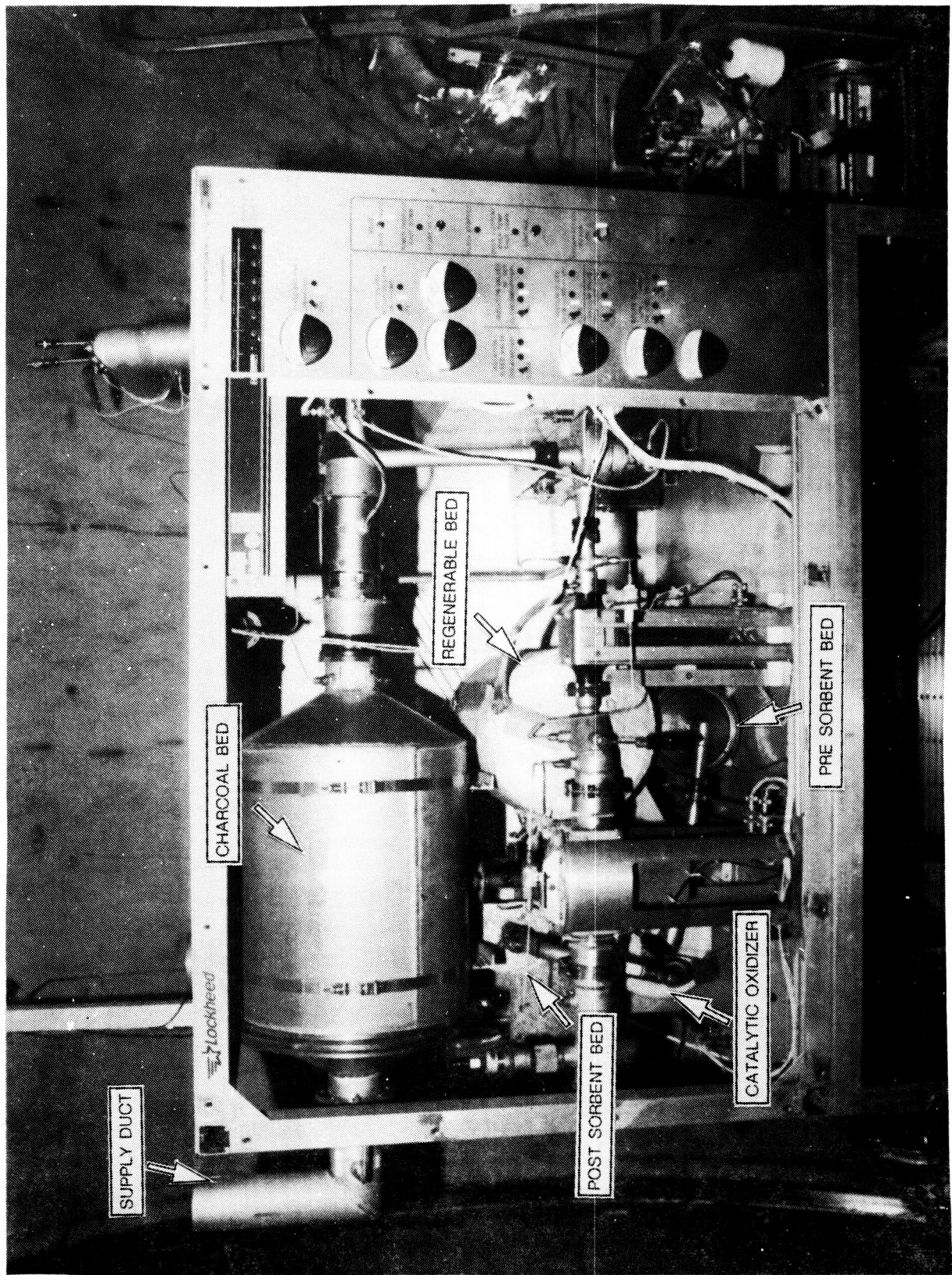


Figure 9. TCCS.

### 3.0 TEST SUMMARY

This section is a condensed narrative of what is contained in the test log (see appendices). A more detailed explanation of each anomaly that occurred during the test is given in the following section. The absolute times that are given in this section are followed by a number in brackets which is the test elapsed time in hr:min format.

The SIT began at 7:00 a.m. (00:00) CST June 9, 1987. At 7:05 a.m. (00:05) the internal TIMES heaters were turned on without activating the subsystem. Since the heaters require 1 to 1.5 hr to warm up, this allowed for a quicker start once the subsystem was activated. The TCCS was activated at 7:22 a.m. (00:22) and after several attempts the SCATS was operational and recording data at 7:44 a.m. (00:44). At 7:46 a.m. (00:46) the molecular sieve was on-line. The SFE startup sequence was initiated with a nitrogen purge at 8:10 a.m. (01:10). By 8:48 a.m. (01:48) the SFE cell current was 8.2 A indicating  $H_2/O_2$  production. At 8:53 a.m. (01:53) the SFE nitrogen purge was terminated; pure oxygen and hydrogen were flowing through the outlet lines. By 9:07 a.m. (02:07) the Molecular Sieve had sufficient pressure in its  $CO_2$  outlet accumulator to open SV13 allowing flow through the facility vent at SV09. At 9:09 a.m. (02:09) the Sabatier startup sequence was initiated with a 4-min nitrogen purge. At 9:17 a.m. (02:17) the Sabatier was receiving a  $H_2/CO_2$  mixture from the SFE and Molecular Sieve subsystems. At this point the SFE cell current was 16.0 A (nom = 29.0 A) indicating that the unit was still warming up to full capacity. At 9:20 a.m. (02:20) the TIMES was fully activated (heaters had been on since 7:05). (It should be noted that the SFE had previously been charged with facility deionized water.) At 9:44 a.m. (02:44) communication was lost between the SFE PDU and the SFE controller. It was decided to continue operation until the vendor could arrive to troubleshoot the problem. The SFE performance could still be monitored from flow sensors mounted externally to the unit. At 10:20 a.m. (03:20) a manual shut down of the TIMES was conducted to investigate a high evaporator pressure reading. At 10:26 a.m. (03:26) the TIMES was reactivated. At 11:00 a.m. (04:00) the SFE shutdown sequence was initiated. By 2:30 a.m. (07:30) the vendor had replaced the PDU/SFE optical communications link with a copper wire communications cable and the startup sequence was again initiated with an automatic nitrogen purge. By 3:08 p.m. (08:08) the SFE current was 8.2 A indicating that the unit was producing hydrogen and oxygen. At 3:20 p.m. (08:20) it was discovered that the Sabatier had shut itself down. This event was not discovered immediately as the Sabatier's DCC was not updating displayed measurements properly. At 3:22 p.m. (08:22) the Sabatier was back on line as the DCC and the unit were restarted. At 3:26 p.m. (08:26) the Sabatier was receiving a  $CO_2/H_2$  mixture from the molecular sieve and the facility  $H_2$  supply (the SFE  $H_2$  output was being diverted to vent). At 3:42 p.m. (08:42) the TIMES product water (after post treat) conductivity was measured at 85 umho/cm which was within the SFE acceptance range. At 3:50 p.m. (08:50) the SFE cell current was 19.0 A and the Sabatier was receiving a  $CO_2/H_2$  mixture from the Molecular Sieve and SFE subsystems.

At this point, the five subsystems were functioning as an integrated system and operation continued without interruption for the next 19 hr. However, several anomalies were reported during this period. At 3:00 a.m. (20:00) on June 10 a flow sensor in the Sabatier vent line (FF03) indicated a value of 2.9 SLPM which was much greater than nominal (nom = 1.0 SLPM). The flow stabilized at 5:00 a.m. (22:00) so no action was taken until 7:51 a.m. (22:51) when a manual flow measurement was made. The manual measurement agreed with the nominal value of 1.0



SLPM although the flow sensor was continuing to report a much higher value, thus indicating a faulty sensor. At 5:02 a.m. (22:02) on June 10 the console fault indicator activated on the DCC. It was later discovered that the event was due to clogging of the cooling fan debris filter. At 9:20 a.m. (26:20) a TIMES low production rate warning was sounded. The TIMES conductivity was observed to be in excess of 50 umho/cm so a brine dump was initiated at 9:34 a.m. (26:34). The TIMES production rate was soon restored to between 2.5 and 3.0 lb/hr. At 11:20 a.m. (28:20) the Sabatier experienced an automatic shutdown. It is believed that this shutdown was caused by manual gas sampling of the SFE product H<sub>2</sub> which was in progress at approximately the same time. The Sabatier possibly shut itself down because of a drop in H<sub>2</sub> flow which caused the reaction to cease. The Sabatier was restarted at 11:30 a.m. (28:30). System operation continued for the next 23 hr without interruption. Aside from a SFE high voltage warning at 7:54 a.m. (48:54) on June 11, operation was uneventful. Beginning at 10:00 a.m. (51:00) on June 11 the subsystems were shut down one at a time and the SIT was concluded. The first ECLSS integrated test had run for a total of 52 hr (including startup and shutdown) with continuous runs of 19 and 23 hr.

## **4.0 TEST ANOMALIES**

The anomalies that occurred during the SIT are listed below for convenience. Detailed explanations are given for each anomaly where possible.

### **4.1 SFE Communication to PDU Failure**

At 9:44 a.m. on June 9, the SFE subsystem lost communication between its internal controller and the PDU. Communication was lost to the SCATS as well. A manual shutdown was initiated at 11:00 a.m. to troubleshoot the problem. The RS-232 optical-fiber communication link between the PDU and the internal controller was tested and the communication loss was believed to have occurred on the internal controller side of the link. The Central Electronics Unit (CEU) card which contains the communication electronics was first suspected; however, replacement of this card did not restore communications. The optical link was then bypassed with a copper wire communications cable and communication to the PDU was restored. The optical-fiber link is being tested at the vendor to determine the exact cause of the problem.

### **4.2 TIMES Manual Shutdown**

At 10:20 a.m. on June 9, the TIMES was manually shut down to investigate a high evaporator pressure. At 10:26 a.m. the unit was reactivated and the evaporator pressure returned to normal and remained normal for the remainder of the test. The TIMES has a pulse valve located between the evaporator passage and an external vacuum source. This valve opens periodically to allow noncondensable gases to escape through the vacuum source. After startup, the TIMES was put in the "manual" mode and the pulse valve was closed to facilitate reaching the process pressure in the evaporator. The TIMES was then taken directly to the "on" mode. The pulse valve was

never reinitialized and therefore stayed in the closed position, causing the rise in evaporator pressure. It was discovered that the characteristics of the software require that in order to return control of the TIMES to the controller from the manual mode, the operator must do a "power reset" before going to the "on" mode. This software characteristic will be revised to allow direct return to the "on" mode from the "manual" mode for the next test.

### **4.3 First Sabatier Shutdown**

At 3:20 p.m. on June 9, the Sabatier subsystem shut down. The shutdown was due to a loss of communication from the Sabatier controller to the DCC and the SCATS. At 3:22 p.m. the unit was successfully restarted. Later troubleshooting revealed that a poor connection of a ground lead in the driver box was the cause of the shutdown. The ground connection has been repaired and subsequent Sabatier testing has shown no reoccurrence of the problem.

### **4.4 External Flow Sensor for Sabatier Product Gas Vent**

Several times during the test the Sabatier vent flow sensor (FF03, not a part of the subsystem) reported large flow rates through the Sabatier product gas vent. It was determined through manual measurements that the sensor was outputting an incorrect value. It was later determined that moisture affected the sensor, as gas samples taken from the vent line contained condensation. To correct this problem, the vent line was replumbed to be more conducive to draining condensed water and a clear bowl water trap was installed upstream of the flow sensor. The Sabatier has since been operated with no reoccurrence of the problem.

### **4.5 Weight Scales**

It was discovered on the second day of testing, June 10, that the SCATS was not updating the facility weight scale measurements for TIMES and Sabatier product water. It was possible to read the value directly from the digital value displayed on the scale, however. Problem resolution is still in work.

### **4.6 DCC Console Fault Indicator**

At 5:22 a.m. on June 10, the DCC fault indicator sounded. This was due to an overheating of the graphics board. Though the DCC display was not updating, this did not effect the operation of the TIMES or the Sabatier subsystems. The cooling air filter was found to be covered with dirt and debris. The filter was cleaned and reinstalled. The DCC has not experienced any further problem.

## **4.7 Second Sabatier Shutdown**

At 11:20 a.m. on June 10, the Sabatier subsystem shut down displaying the message "...H<sub>2</sub>O/CH<sub>4</sub> Delta P is out of range..." This shutdown is believed to have been caused by manual gas sampling of the SFE product H<sub>2</sub> outlet line which was taking place at approximately the same time. The sampling reduced the Sabatier inlet H<sub>2</sub> flow causing a decrease in water production and producing a much higher product gas to water ratio outlet pressure thereby increasing the delta pressure. The unit was restarted at 11:30 a.m. and the anomaly was not observed for the remainder of the test. Since the integrated test, the sampling valve for H<sub>2</sub> has been replaced with a 0.032-in. diameter orifice metering valve to prevent out of tolerance H<sub>2</sub> input flows to the Sabatier during sampling. Later Sabatier sampling has shown that the metering valves have solved the problem.

## **4.8 SFE High Voltage Warning**

At 7:54 a.m. on the final day of testing, June 11, the SFE subsystem displayed a high voltage warning. This was due to a low operating temperature on T1, the feed water recirculation loop temperature. No action was taken to correct the problem because the integrated test was scheduled to be completed that morning. Because little data was available, the exact cause of the low temperature could not be determined. It has been recommended by the vendor that the control point for T1 be raised 5°F prior to the next integrated test to avoid reoccurrence of this anomaly in the future.

## **4.9 O<sub>2</sub> in Molecular Sieve CO<sub>2</sub> Output**

A steadily degrading situation was observed during the test where the oxygen in the Molecular Sieve CO<sub>2</sub> output stream rose from about 0.7 percent to 2.5 percent over the course of the test. The upper limit for this value was 3.0 percent indicating that some type of correction will be necessary for longer duration tests. For a complete discussion of the modifications made to the molecular sieve see Section 5.4.3.

## **5.0 SUBSYSTEM DISCUSSIONS OF RESULTS**

The following sections discuss the test results for each individual subsystem in detail. At the beginning of each section is a brief description of each subsystem including theory of operation. Results for the TCCS are not available due to an anomaly in the data link between the TCCS and the data management computer.

## 5.1 TIMES

### 5.1.1 Subsystem Description

A schematic of the TIMES utilized in the SIT is provided in Figure 10. The main elements of the subsystem are the dual evaporators and the thermoelectric regenerator (TER). The function of these two elements is to produce a low temperature, purified steam distillate from a concentrated wastewater while reducing the inherent power requirement associated with any phase-change process.

Each evaporator consists of three hollow fiber membrane (HFM) assemblies. Each assembly includes 100 tubes (0.04-in. ID, 0.05-in. OD, 7.5-ft long) made of Nafion, a fluorocarbon-based cation exchange material. The function of the tubes is to control the vapor/liquid interface in microgravity. Heated wastewater, at a temperature of approximately 140°F, flows through the inner diameter of these tubes. Water is transported through the walls of the tubes by diffusion and ion exchange mechanisms. Vaporization occurs at the outer surfaces of the tubes which are maintained at a pressure of 2.7 psia.

The TER is an integrated package consisting of two wastewater heat exchangers and two arrays of thermoelectric devices (TED) as well as a common condensing heat exchanger. The hot sides of the TEDs are in contact with the two wastewater heat exchangers and the cold sides with the condenser. In this arrangement the TEDs are able, through application of power (28 Vdc, 9 A total), to transfer heat from the condenser to the heat exchangers, thereby effectively recovering the heat of vaporization for reuse.

Wastewater is gravity-fed to the TIMES from a facility storage tank. Within the subsystem, the wastewater feed is preheated via a regenerative heat exchanger and combined with a concentrated brine solution that is recirculated internally at a rate of 600 lb/hr. The brine is passed through a 25 micron polypropylene filter which protects the HFMs from gross particulate contamination. Effluent from the filter is split and flows through the wastewater heat exchangers which raise the temperature of the brine to approximately 140°F. The heated brine flows through the two HFM bundles. The portion of the brine that does not evaporate during a single pass through the HFMs is recirculated via the recycle pump for additional processing.

Steam generated in the evaporators is partially condensed in the condenser. The latent heat that is released is transferred by the TEDs to the wastewater heat exchangers. Additional condensation occurs through heat transfer to the incoming wastewater in the regenerative heat exchanger. Final condensation is accomplished with an air-cooled heat exchanger. Noncondensable gases such as carbon dioxide are removed from the condensate via a centrifugal air/water separator, stored in an accumulator, and periodically purged to a facility vacuum source to maintain a subsystem reference pressure of 1.6 to 2.0 psia. A check of condensate quality is provided by a conductivity sensor prior to delivery to a facility product water storage tank. Condensate with a conductivity in excess of 250 umho/cm triggers an alarm and results in the condensate being returned, via the reject valve, to the recirculation loop for reprocessing.



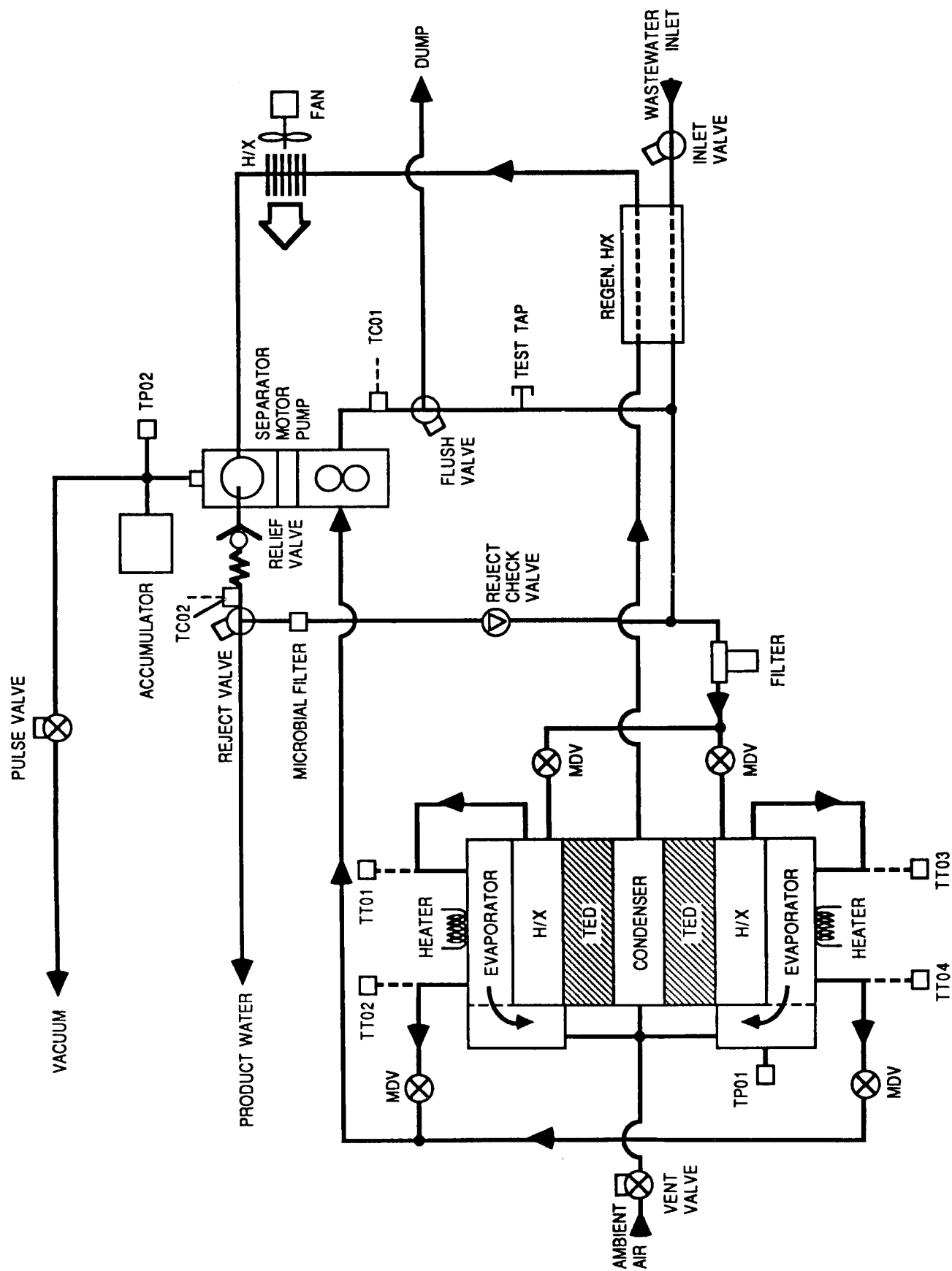


Figure 10. TIMES schematic.

Heaters are installed on the exterior surfaces of the two evaporators. These heaters are utilized during the initial startup of the unit to prevent excessive condensation from accumulating in the evaporators before steady-state operating temperatures are reached. The heaters are turned off once the temperature of the evaporator, as inferred from the HFM inlet and outlet temperatures, reaches approximately 130°F. The heaters remain off under nominal processing conditions.

## 5.1.2 Post-Treatment Module Description

A post-treatment sorbent bed was provided to polish the aggregate distillate produced by the TIMES. The bed contained both activated carbon and a mixed ion exchange resin. Because this phase of system testing is not addressing microbial control, the bed did not have any provisions (such as the inclusion of iodinated resin or heaters) for microbial control.

The bed was located between the TIMES product water tank and the TSA for the water electrolysis subsystem. A pump was used, on a periodic basis, to pump aggregate distillate from the TIMES product water storage tank, through the post treatment bed, and into the TSA storage tank or out through a facility sampling port.

## 5.1.3 Discussion of Results

### 5.1.3.1 General

Throughout the test the TIMES processed a wastewater mixture comprised of 75 percent pretreated urine and 25 percent deionized water by volume. The addition of deionized water is required to simulate the amount of urinal flush water projected to be required for space station operations. The pretreatment formulation used is listed in Table 1. Throughout the remainder of this report, the mixture of pretreated urine and deionized water will be referred to simply as pretreated urine.

TABLE 1. PRETREATED URINE COMPOSITION

<u>Pretreatment Chemicals</u>	<u>Dosage (g/l)*</u>
Sulfuric Acid	2.52
Oxone	5.00
 <u>Pretreat Urine/Deionized Water Mixture Ratio</u>	
Pretreated Urine	75% by vol
Deionized Water	25% by vol

\* refers to grams of chemical per liter of raw urine  
(i.e., urine without flush water)

The TIMES operated nearly continuously for 47.66 hr following the initial warmup period of 2.33 hr. The one exception was a period of approximately 6 min during the early stages of the test when the unit was temporarily shut down to investigate a high evaporator pressure reading (see below). Throughout the remainder of the test, the TIMES operated nominally with no significant anomalies.

Due to a communication problem between the SCATS data acquisition computer and the scales located under the facility product water and brine storage tanks, accurate data detailing the overall TIMES water balance is not available. In addition, provisions to measure the quantity of water lost to vacuum through periodic purging were not available. Without this data, the overall water recovery efficiency of the TIMES was not determined for this test.

### **5.1.3.2 Pretreated Urine Processing Rate**

As shown in Figure 11, the TIMES processed a total of 115.2 lb of pretreated urine following the initial warmup period. This translates into an average urine processing rate of 2.42 lb/hr. During the test, two brine dumps were initiated manually. The first occurred at 26:34 hr in response to a low production rate warning and appears as a sharp drop of approximately 6.2 lb in the wastewater tank scale reading. This drop was due to the rapid replacement of brine within the internal recycle loop with fresh pretreated urine. The second brine dump occurred at approximately 40:00 hr. The reason this brine dump appears as a slight peak in Figure 11 is that immediately following the dump, fresh pretreated urine was added to the wastewater storage tank thereby offsetting the drop in wastewater quantity attributable to the dump. Fresh pretreated urine was also added to the wastewater storage tank at approximately 29:30 hr accounting for the sharp increase evident in Figure 11 at that time.

The maximum urine processing rate observed during the test was 3.42 lb/hr in the early stages of operation. The minimum urine processing rate occurred just prior to the first brine dump and triggered the low production rate warning set at 0.8 lb/hr.

As noted above, the overall water recovery efficiency cannot be directly determined due to the problems associated with the product water tank weight scale. An estimate can be determined, however, from the total solids concentrations of both the pretreated urine and the raw distillate. The total solids concentration of the pretreated urine was not directly measured during this test. Given the typical total solids content of human urine (3.7 percent) the amounts of pretreatment solids added per liter of urine, and the ratio of urine to flush water used in the test, it is possible to calculate an estimated total solids content for the pretreated urine of 2.7 percent. The measured total solids concentration of the raw distillate was approximately 3.5 ppm ( $= 3.5 \times 10^{-4}$  percent by weight). Combining the definition of overall water recovery (i.e., total mass of water produced divided by the total mass of water fed) with an overall solids balance yields a calculated overall water recovery efficiency of 87.4 percent. (It should be noted, however, that the accuracy of this calculated efficiency is only as good as the accuracy of the assumption relative to the total solids content of the pretreated urine.)

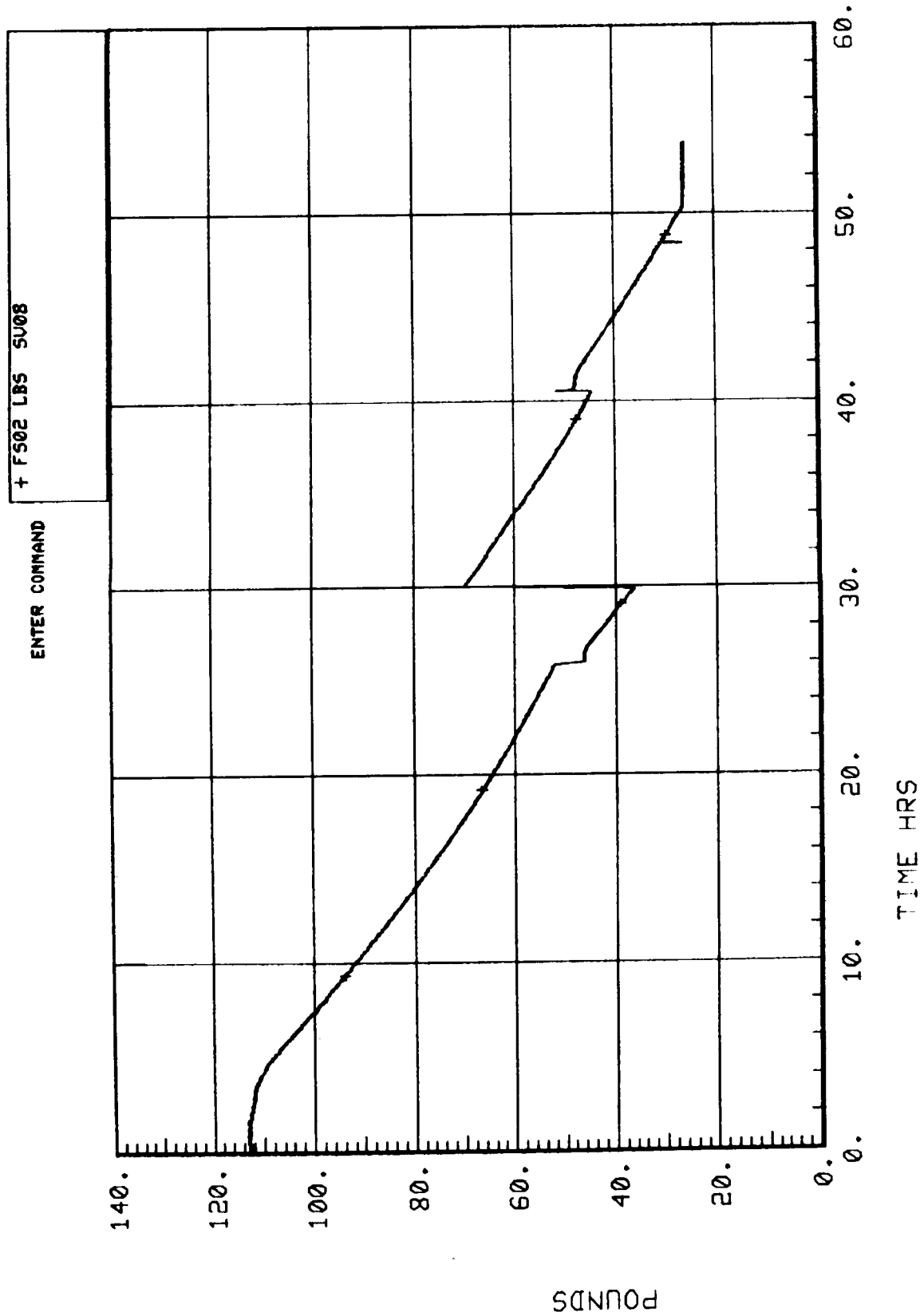


Figure 11. TIMES facility wastewater weight.

### **5.1.3.3 Product Water Quality**

Analyses of water quality were not conducted throughout the test. A spot check of the conductivity of non-post-treated distillate measured 85 umho/cm at 8:46 hr.

Detailed water quality analyses of raw and post-treated distillate, as well as of concentrated brine, were conducted near the conclusion of the test. A complete summary of these analyses is provided in Section 6.0. Both the raw distillate and brine samples were taken from the pooled sources in the respective facility tanks whereas the post-treated distillate samples were obtained directly from the post-treatment module effluent.

As described in Section 6.0, the aggregate raw distillate had a pH of approximately 3.4, a conductivity of 94 umho/cm, and a total solids concentration of 3.5 ppm. The TOC concentration of the aggregate raw distillate cannot be determined due to the discrepancies apparent in the analytical results.

Post-treated distillate generally met the water quality requirements currently defined by JSC 3000, sec. 3, rev D for space station hygiene water. A comparison of the hygiene water specification and the post-treated distillate is provided in Table 2. Of the 52 parameters defined in JSC 3000, sec. 3, rev D for hygiene water, 35 were measured analytically. Of these, only pH was found to be out of specification in two parallel laboratory analyses that were conducted. One of the two analyses for magnesium showed it to be above specification. Only one of the analyses conducted for arsenic and mercury, respectively, had a lower limit of detection sufficiently accurate to verify compliance with the specification. Residual bacteriacide, in the form of iodine, was below the minimum required concentration because appropriate iodine dosing equipment was not included in this test. Finally, the relatively large levels of microorganisms detected are attributable to the fact that active measures to control microbial contamination in the post-treatment beds, product water storage tank, and all the associated plumbing, were not included as a part of this test.

### **5.1.3.4 Discussion of Individual Measurements**

#### **5.1.3.4.1 Evaporator Temperatures – TT01-TT04**

Figures 12 through 15 show the temperatures at the inlets (TT01 and TT03) and outlets (TT02 and TT04) of the HFMs. Following the initial startup, the inlet and outlet temperatures averaged 139° to 142°F and 132° to 135°F, respectively. The drop in temperatures between inlets and outlets is typical of that associated with the heat loss through evaporation. The sharp drops in temperatures at approximately 26.5 hr and 40 hr correspond to the rapid influx of fresh pretreated urine during the two brine dumps.

#### **5.1.3.4.2 Steam and Reference Pressures – TP01 and TP02**

Figures 16 and 17 show the steam pressure measured inside the evaporator (TP01) and the reference pressure measured at the purge gas accumulator (TP02). Both pressures exhibit the cyclic behavior associated with the gradual buildup of noncondensable gases within the subsystem and the

TABLE 2. COMPARISON OF POST-TREATED DISTILLATE TO HYGIENE WATER  
QUALITY SPECIFICATION

PARAMETER	SPECIFICATION LIMIT	MAXIMUM CONCENTRATION DETECTED IN POST TREATED DISTILLATE
Physical		
total solids (ppm)	TBD < 500	35
color, true (Pt/Co)	15	0
taste & odor (TTN/TON)	<3	N.A. (1)
pH	5.0-8.0	<u>4.6-4.96</u>
particulate (max size)	40 microns	N.A.
turbidity (NTU)	11	0.26
dissolved gas	no free gas at 35 C	N.A.
free gas	none at STP	N.A.
Inorganics (mg/l)		
ammonia	0.5	0.03-<0.25
arsenic	0.01	<0.005-< <u>0.023</u>
barium	1.0	<0.026-<0.5
cadmium	0.01	N.A.
calcium	TBD	0.02-0.806
chloride	TBD	8.16-11.1
chromium	0.05	0.008-<0.025
copper	1.0	0.092-<0.50
fluoride	1.0	<0.05-<0.5
iodide	TBD	<0.1
iron	0.3	0.00006-<0.15
lead	0.05	<0.07-0.017
manganese	0.05	0.002-<0.025
magnesium	0.05	0.03- <u>0.115</u>
mercury	0.002	<0.00005-< <u>0.005</u>
nickel	0.05	0.013-<0.025
nitrate	TBD	<0.05-<0.5
potassium	TBD	<170
selenium	0.01	<0.000014-<0.005
silver	0.05	<0.02
sulfide	0.05	N.A.
sulfate	TBD	0.14-<0.5
zinc	5.0	0.044-<2.5

\* Underlined values denote out of tolerance condition

TABLE 2. (Concluded)

Organics (mg/l)		
TOC	TBD<10	5.3-6.87
TOC (less-nontoxics)	TBD<1	N.A.
organic acids	TBD	<10-<200
cyanide	TBD	0.1349-0.17
phenols	1	N.A.
halogen'd hydrocarbons	TBD	0.47 (2)
organic alcohols	TBD	<1.4 (3)
specific toxicants	TBD	N.A.
Microbial (CFU/100ml)		
total bacteria	TBD	$2 \times 10^4$
anaerobes	TBD	$7.5 \times 10^3$
aerobes	TBD	$1.25 \times 10^4$
gram positive	TBD	N.A.
gram negative	TBD	N.A.
E-coli	TBD	N.A.
enteric	TBD	N.A.
virus	TBD	$<1 \times 10^2$ (4)
yeast and molds	TBD	N.A.
Bactericide (mg/l)		
residual (min - max)	0.5-6.0	<0.5-<1.0 (5)
Radiological (pCi/l)		
alpha 90 Sr	TBD	N.A.
alpha 226 Ra	TBD	N.A.
beta 3H	TBD	N.A.

(1) no analysis performed for the particular parameter

(2) as determined by EPA 625

(3) ethanol, as determined by EPA 624

(4) determined by electron microscopy and lack of growth on  
4 cell lines

(5) iodine

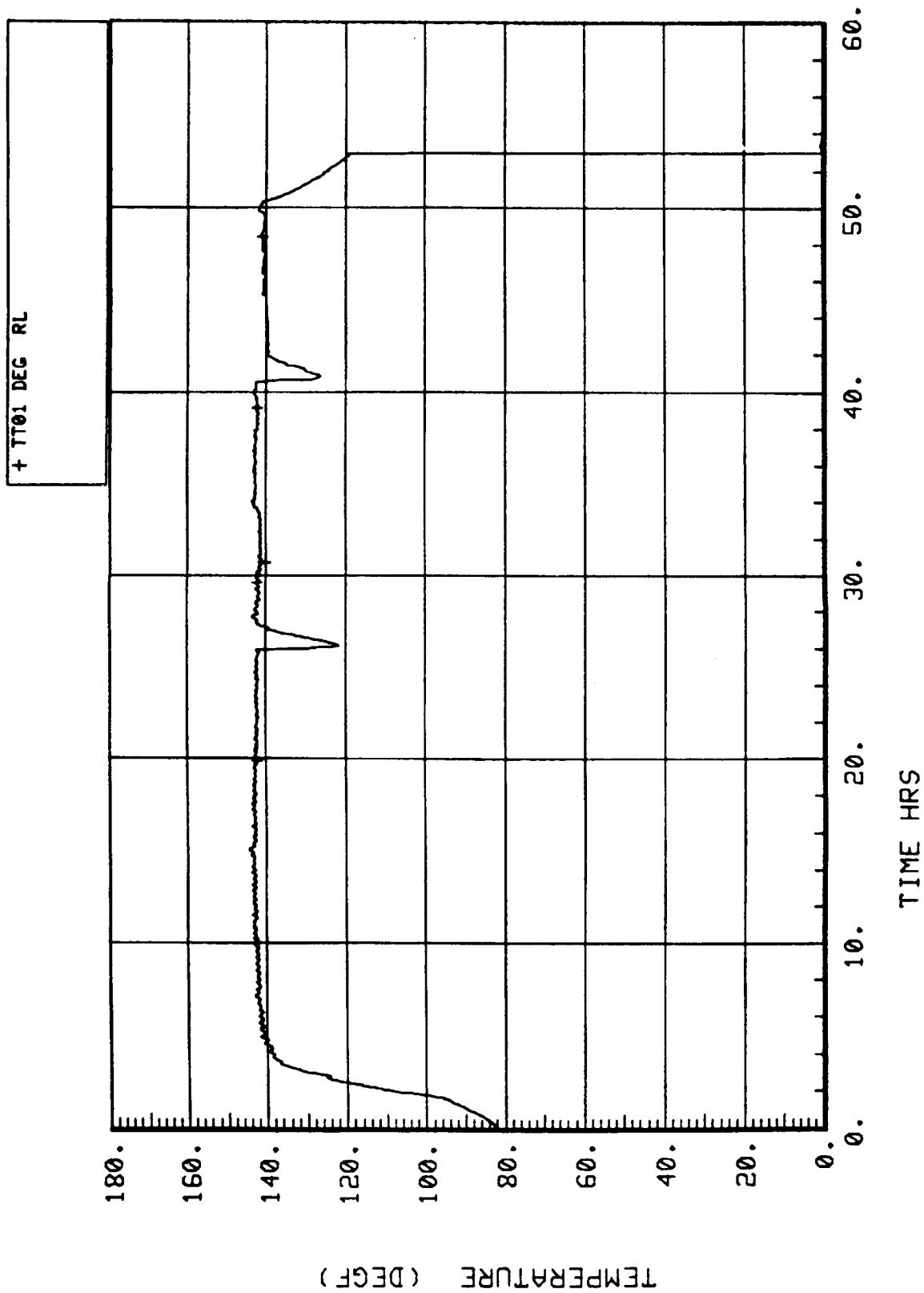


Figure 12. TIMES evaporator temperature TT01.



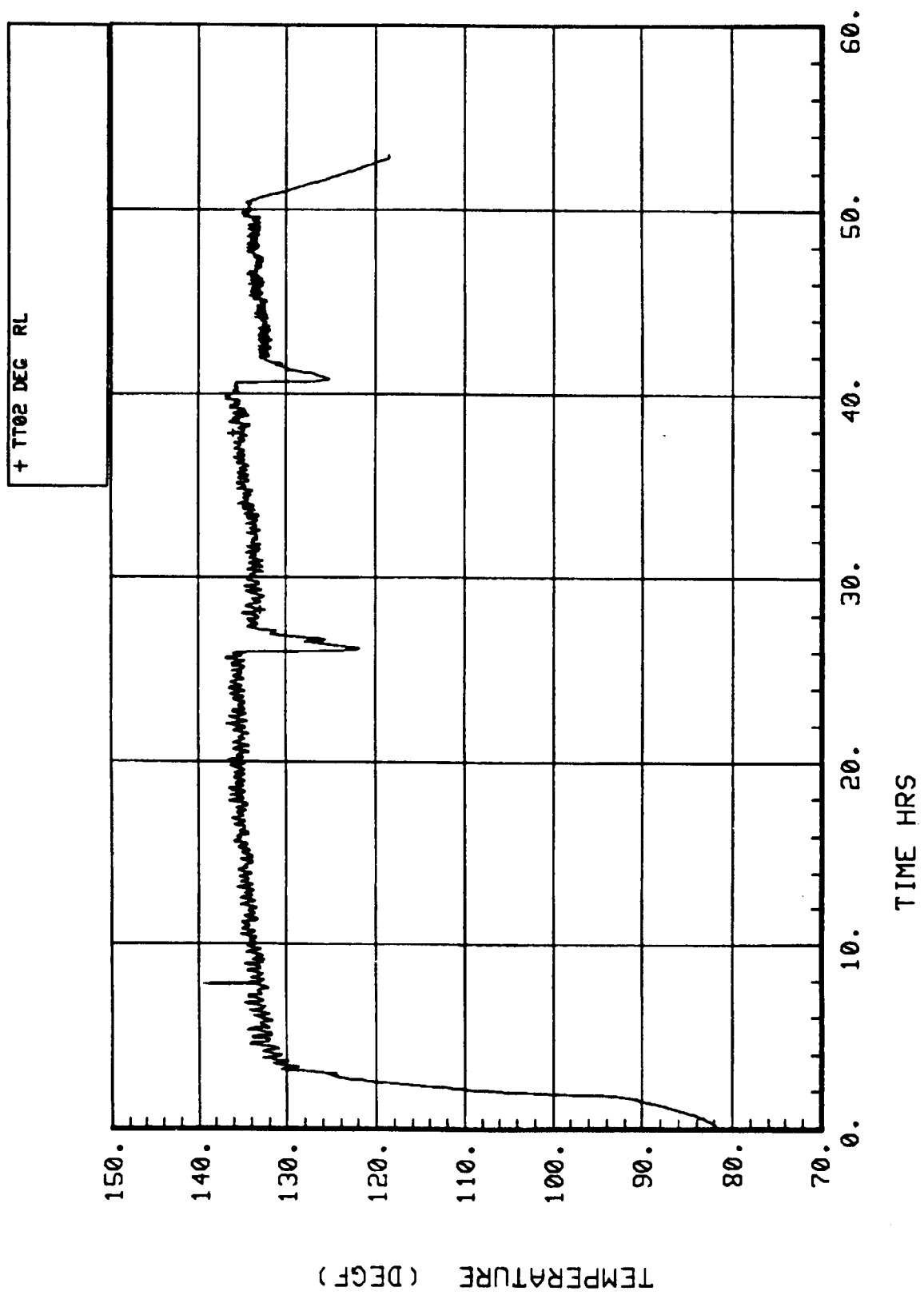


Figure 13. TIMES evaporator temperature TT02.

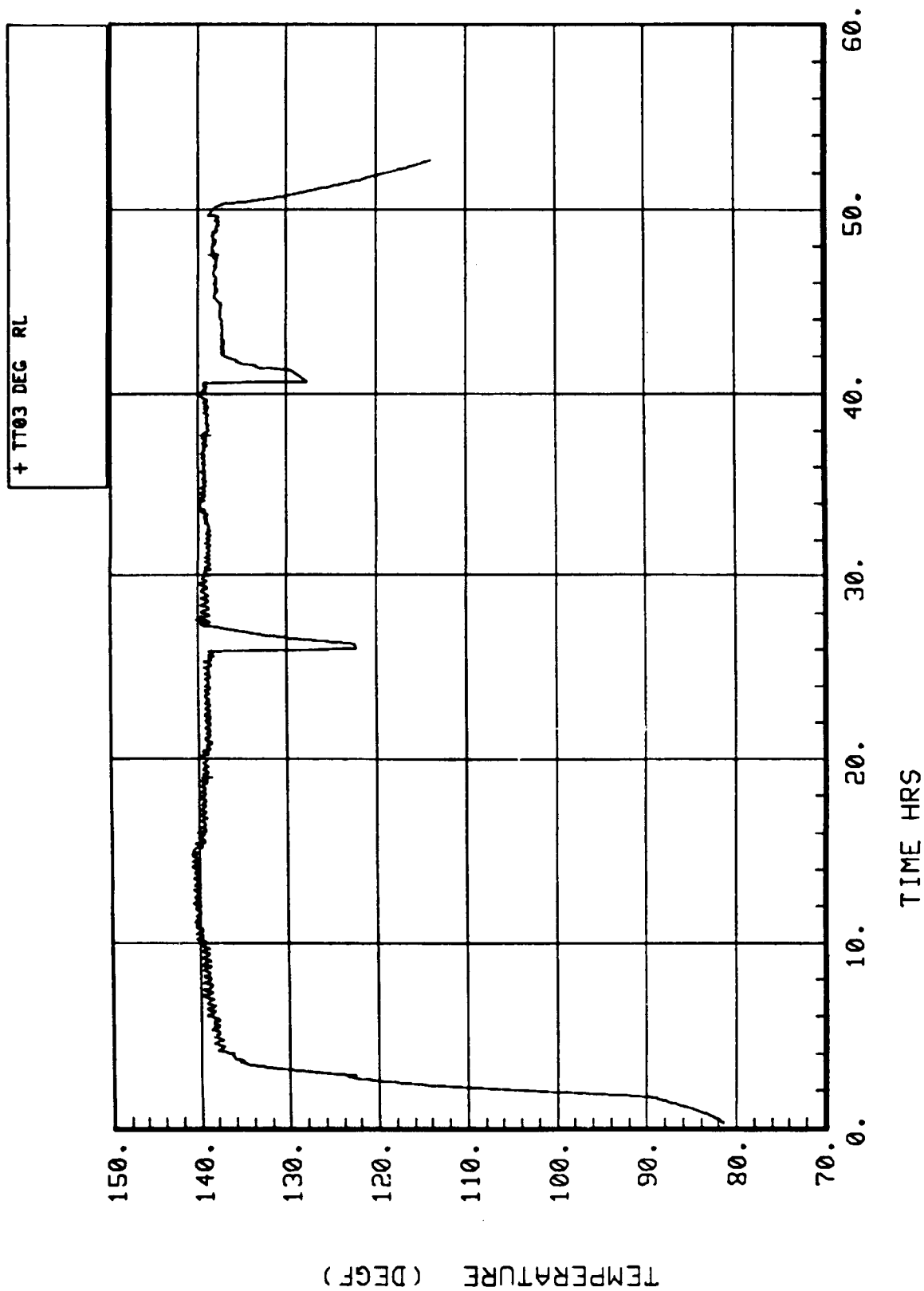


Figure 14. TIMES evaporator temperature .T03.

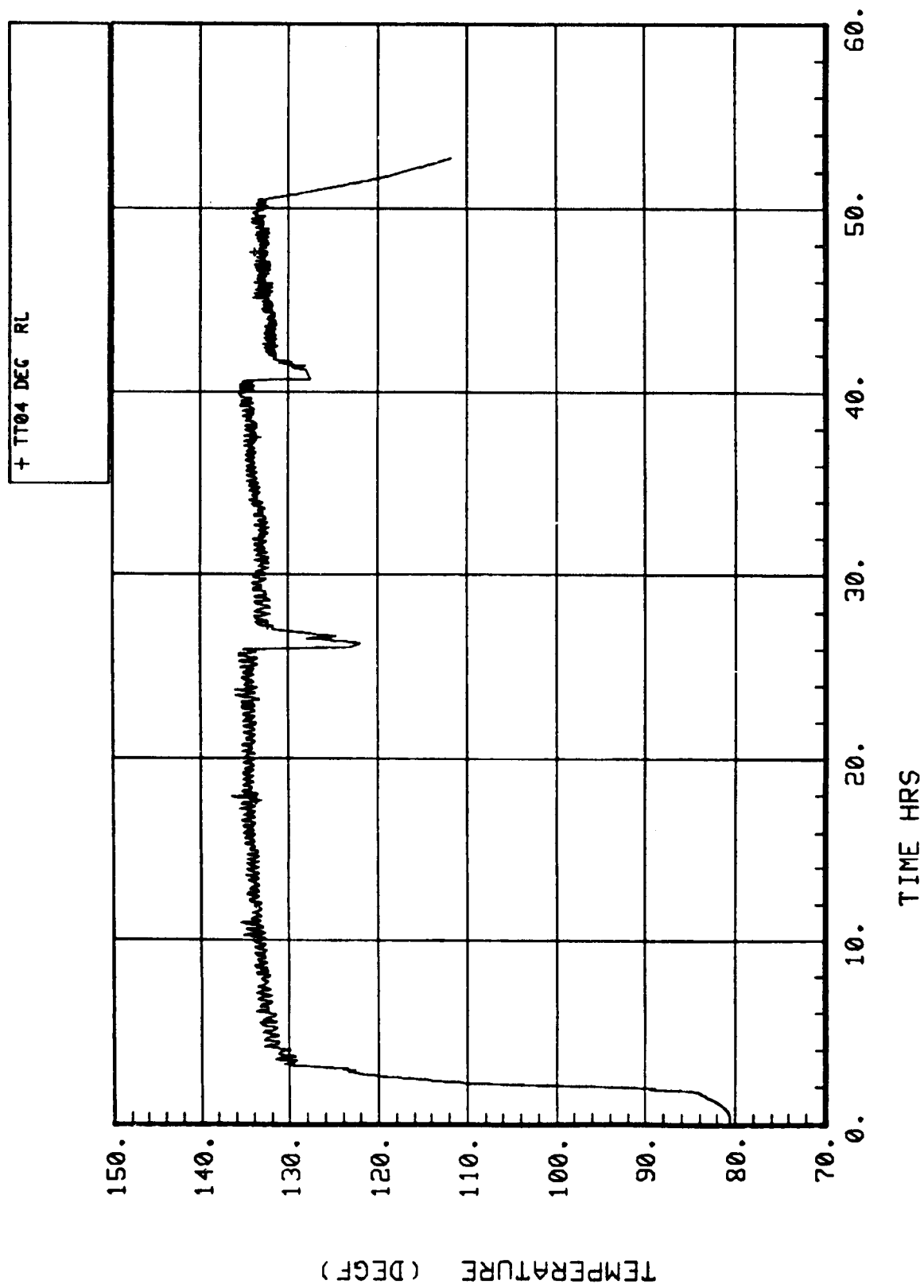


Figure 15. TIMES evaporator temperature TT04.

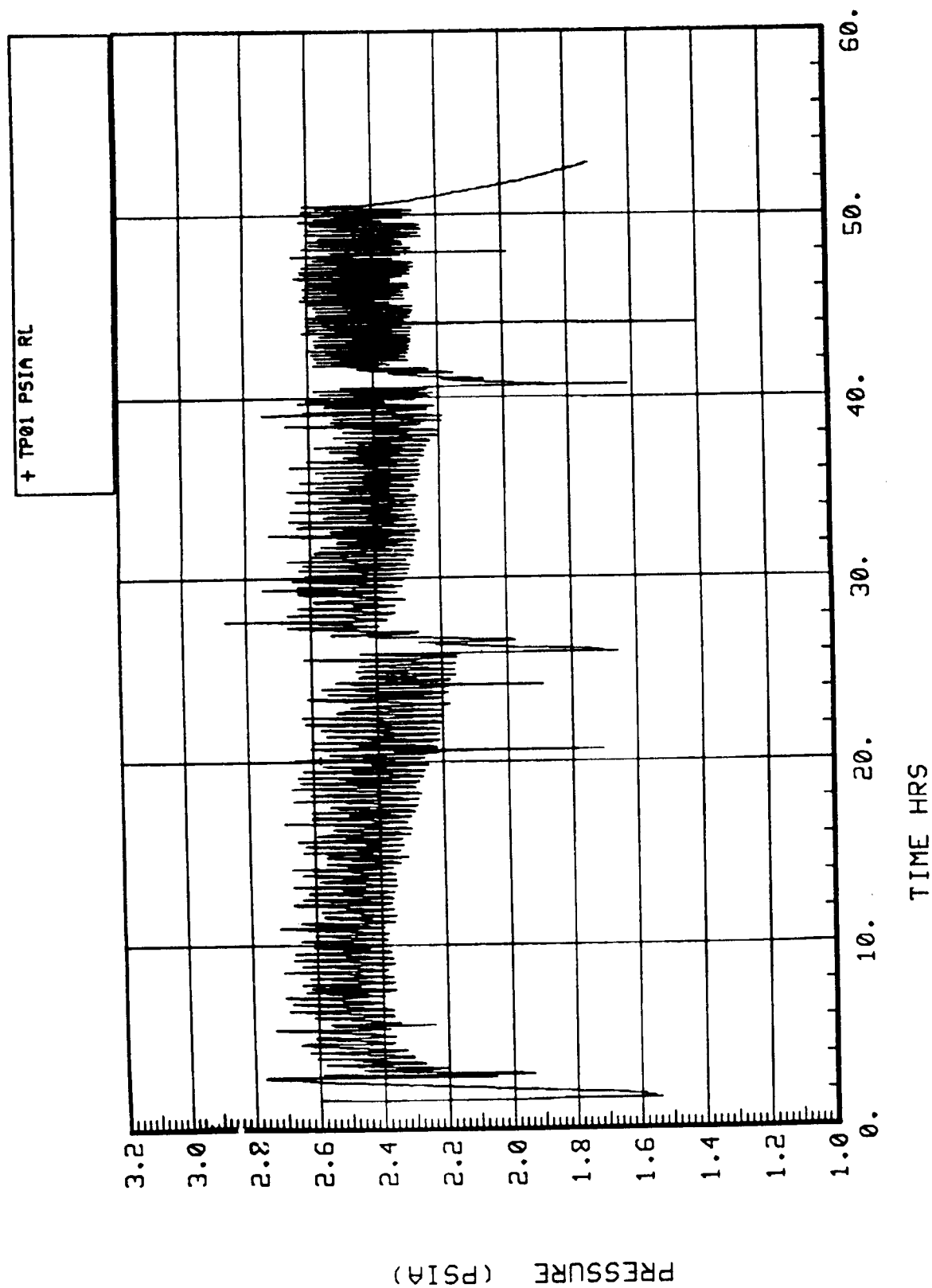


Figure 16. TIMES steam pressure TP01.

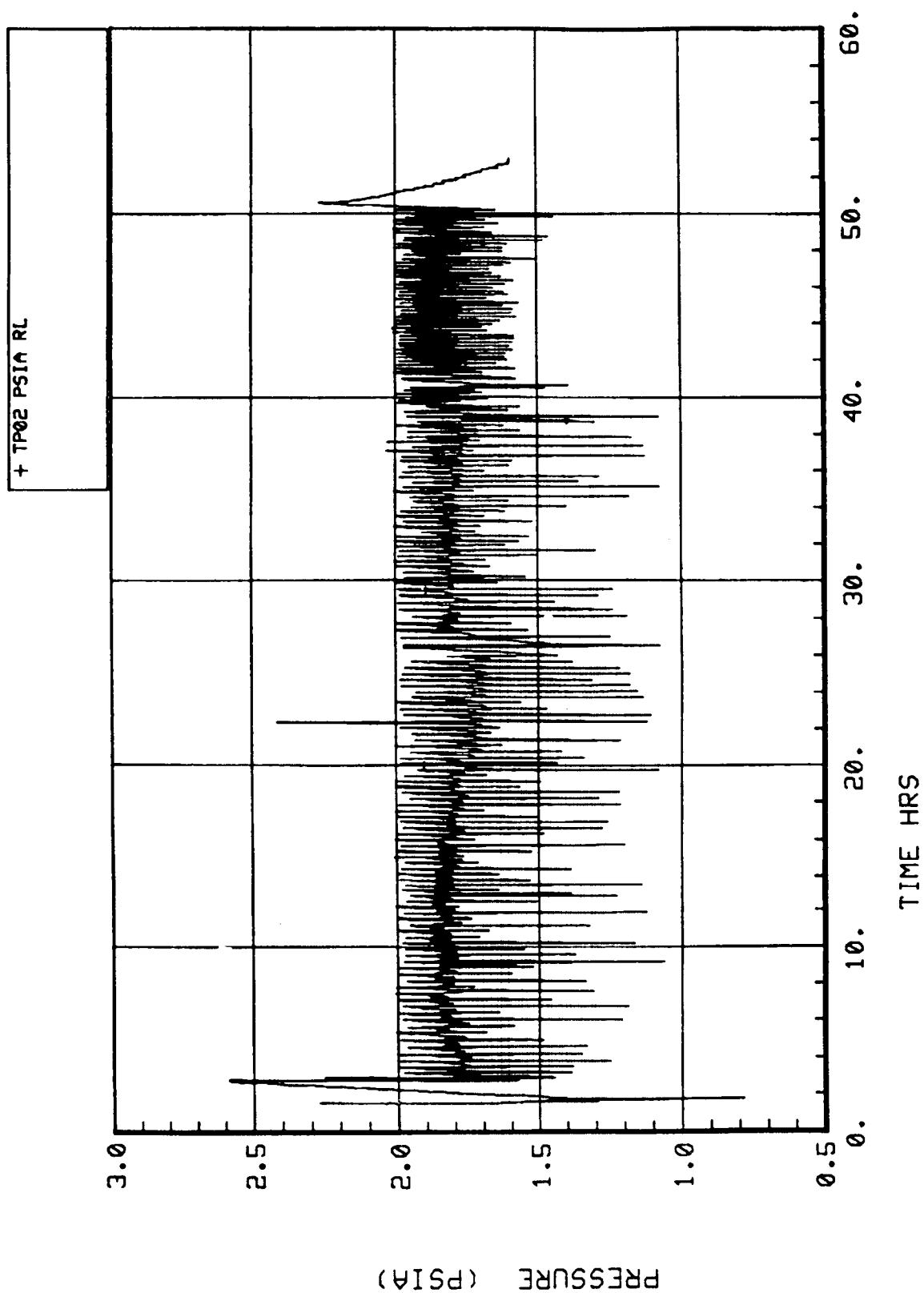


Figure 17. TIMES steam pressure TP02.

periodic purging of these gases to the facility vacuum source. The reference pressure varied between 1.1 and 2.0 psia, with two exceptions. The first occurred during the initial startup when the reference pressure rose to approximately 2.6 psia. This anomaly was tracked to the manual mode operations which were utilized during startup. In manual mode, the pulse valve which controls the venting process remained closed thereby allowing pressure to build. When this situation was detected, the TIMES was switched to "off" mode and then allowed to proceed through an automatic, rather than a manual, startup transition sequence. Under automatic control, the pulse valve functioned properly and regulated the reference pressure within the prescribed limits. A second temporary increase in the reference pressure is apparent at approximately 22 hr. This increase was not of sufficient magnitude to trigger a high pressure alarm or to detectably affect performance. The anomaly was corrected without any intervention by test personnel and most probably represents a temporary sticking of the vent valve or an extraneous electrical signal (which is suggested by the fact that a corresponding increase in the evaporator steam pressure was not detected at the same time).

The steam pressure within the evaporator varied periodically between 2.2 to 2.7 psia. The difference between the reference and evaporator pressures is attributable to pressure losses between the two locations. The gradual reduction in evaporator pressure is due to the corresponding vapor pressure depression associated with the increasing solids concentration of the brine over time. Sharp drops in evaporator pressure at 26.5 and 40 hr corresponds to the introduction of fresh pretreated urine during the two brine dumps.

#### **5.1.3.4.3 Brine Conductivity – TC01**

Figure 18 shows the conductivity of the internal brine solution measured by sensor TC01. The function of the sensor is to trigger brine dumps. However, during this test both brine dumps were initiated manually. The conductivity measured by TC01 varied between 21 and 55 millimho/cm. The gradual increase is due to the increasing concentration of contaminants within the internal brine loop as water is continually removed. Drops in conductivity at 26.5 and 40 hr are due to the influx of fresh pretreated urine during brine dumps. The fact that the conductivity does not return to the level measured for fresh pretreated urine at the beginning of the test (21 millimho/cm) suggests that the brine loop is not completely purged of concentrated brine during the dumps. Several unexplained spikes in the conductivity are apparent and are most probably due to the extremely heterogeneous nature of the brine or to extraneous electrical signals.

Although the relative behavior of the brine conductivity as measured by TC01 is expected, the accuracy of the absolute magnitude of the measurements is questionable. According to Figure 18, the maximum conductivity of the brine (50 to 55 millimho/cm prior to the first two brine dumps, 47 millimho/cm at the end of the test) is significantly below the measured conductivity of the aggregate brine at the end of the test (approximately 101 millimho/cm). This suggests that sensor TC01 may require recalibration, as is often the case for conductivity sensors.

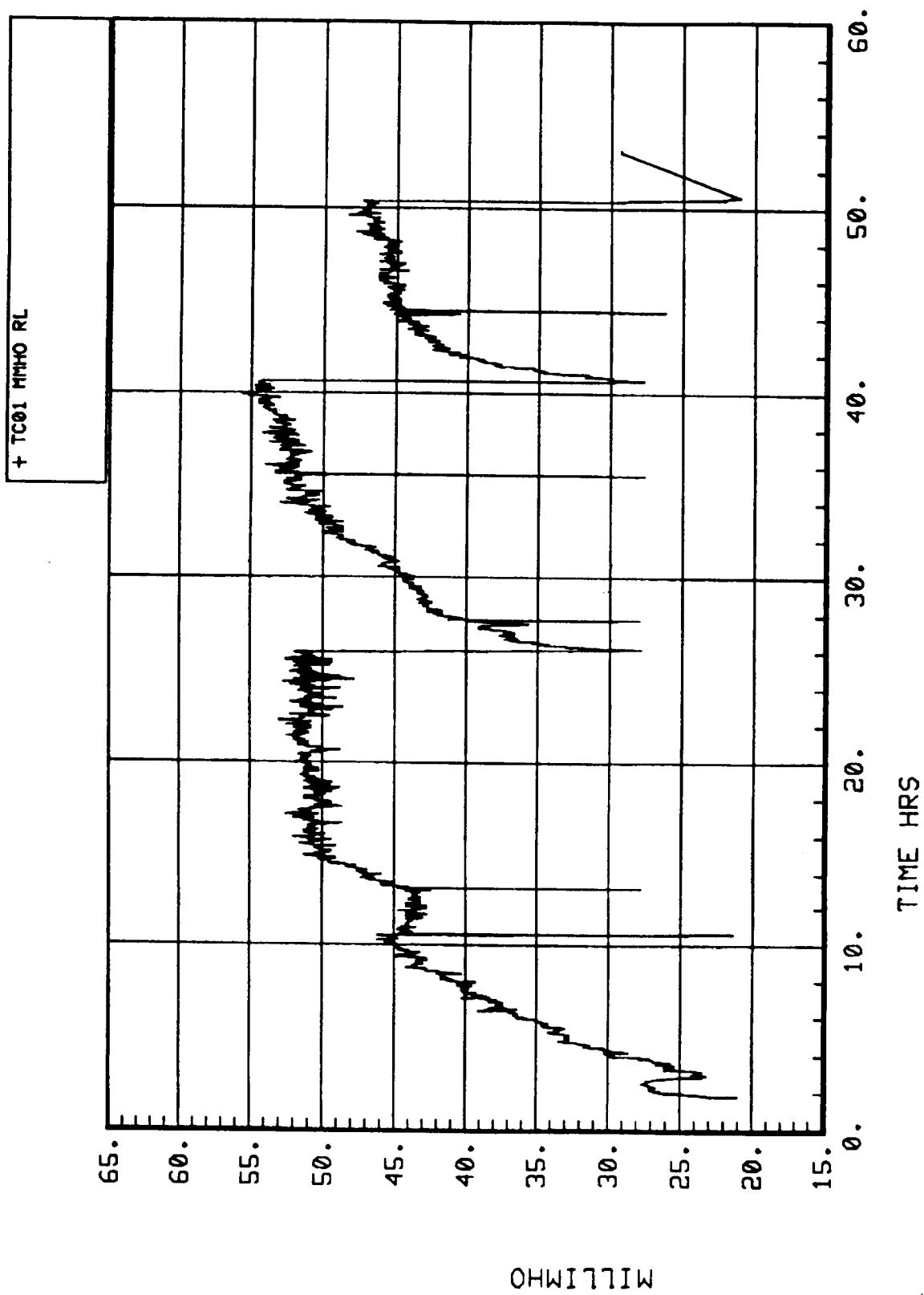


Figure 18. TIMES brine conductivity TC01.

#### **5.1.3.4.4 Condensate Conductivity – TC02**

The conductivity of the distillate is checked by TC02 prior to delivery to the subsystem outlet. Prior to the beginning of the SIT, it was noted that sensor TC01 was not operating properly. A replacement sensor was not available for the test. Therefore, the measurements obtained from TC02 are erroneous and are not included in this report.

#### **5.1.3.4.5 TER Voltage – TV02 and Current – TI01 and TI02**

Figure 19 shows that the TER operated at a nominal voltage of 27.7 V. Extraneous voltage spikes are also apparent in the figure. The voltage spikes are interpreted as electrical noise and are not believed to reflect actual operating conditions.

The operating current for the two arrays of TEDs are shown in Figures 20 and 21. Each array had current draws of approximately 3.5 to 4.3 A, for a combined current draw of about 7.4 to 8.5 A. The numerous spikes in the current curves are typical of the on/off operation of the TEDs during normal operation. The gradual declines in current draw for each array are attributed to the reduced vapor evolution rate, and hence the reduced heat load, resulting from the accumulation of contaminants within the brine loop.

#### **5.1.4 Recommendations/Lessons Learned**

The following recommendations were compiled based on the experiences in the SIT.

The data communications between the SCATS and the facility tank scales must be established in order to provide sufficient data required for the determination of the overall water production rate and water recovery efficiency. Detailed records should be kept of all additions to, and removals from, all facility storage tanks.

Provisions should be made to collect and quantify the amount of water lost to vacuum during the normal purging of the subsystem. This data is required to complete the overall water balance around the TIMES.

Routine analyses of the total solids content of the pretreated urine supply, brine, and product water should be conducted in order to eliminate the need for the engineering assumptions outlined in this report relative to the calculation of the overall water recovery.

An optimized post-treatment bed should be used for the polishing of TIMES distillate. Such a bed should contain known quantities of specified sorbents and resins and should have appropriate provisions for the control of microorganisms.

All storage tanks, especially the product water tank, should be sanitized prior to each test and should be vented to ambient in such a way as to preclude the introduction of microbial contaminants from the atmosphere. Plumbing lines should be arranged to allow sanitization and flushing prior to all tests. Without these provisions, the capacity of the TIMES and post-treatment elements to meet potential microbial specifications cannot be adequately determined.



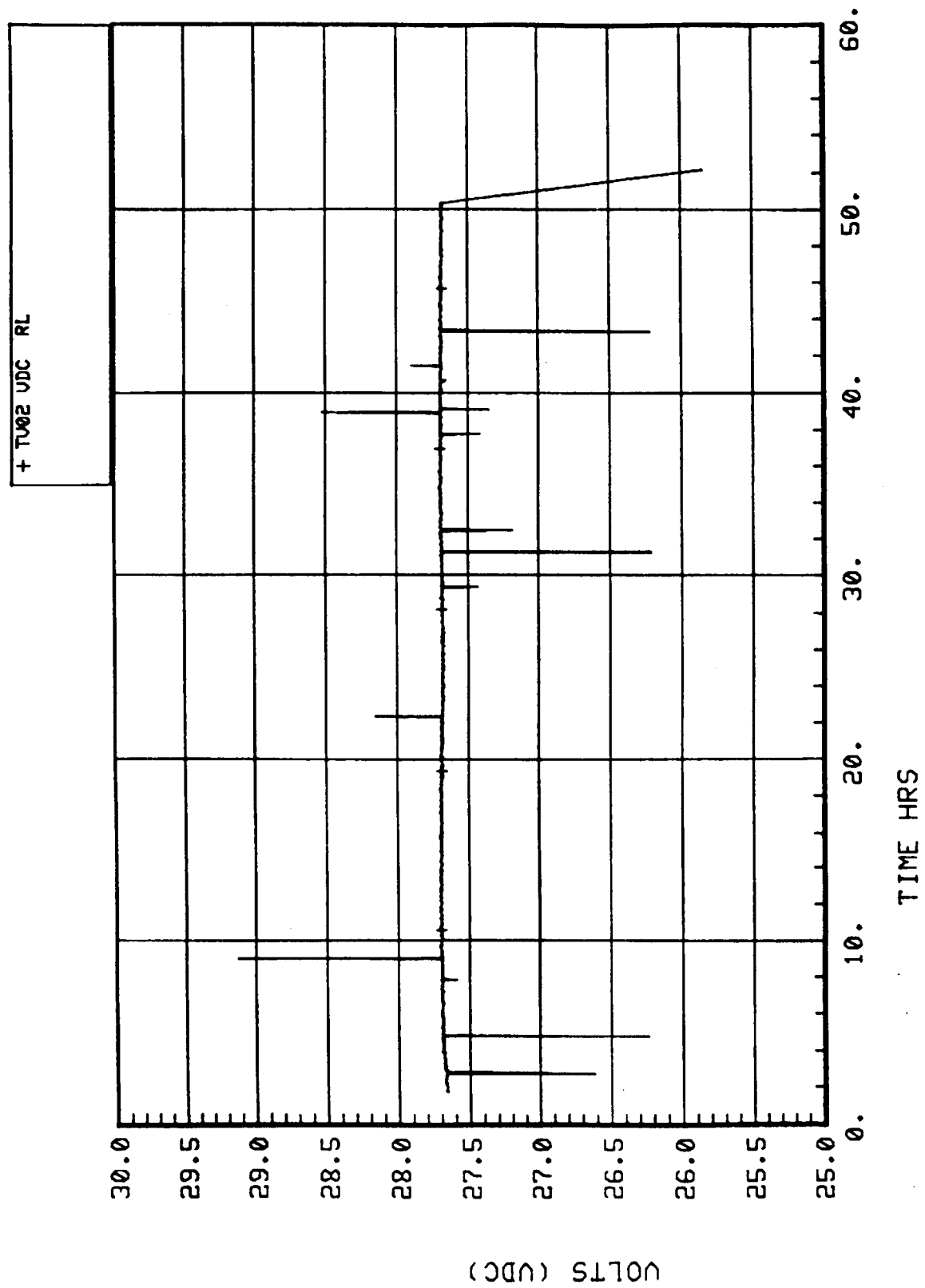


Figure 19. TIMES TER voltage TV02.

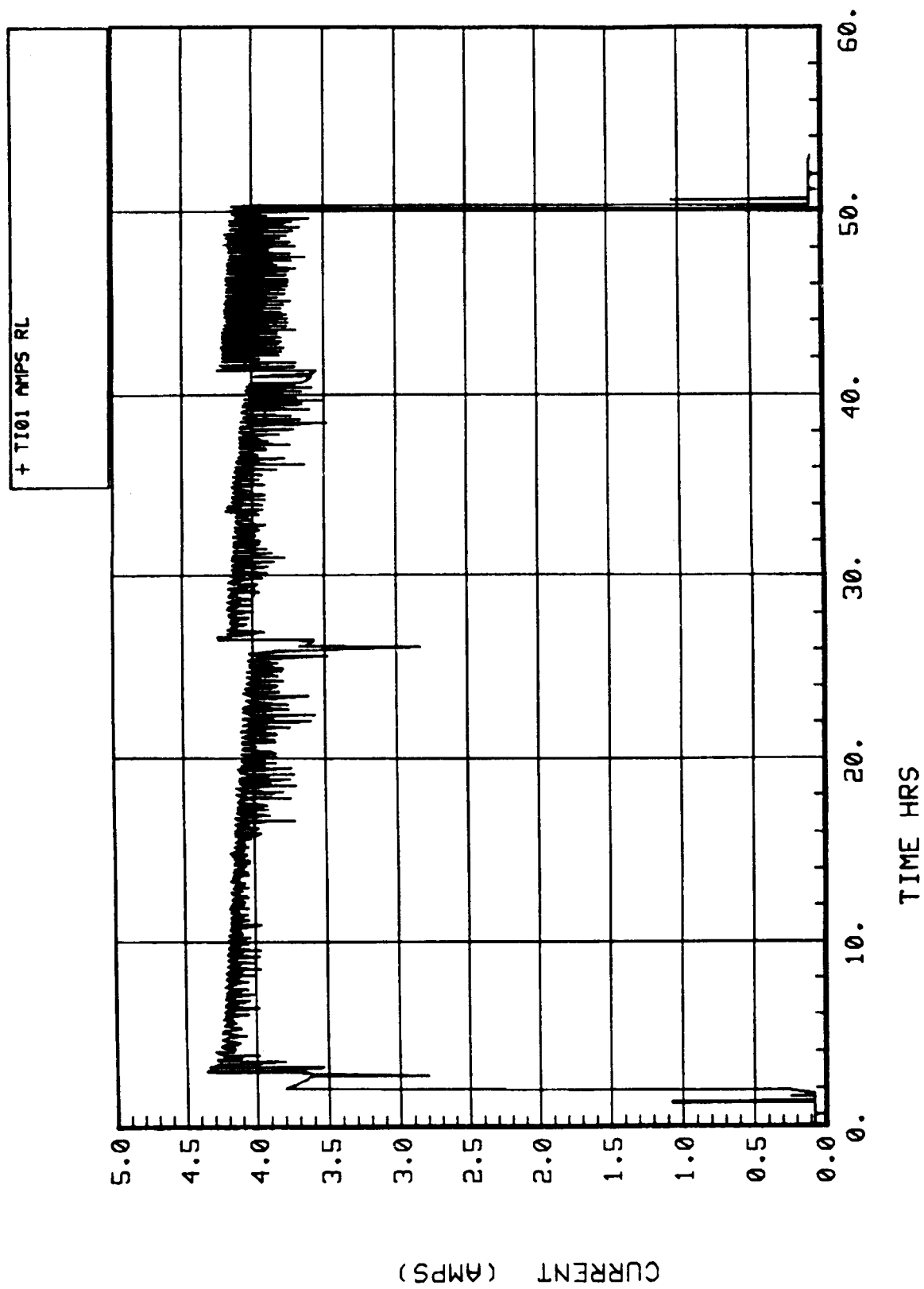


Figure 20. TIMES TER current TI01.

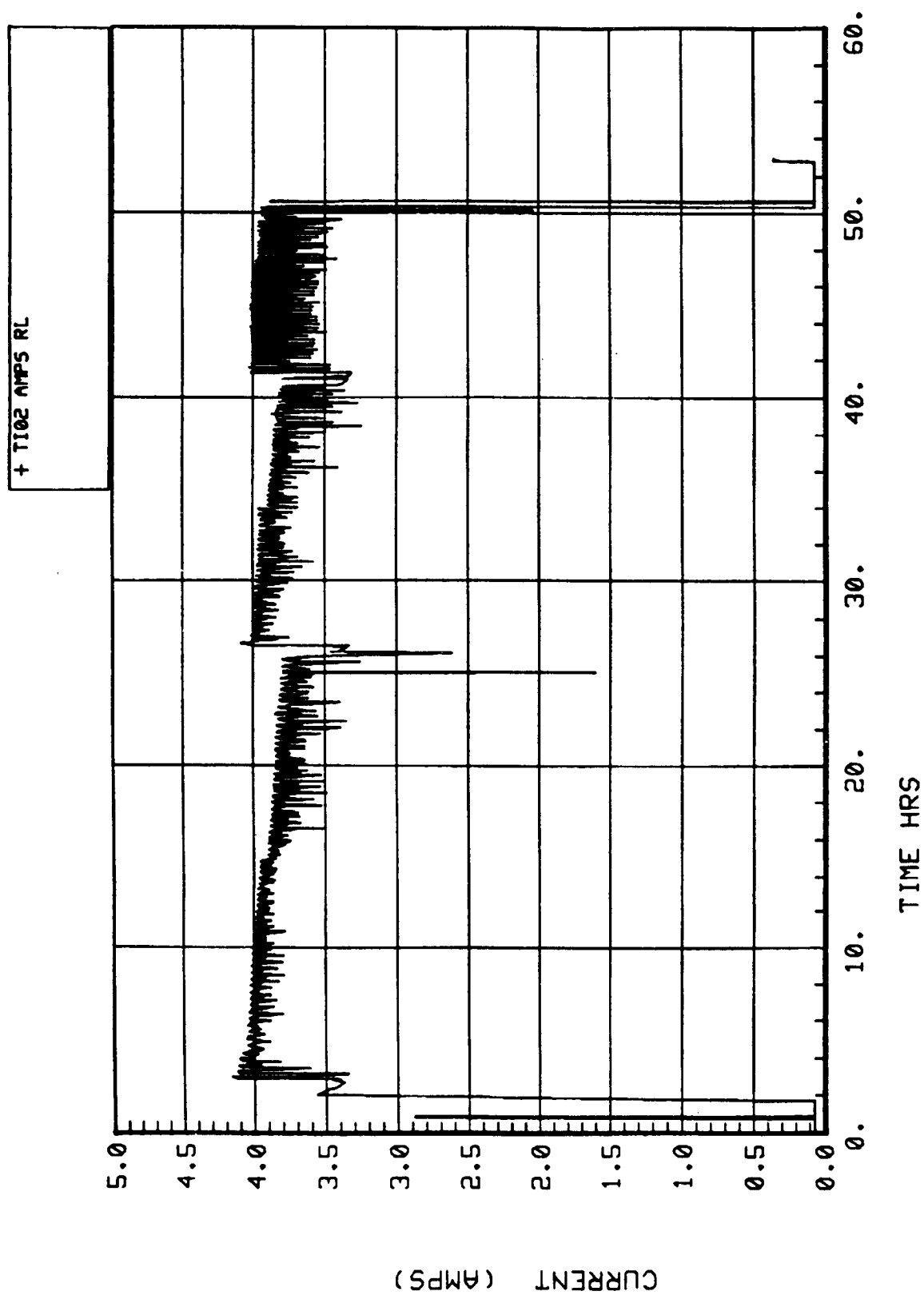


Figure 21. TIMES TER current TIO2.

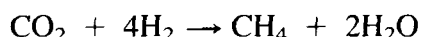
The condensate conductivity sensor (TC02) in the TIMES should be replaced and the brine conductivity sensor (TC01) should be recalibrated. An independent conductivity sensor should be provided by the facility in-line downstream of the post-treatment bed in order to have real-time monitoring of post-treated distillate quality.

## 5.2 Sabatier

### 5.2.1 Subsystem Description

The Sabatier CO<sub>2</sub> reduction subsystem was used in the SIT to catalytically reduce carbon dioxide and hydrogen into methane gas and water. A schematic of the Sabatier subsystem along with associated facility inputs and outputs is shown in Figure 22. Subsystem and facility sensor designations are also noted on the schematics of individual measurements included in this section.

The input carbon dioxide and hydrogen are combined before entering the Sabatier. The CO<sub>2</sub>/H<sub>2</sub> mixture passes first through an activated charcoal filter which removes any contaminants present which could poison the reactor catalyst, and enters the preheated reactor. The reaction



takes place in a packed Ruthenium on Alumina catalyst bed. The reaction, as written, is exothermic and self-sustaining up to a temperature of about 1100°F and is at least 99 percent efficient in converting the lean reactant in a single pass. The reactor heaters are used only at startup to initiate the reaction and automatically shut off when the bed reaches 350°F. Two thermocouples, located in the center and outside radius of the reactor bed, monitor the reaction temperature. After passing through the catalyzed portion of the reactor, the reaction products methane, water vapor, and either excess carbon dioxide or hydrogen flow through two successive air-cooled heat exchange zones in the reactor and exit to the air-cooled condensing heat exchanger. A 25-cfm blower provides the cooling air for the reactor and condensing heat exchanger. The water vapor is condensed from the gas stream and is then separated by a rotary motor-driven water separator. A relief valve in the water outlet line provides back pressure to the water separator to prevent gas from exiting with the water. The product water may be, depending on the configuration of the three-way valve, pressurized out to facility storage or measured by an internal water quantity sensor before exiting to facility storage. The gas exiting the water separator is vented outside of the building. There is a sample port in the gas outlet line for taking grab samples for analysis.

The subsystem is purged with nitrogen gas at subsystem startup and cooldown. A nitrogen accumulator tank inside the Sabatier ensures that enough nitrogen is always present to purge the reactor in case of loss of power or N<sub>2</sub> pressure.

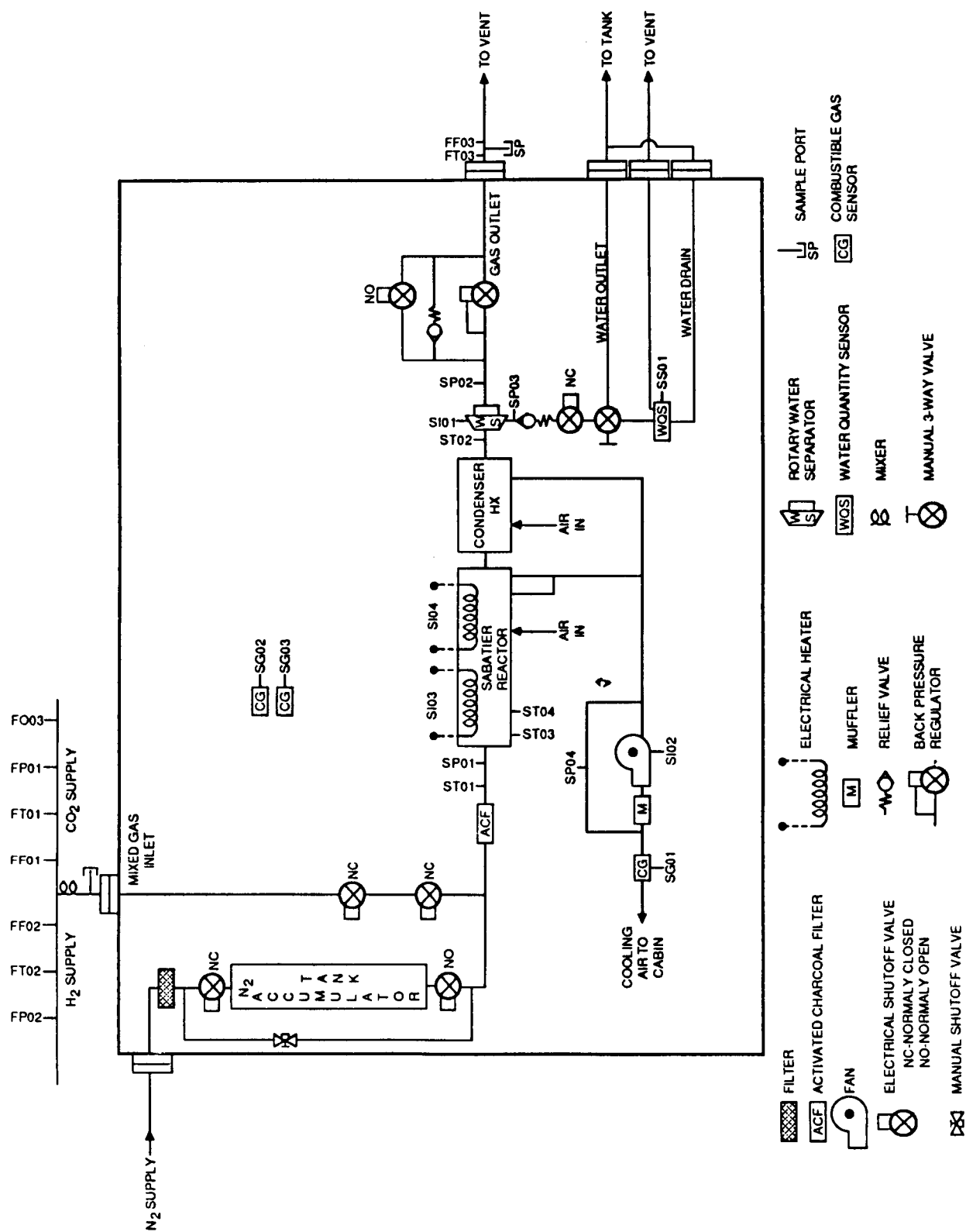


Figure 22. Sabatier subsystem schematic.

## 5.2.2 Discussion of Results

### 5.2.2.1 General

The Sabatier subsystem was run for a total of 48 hr of integrated testing with two subsystem initiated shutdowns. The unit received CO<sub>2</sub> from the Molecular Sieve subsystem at an average rate of 4.4 lb/day and H<sub>2</sub> from the SFES at 2.85 SLPM or 0.74 lb/day. However, analysis of CO<sub>2</sub> samples taken during testing showed that the actual purity of the CO<sub>2</sub> was approximately 82 to 85 percent, with 1.5 percent oxygen included. Therefore, the corrected flow of CO<sub>2</sub> was approximately 3.7 lb/day with about 0.05 lb/day of oxygen. The resulting mixture ratio of moles of hydrogen to moles of carbon dioxide delivered to the Sabatier was 4.3 to 4.4, which is slightly hydrogen rich. Based on the above values, the theoretical production rates of the products methane, water, and any excess hydrogen would have been 1.4 lb/day, 3.2 lb/day, and 0.05 lb/day, respectively, assuming that the oxygen would have reacted with any excess hydrogen to produce water. In addition, nitrogen was found to be in the inlet CO<sub>2</sub> at approximately 9 percent, or 0.25 lb/day. Aside from a small quantity of ammonia discovered in the product water, it is assumed that the nitrogen would have acted as an inert gas and would have passed through the subsystem unreacted. Sample results from the outlet vent gas (see Section 6 for tabulated results) indicated 74.4 percent methane, 15.5 percent hydrogen, 8 percent nitrogen, 1.5 percent oxygen, and 1 percent carbon dioxide. The approximate vent flowrate was 1 SLPM, although problems with condensation in the flowmeter caused the reading to be much higher later in the test. Assuming a 1 SLPM flowrate, the above sample results would translate to mass flowrates of 1.6 lb/day methane, 0.04 lb/day hydrogen, 0.30 lb/day nitrogen, 0.06 lb/day oxygen, and 0.06 lb/day carbon dioxide in the vented gas. These flowrates correspond well with the predicted theoretical values; however, the presence of some carbon dioxide in the outlet gas suggests that the reaction was somewhat less than complete and it appears that the oxygen did not react at all.

Actual product water flowrate from the subsystem was estimated at 2.3 to 2.5 lb/day based on manual scale readings (data transmission was lost from FS04) and total water collected. This value was considerably less than the predicted 3.2 lb/day; however, condensed water was also exiting along with the vent gas as was discovered while taking samples, which could account for some of the difference. In addition, it has since been discovered that the configuration of the facility plumbing from the Sabatier to its water storage tank prevents a uniform flowrate resulting in water remaining in the lines after testing. It is therefore believed that, although near to theoretical water production from the reaction did occur, problems with condensation, separation, and measurement of the water resulted in the low collection rate value. This will be validated in later tests.

### 5.2.2.2 Discussion of Individual Measurements

#### 5.2.2.2.1 Inlet H<sub>2</sub> Flowrate – FF02

The Sabatier inlet hydrogen flow is shown in Figure 23. Flow from the SFES to the Sabatier averaged approximately 2.85 SLPM during the test. The Sabatier experienced an automatic shutdown between 7 and 8 hr into the test due to a loss of communication between the subsystem controller and the DCC. This shutdown is evident in the FF02 plot by a drop in flowrate due to the Sabatier inlet mixed gas valves closing. After restart, operation continued normally to the next

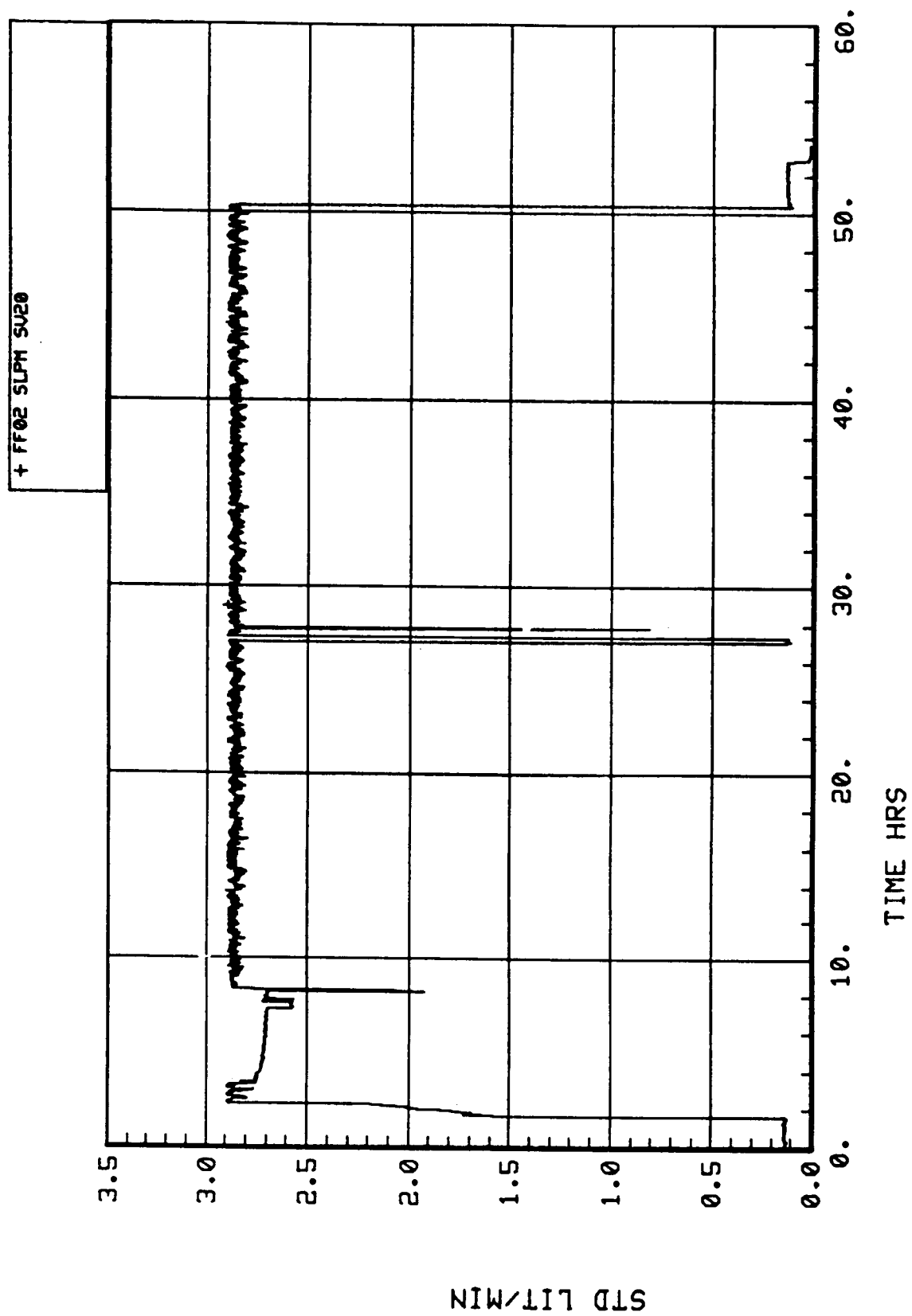


Figure 23. Sabatier inlet H<sub>2</sub> flow FF02.

morning. A sample of the hydrogen was drawn at about 27 hr. To manually sample, hand valve 12 was opened and gas was sampled while flowing to the Sabatier as well. However, the flow split was such that most of the hydrogen went to the sample and little to the Sabatier, causing a cessation of the reaction. The drop in flow to the Sabatier can be seen on the plot at the time of sampling. As a result, water production temporarily ceased and the pressure out of the water separator (SP03) dropped from 40 psia to less than 20 psia. An automatic shutdown which is initiated when the difference between the water outlet pressure and the gas outlet pressure drops below 10 psid (designed to prevent gas from exiting with the water) occurred and can be seen in the FF02 plot by a similar drop in flow when the inlet valves were shut. The Sabatier was restarted, and operation continued normally for the remainder of the test.

#### **5.2.2.2.2 Inlet H<sub>2</sub> Pressure – FP02**

The Sabatier inlet hydrogen pressure is shown in Figure 24. The Sabatier hydrogen supply pressure from the SFES was approximately 1.8 psig throughout the test. The only deviations were due to the three events mentioned in the above discussion: the first Sabatier shutdown, the hydrogen sampling, and the second Sabatier shutdown (due to the hydrogen sampling). A pressure rise on the FP02 plot signifies the first shutdown when the inlet mixed gas valves closed and flow of hydrogen to the Sabatier ceased. A drop in pressure due to the sampling can be seen at 28 hr, followed by another pressure peak when the Sabatier shut down.

#### **5.2.2.2.3 Inlet H<sub>2</sub> Temperature – FT02**

The hydrogen supply temperature (Fig. 25) ranged from 80° to 88°F and fluctuated in a 24-hr cycle as the room temperature varied.

#### **5.2.2.2.4 Inlet CO<sub>2</sub> Flowrate – FF01**

Carbon dioxide flowrate (Fig. 26) to the Sabatier ranged from 4.5 to 5.1 lb/day in cycle with the Molecular Sieve. The two Sabatier shutdowns may be seen on the plot as the flowrate of CO<sub>2</sub> dropped due to the Sabatier inlet mixed gas valves closing.

#### **5.2.2.2.5 Inlet CO<sub>2</sub> Pressure – FP01**

The carbon dioxide supply pressure (Fig. 27) was nominally 1.8 psig and remained steady throughout the test. A peak in pressure could be seen at Sabatier startup as CO<sub>2</sub> built in the line before the Sabatier inlet valves were opened. Two other pressure peaks, corresponding to the two Sabatier shutdowns, are also shown in the data plot.



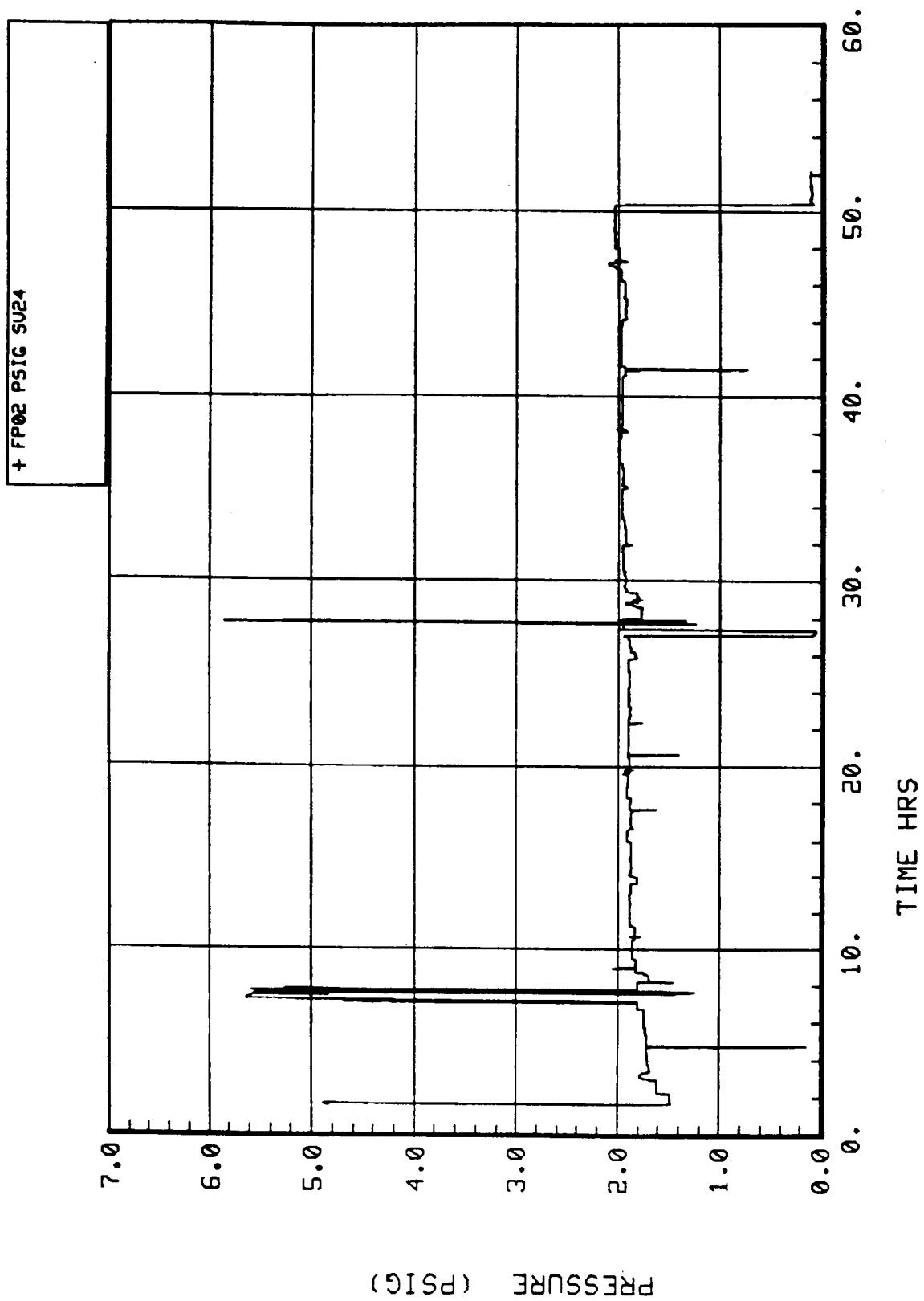


Figure 24. Sabatier inlet H<sub>2</sub> pressure FP02.

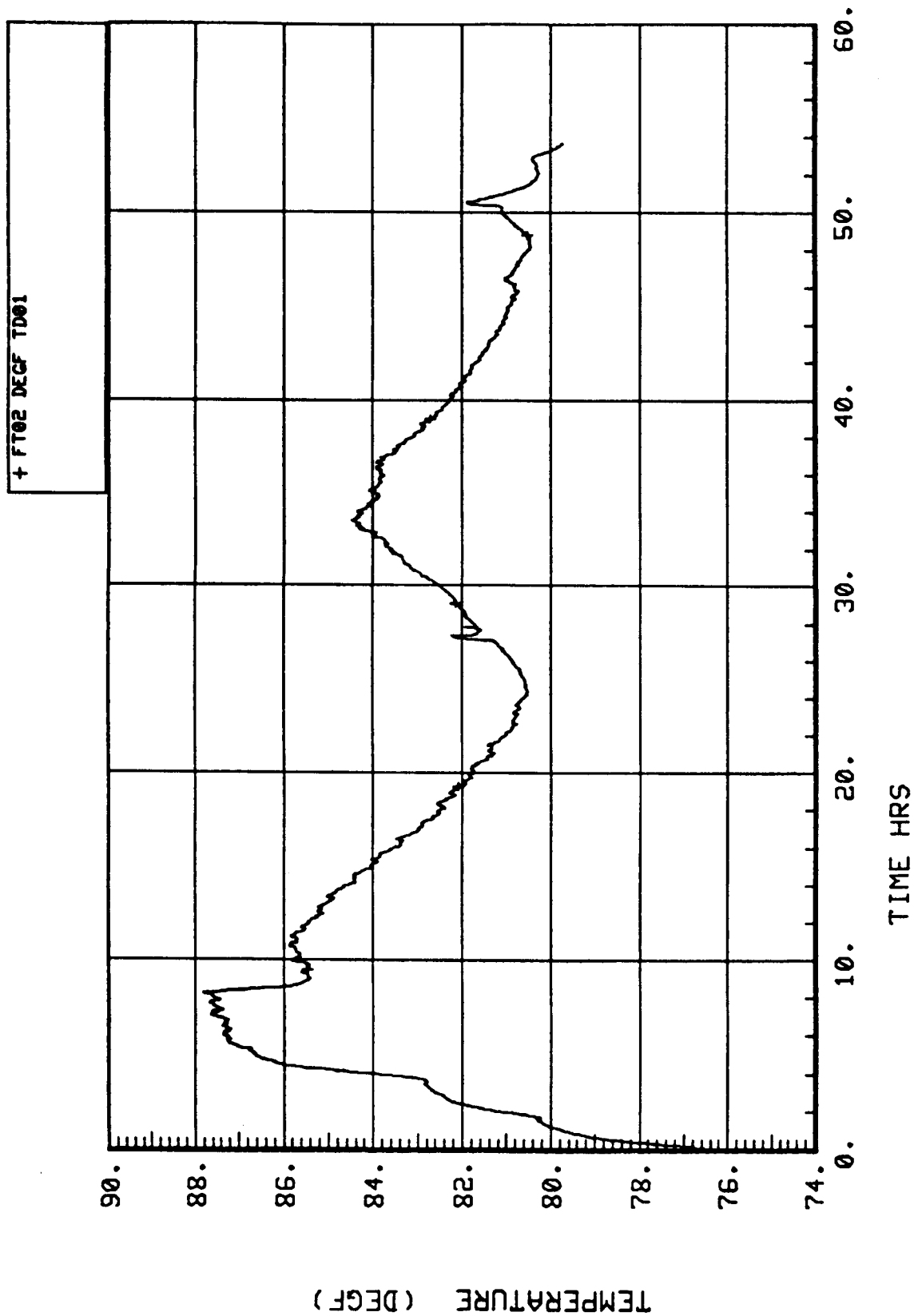


Figure 25. Sabatier inlet H<sub>2</sub> temperature FT02.

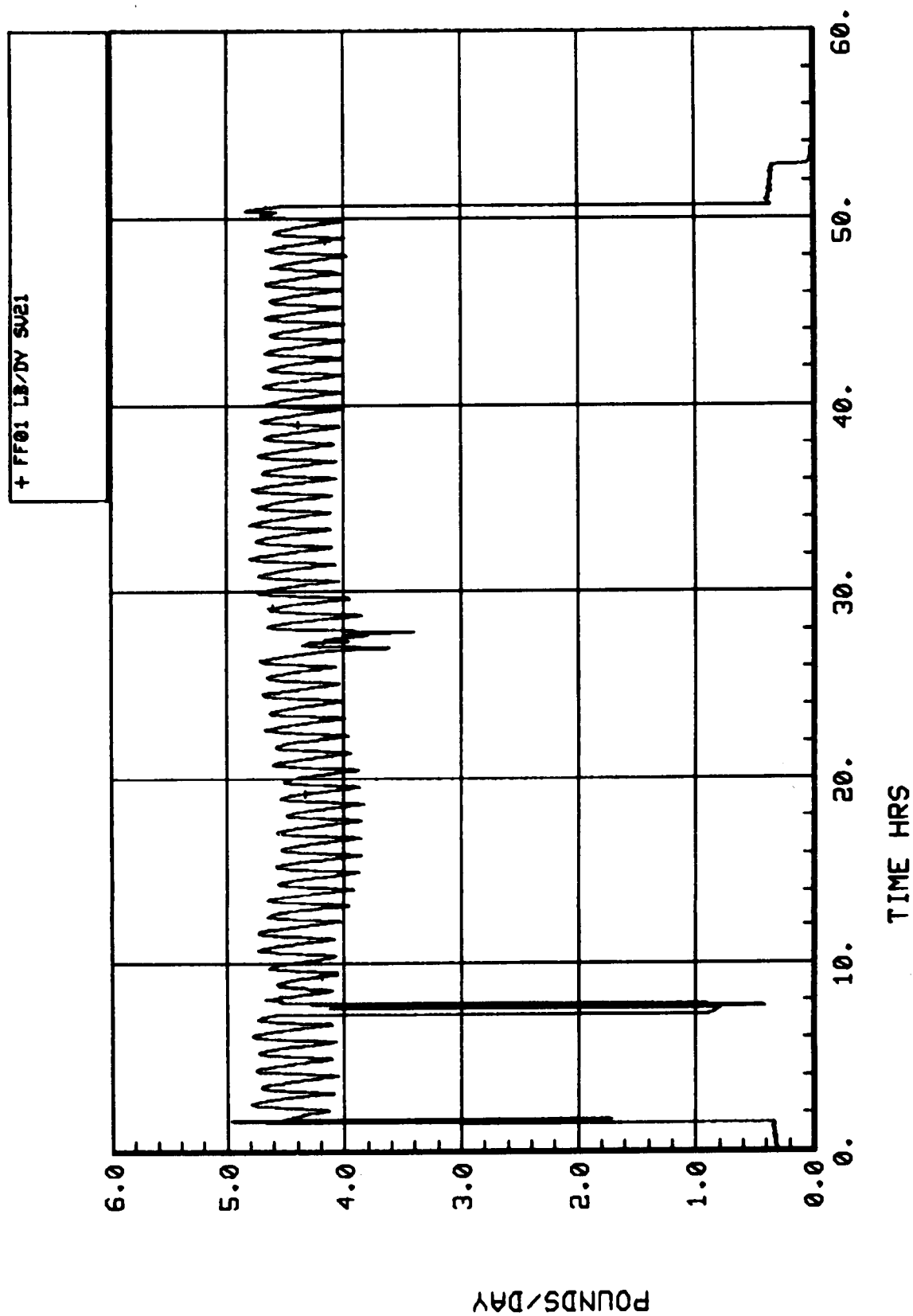


Figure 26. Sabatier inlet CO<sub>2</sub> flow FF01.

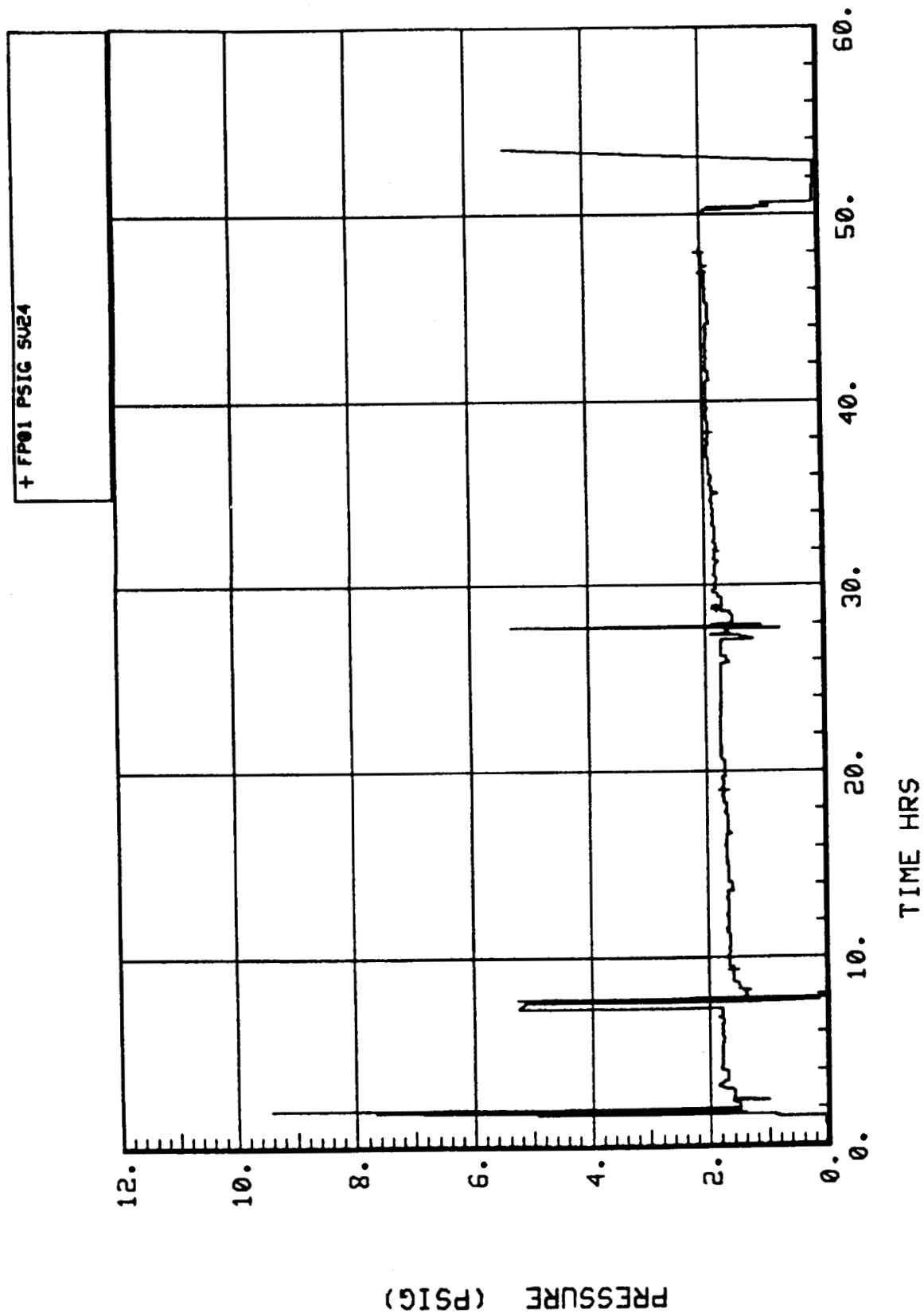


Figure 27. Sabatier inlet CO<sub>2</sub> pressure FP01.

#### **5.2.2.2.6 Inlet CO<sub>2</sub> Temperature – FT01**

The Sabatier inlet carbon dioxide temperature is shown in Figure 28. The CO<sub>2</sub> temperature ranged from 78° to 84°F during the course of the test with about 0.5°F cycles every 55 min due to the Molecular Sieve cycles and overall 24-hr temperature cycles due to room temperature effects. The temperature sensor seems to have been affected somewhat by the two Sabatier shutdowns. The corresponding drops in temperature may have been in part due to changes in flow during those times.

#### **5.2.2.2.7 CO<sub>2</sub> Oxygen Content – FO03**

The oxygen content of the Sabatier carbon dioxide inlet stream is shown in Figure 29. The oxygen sensor, the CO<sub>2</sub> line to the Sabatier, is necessary for safety purposes to prevent a possible explosive mixture of hydrogen and oxygen in the reactor. An alarm is sounded if the oxygen content reaches 3 percent or higher. The sensor readings during the test ranged from 1 percent to a little over 2 percent oxygen and cycled about 0.5 percent with the Molecular Sieve. Slight Drops in readings at the two Sabatier shutdowns were probably due mostly to flow changes.

#### **5.2.2.2.8 Reactor Inlet Temperature – ST01**

The temperature at the inlet to the Sabatier reactor (Fig. 30) ranged nominally from 85° to 89°F during the test. Cycles may be seen due to the cyclic CO<sub>2</sub> temperature and room temperature during the day. During the two Sabatier shutdowns, the temperature dropped about 4°F as an automatic nitrogen purge of the reactor occurred.

#### **5.2.2.2.9 Reactor Inlet Pressure – SP01**

The Sabatier reactor inlet pressure is shown in Figure 31. The nominal pressure at the inlet to the Sabatier reactor was slightly over ambient at 15.3 to 15.7 psia. Peaks to 28.0 psia during the two shutdowns were due to the higher pressure nitrogen purges.

#### **5.2.2.2.10 Reactor Bed Temperature 1 – ST03**

Thermocouple ST03 (shown in Fig. 32) is located at the center of the reactor bed and measures the reaction temperature, which ranged nominally from 800° to 875°F – typical values for the Sabatier. Molecular Sieve temperature cycle affects can be seen, as well as significant cooldowns (600°F) during the two Sabatier shutdown purges.

#### **5.2.2.2.11 Reactor Bed Temperature 2 – ST04**

Like ST03, thermocouple ST04 (Fig. 33) measures reactor temperature, but is located at the outside radius of the reactor bed, rather than in the center. It recorded the same cycles and drops in temperature, but was significantly lower in absolute temperature (550° to 650°F).

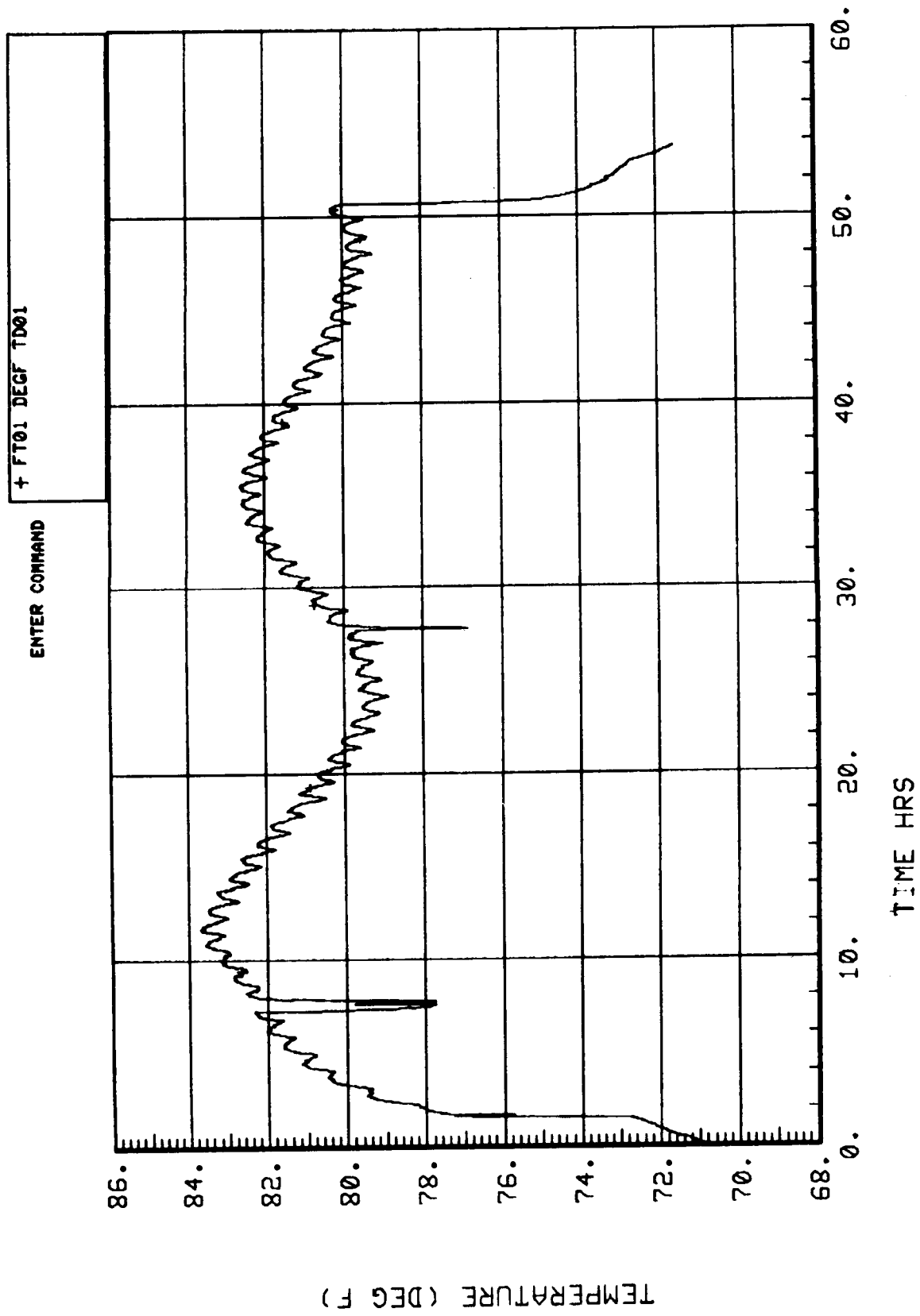


Figure 28. Sabatier inlet CO<sub>2</sub> temperature FT01.

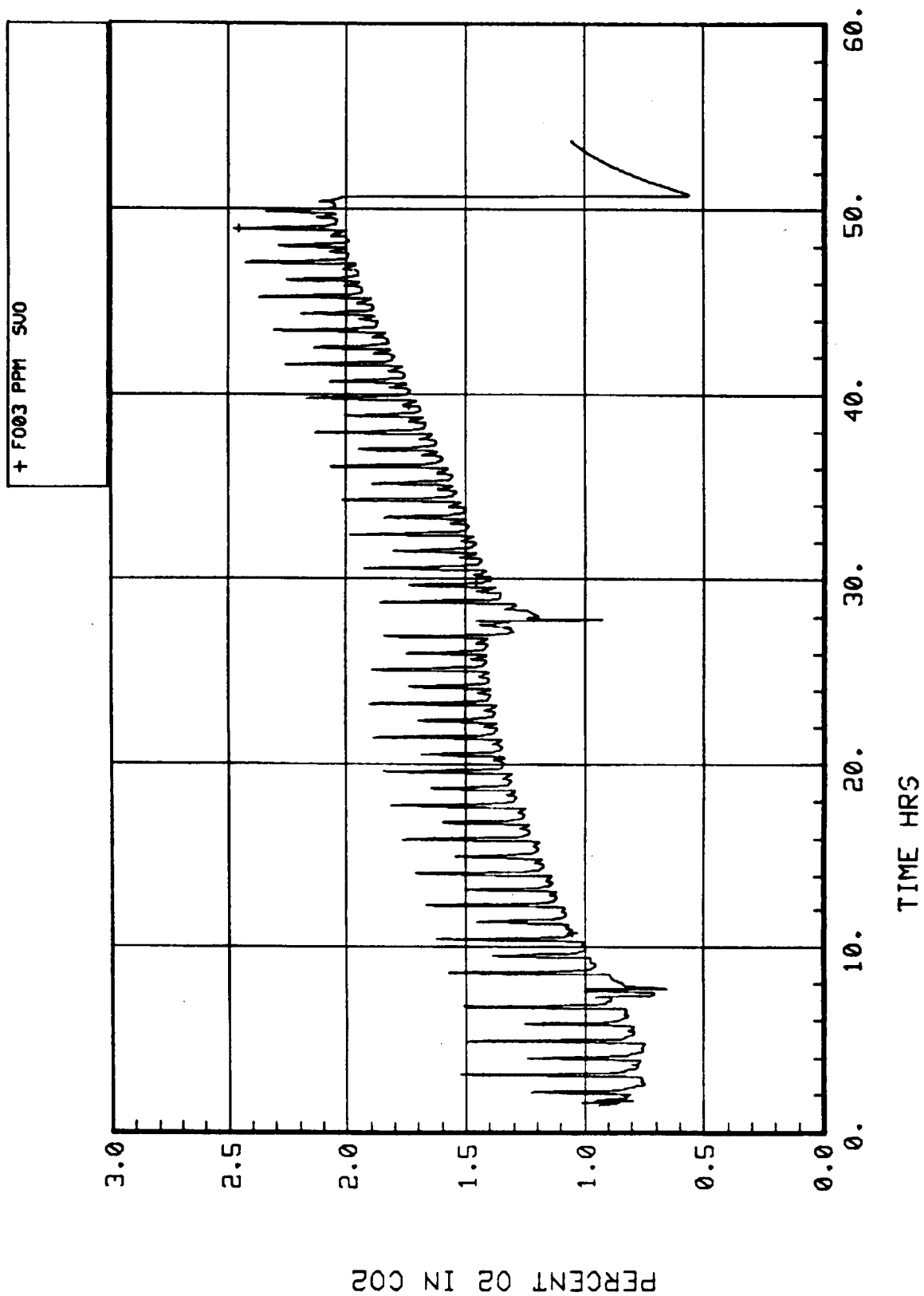


Figure 29. Sabatier inlet CO<sub>2</sub> oxygen content FO03.

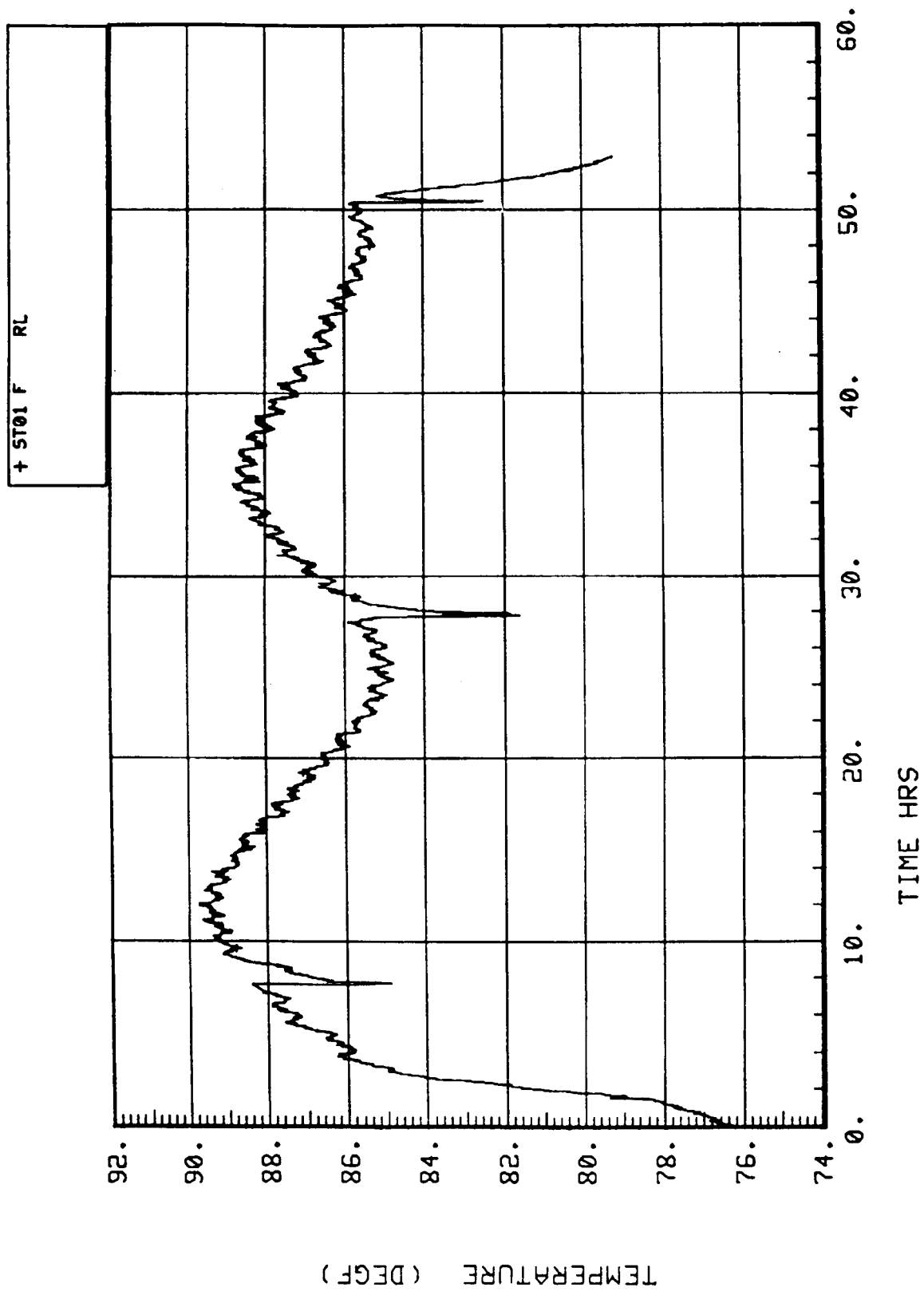


Figure 30. Sabatier reactor inlet temperature ST01.



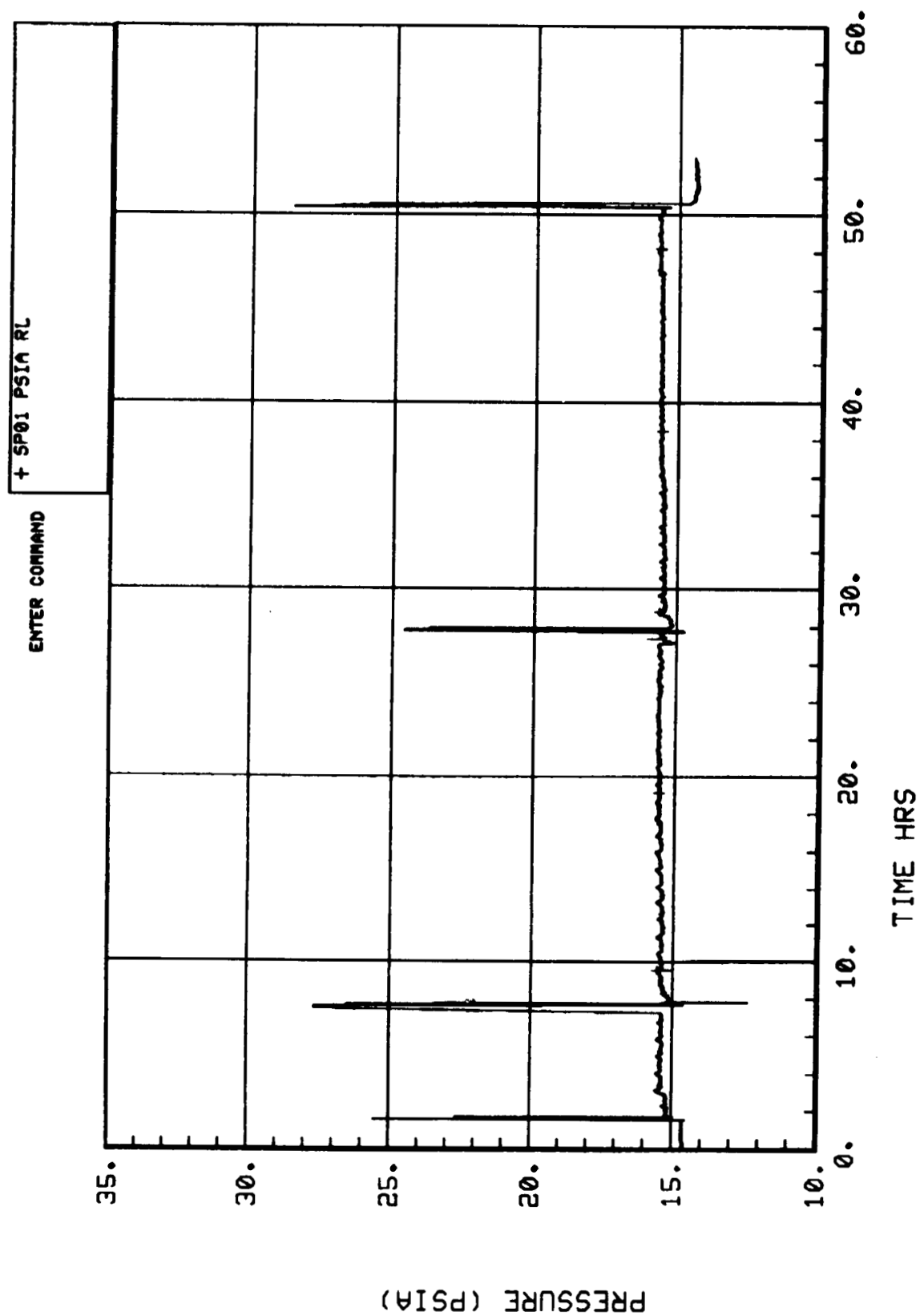


Figure 31. Sabatier reactor inlet pressure SP01.

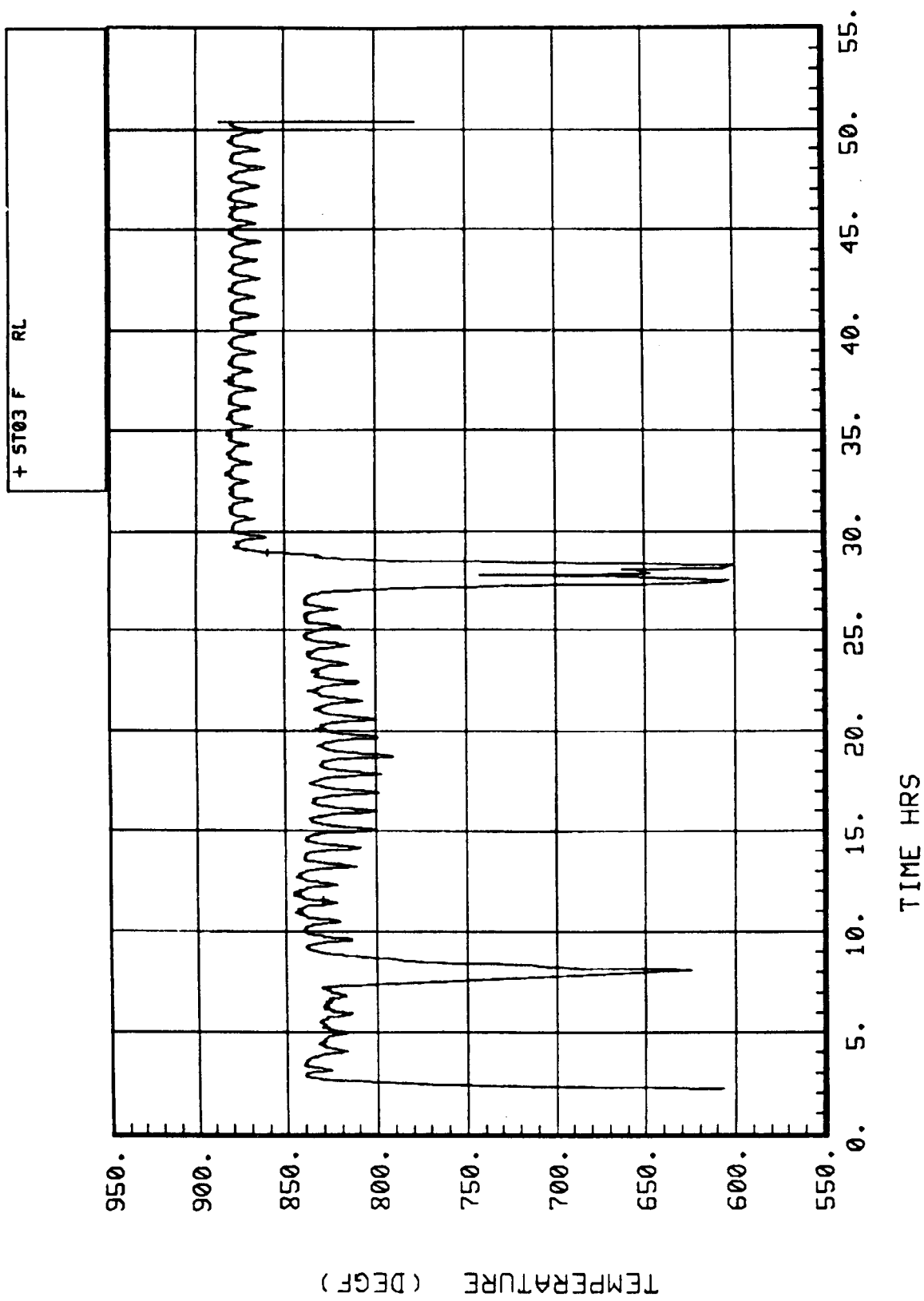


Figure 32. Sabatier reactor bed temperature 1 ST03.

#### **5.2.2.2.12 Condenser Exit Temperature – ST02**

The temperature of the gas/water stream exiting the condensing heat exchanger (Fig. 34) ranged from 91° to 96°F. A 24-hr cycle in the temperature may be seen as the condenser was cooled with ambient air from the simulator environment. Two slight drops in temperature are evident and correspond with the two Sabatier shutdowns.

#### **5.2.2.2.13 Water Outlet Pressure – SP03**

The water outlet pressure is shown in Figure 35. After startup, the water produced in the Sabatier reaction must accumulate in the water separator and pressure must build for some time before it will begin to be output. The relief valve in the water outlet line opens at an approximate pressure of 40 psia to allow water flow out of the subsystem, and will cycle open and closed during steady-state operation. On the SP03 plot, the first output of water may be seen at about three hours and continues until the first Sabatier shutdown. After restart, water production quickly recovered and continued until the next morning when sampling of the hydrogen caused the pressure to drop in the water line and initiated a shutdown of the subsystem. The remainder of the test was nominal with a steady water outlet pressure.

#### **5.2.2.2.14 Gas Outlet Pressure – SP02**

The average Sabatier gas outlet pressure (Fig. 36) was slightly over ambient at 14.8 to 15.0 psia. Peaks to 18 psia occurred at subsystem startup and during the two automatic shutdowns due to the higher pressure nitrogen purge.

#### **5.2.2.2.15 Outlet Vent Flowrate – FF03**

The flowmeter which measures the product gas outlet rate (Fig. 37) was found to be susceptible to water condensation which collected in it during the test. It started at a nominal reading of about 1 SLPM, but gradually drifted upward throughout the test to 8 SLPM. When the Sabatier shut down around 28 hr, the automatic nitrogen purge of the subsystem served to blow out the water which had accumulated in the flowmeter and, shortly afterwards, the sensor reading returned to normal. Eventually, it began drifting up again and returned to the 8 SLPM level. A parallel check measurement of vent flow was made using an analog flowmeter and was found to read 1 SLPM, which proved that FF03 was in error. A water trap has since been installed upstream of FF03 to prevent moisture from reaching the sensor.

#### **5.2.2.2.16 Outlet Vent Temperature – FT03**

The temperature of the outlet gas (Fig. 38) ranged from 79° to 86°F nominally during the test with some cooling during the subsystem startup purge and two shutdown purges.

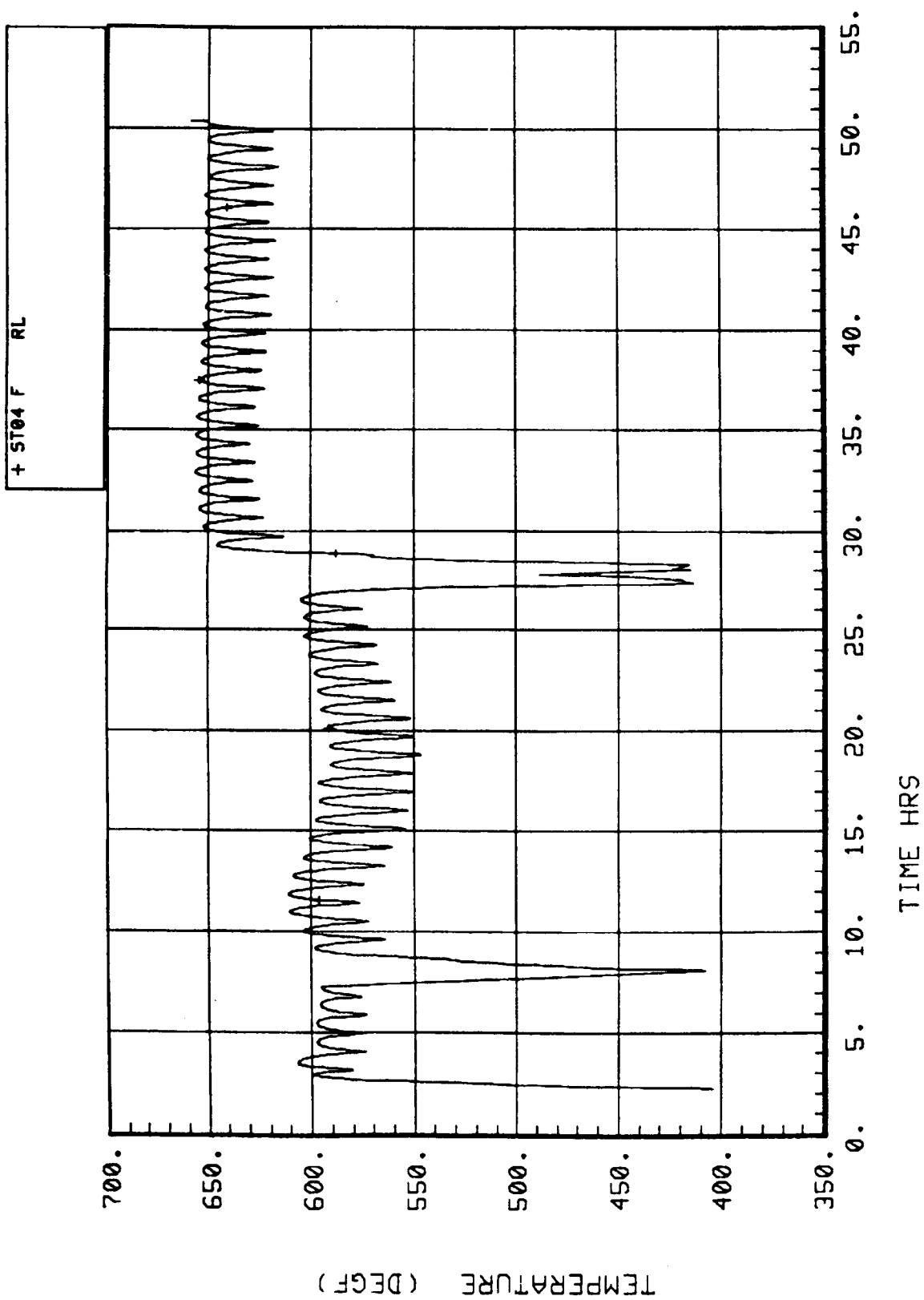


Figure 33. Sabatier reactor bed temperature 2 ST04.

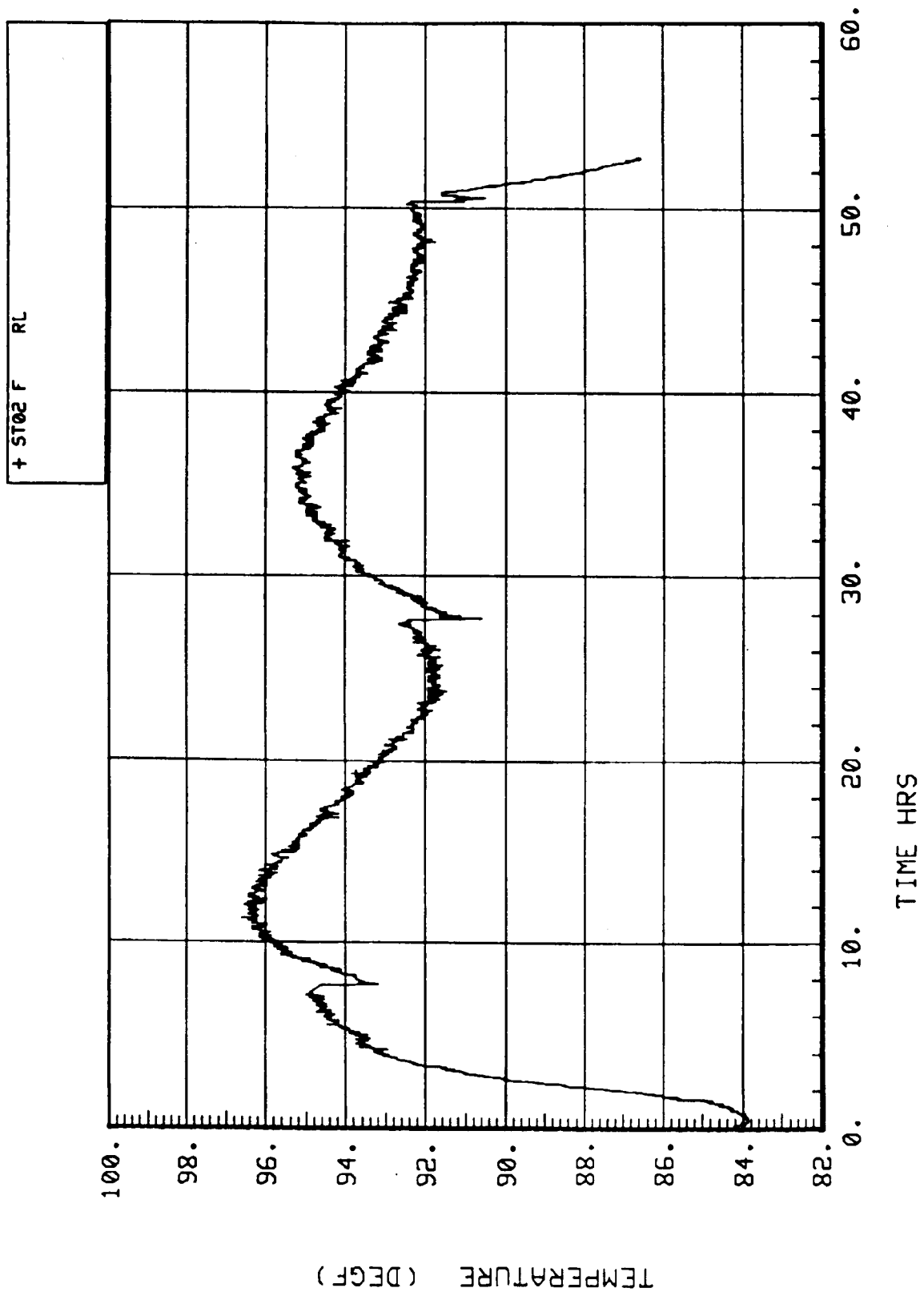


Figure 34. Sabatier condenser exit temperature ST02.

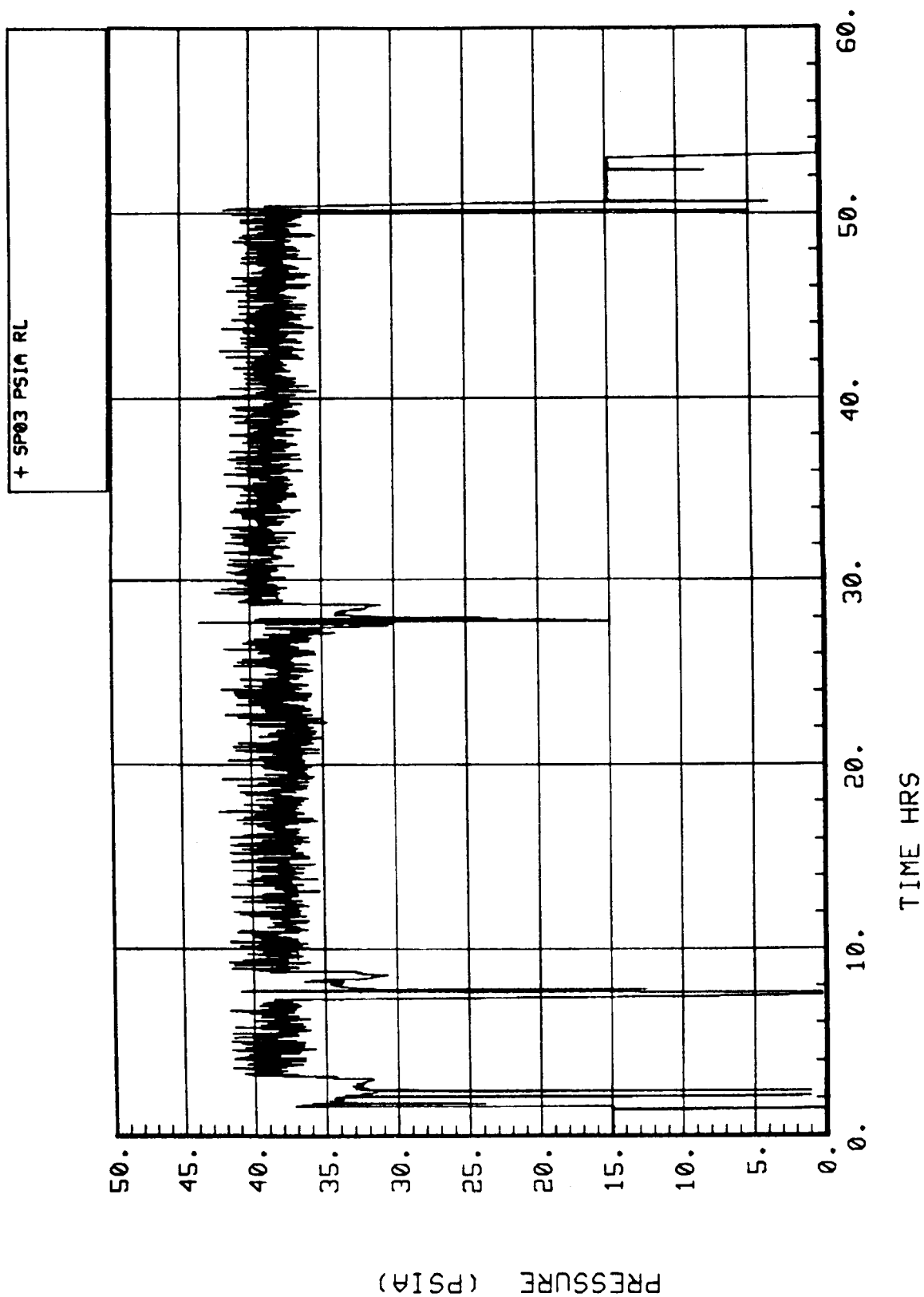


Figure 35. Sabatier water outlet pressure SP03.

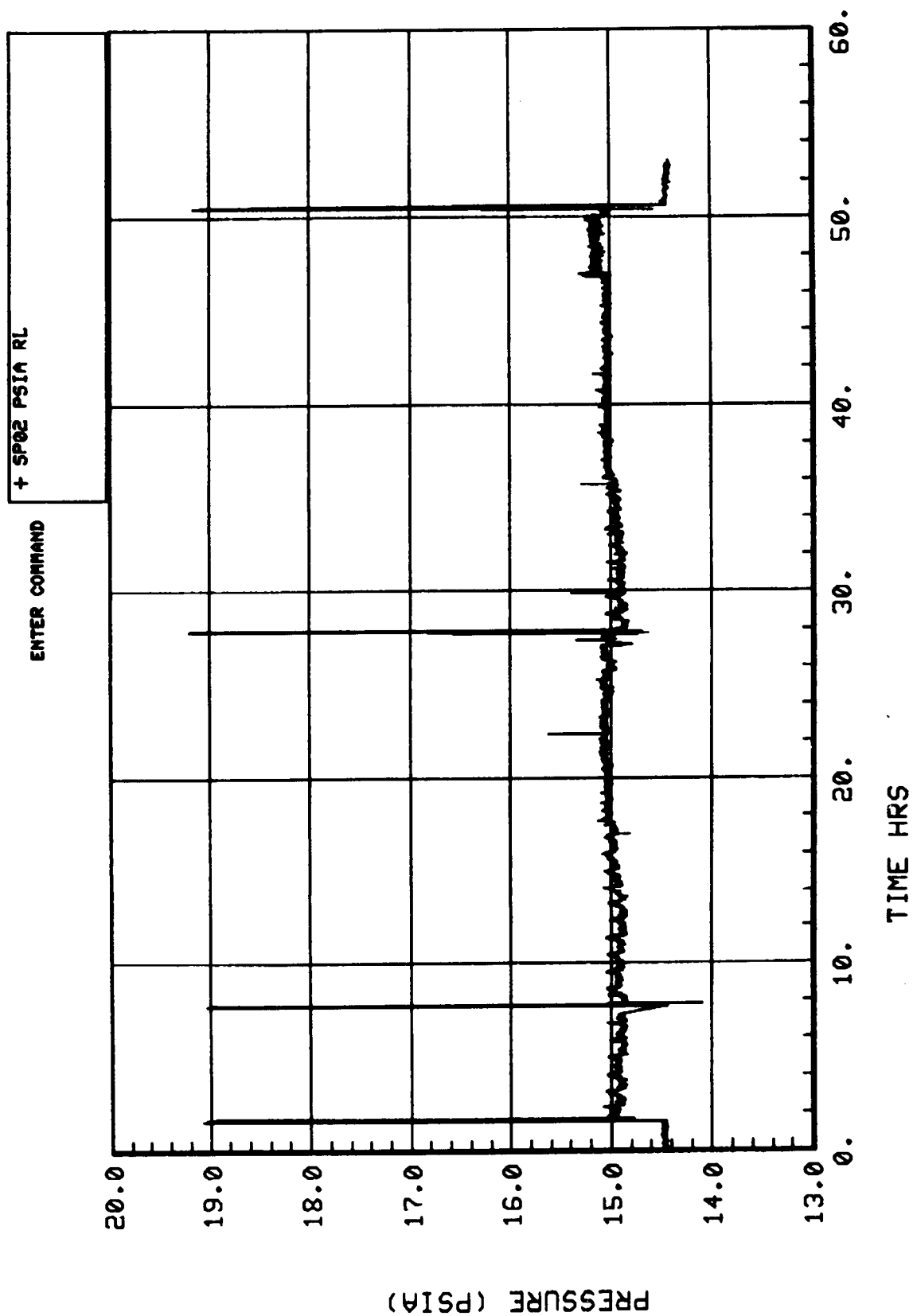


Figure 36. Sabatier gas outlet pressure SP02.

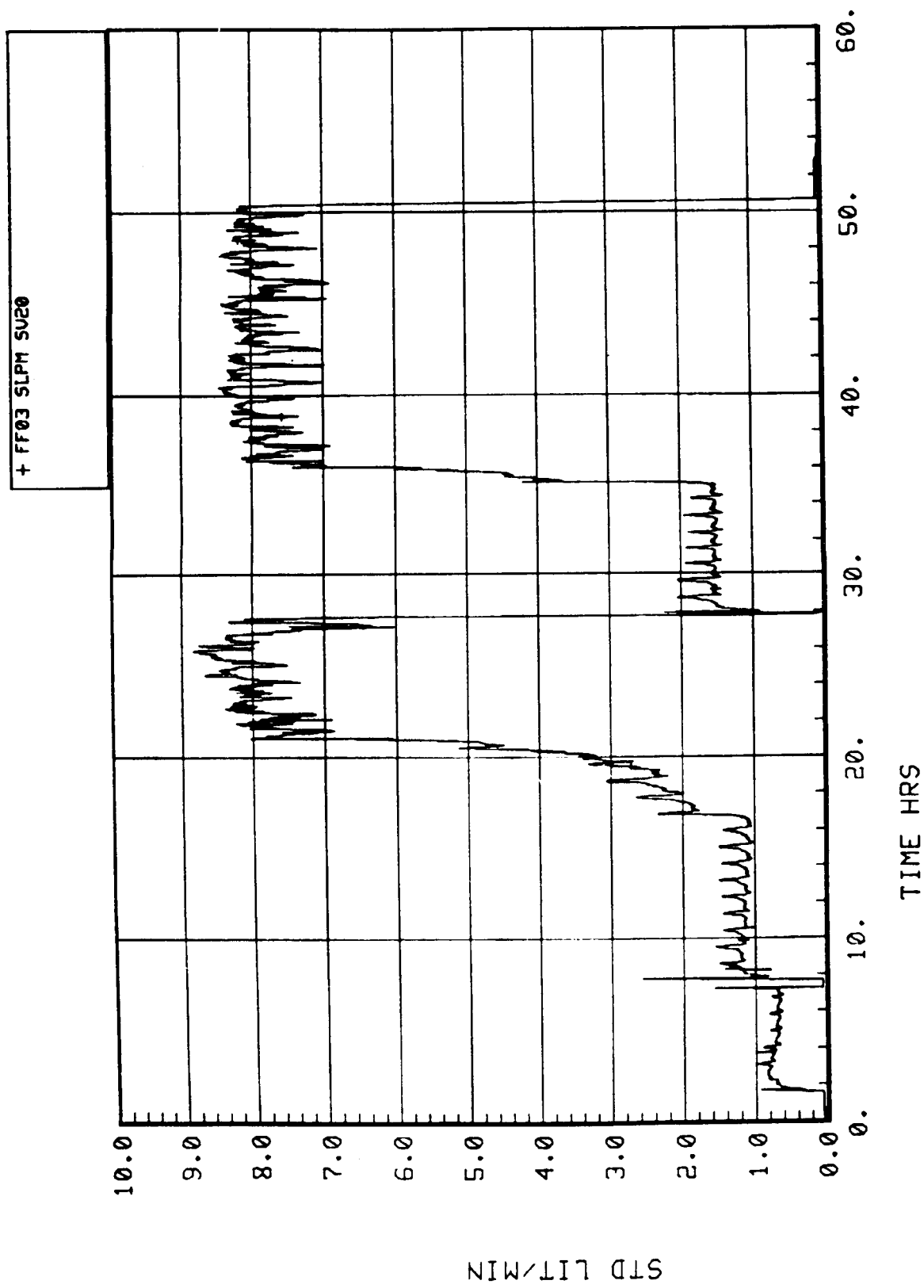


Figure 37. Sabatier outlet vent flowrate FF03.



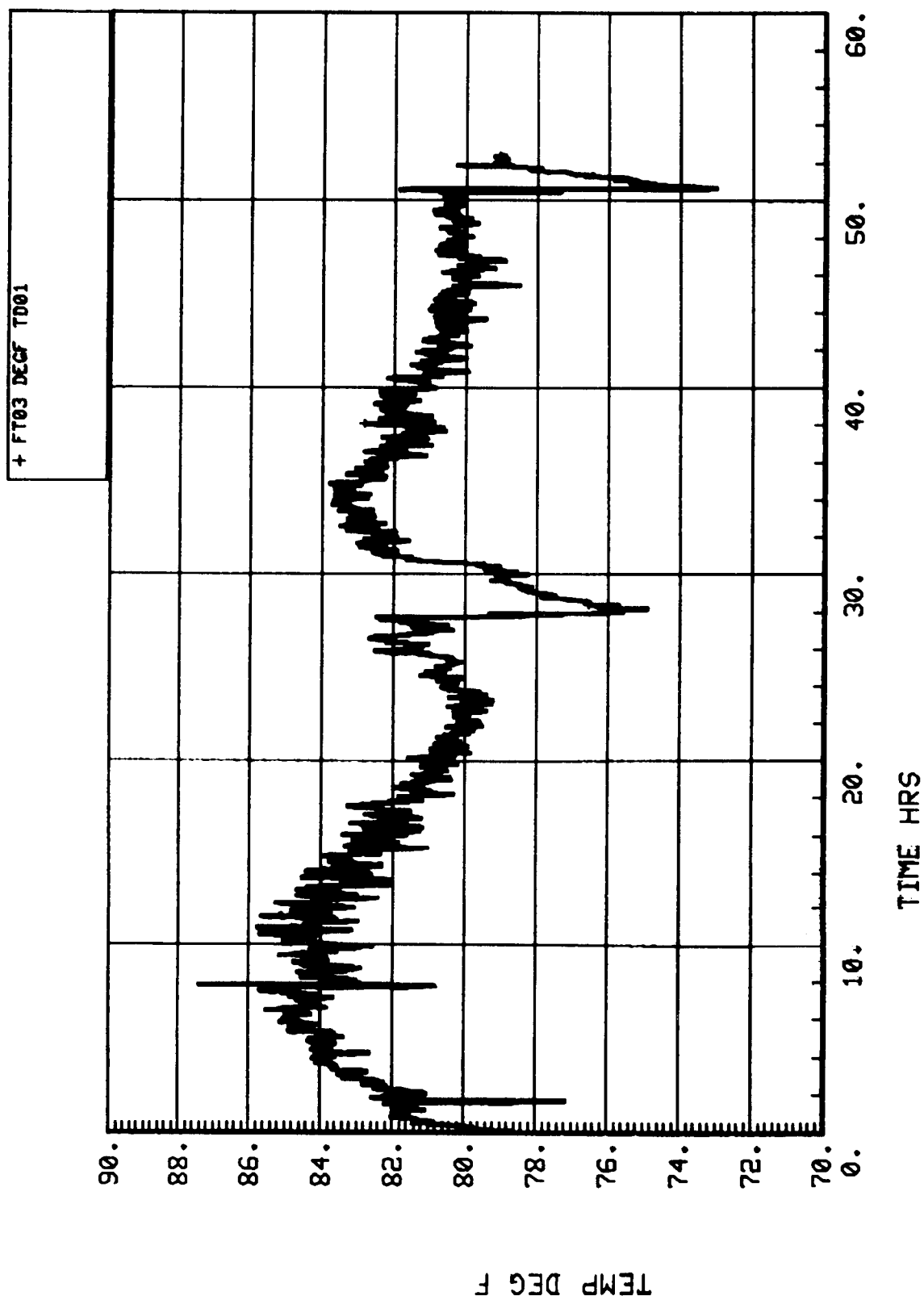


Figure 38. Sabatier outlet vent temperature FT03.

#### 5.2.2.2.17 Product Water Scale – FS04

Communication was lost from scale reading FS04 and the resulting plot is meaningless. Readings were taken of the scale LED readout and recorded to try to estimate a water production rate. Results of these readings have been discussed in the summary of results section.

### 5.2.3 Recommendations/Lessons Learned

Since the SIT, a water trap has been installed upstream of FF03 in the Sabatier outlet vent line. This trap serves to collect the condensed water which exits along with the gas and prevents it from disturbing the flow sensor. Testing has been accomplished with the new configuration resulting in nominal readings from FF03 throughout operation.

The tubing which carries the Sabatier product water from the subsystem to facility storage has been rerouted so that a gradual downward slope to the product water tank is achieved. The prior configuration of the plumbing contained a small upward section which caused the water to collect in the lines before being forced out, resulting in a variable water production rate. It is believed that the new plumbing configuration will help achieve a steadier flow of product water.

To prevent any gas sampling from depleting the supply so much that it causes a Sabatier shutdown, metering valves have been placed in the sample lines of the Molecular Sieve CO<sub>2</sub>, SFES H<sub>2</sub>, and Sabatier inlet mixed gas. The metering valves have been set so that sampling will occur much more slowly. It has also been decided that for future testing all sampling will be done after completion of the required test time so that perturbations caused by sampling will not occur in the data in the middle of the test and longer steady-state run times may be seen.

## 5.3 Static Feed Electrolysis

### 5.3.1 Subsystem Description

The SFE subsystem was used to generate oxygen at a three-man metabolic rate and hydrogen for use by the Sabatier subsystem. A schematic of the SFE is shown in Figure 39. The SFE consists of five major components (1) the electrolysis module, (2) the Fluids Control Assembly (FCA), (3) the Pressure Control Assembly (PCA), (4) the Coolant Control Assembly (CCA), and (5) the feed water tank.

The electrolysis of water to oxygen and hydrogen takes place in the electrolysis module which consists of 12 cells stacked together between two insulation plates and two end plates. Each cell contains a water compartment, an oxygen compartment, and a hydrogen compartment. The water and hydrogen compartments are separated by a water feed membrane, while the two gas compartments are separated by the electrolyte matrix/electrode assembly. The electrolyte is aqueous potassium hydroxide (KOH).

The reactions which occur in the cells are:



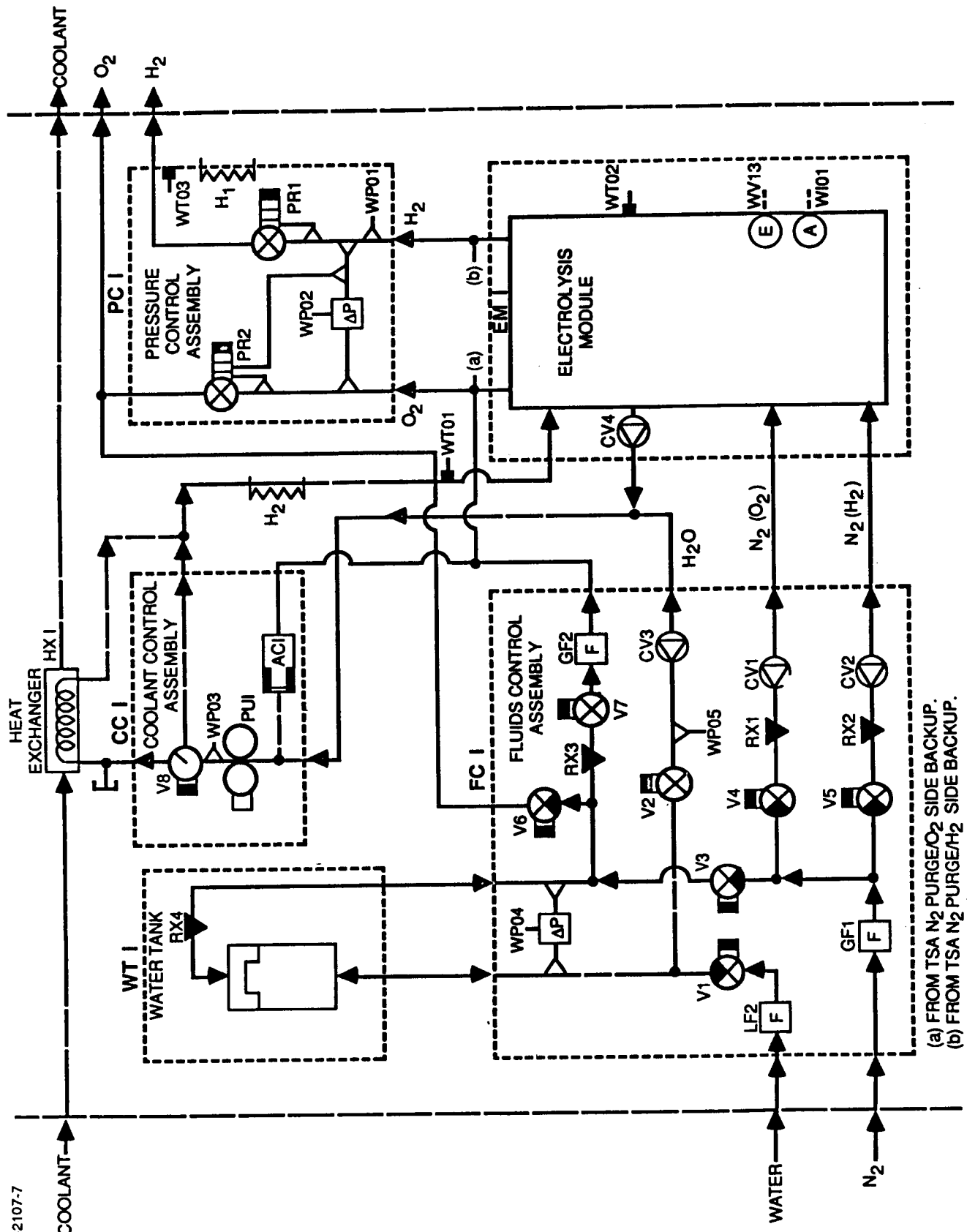
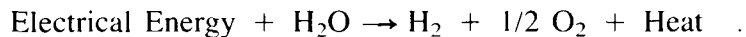


Figure 39. SFE subsystem schematic.

The resulting overall reaction is:



Before power is applied to the module, the water feed cavity and the electrolyte matrix contain equal concentrations of KOH electrolyte. As power is applied to the electrodes, water is electrolyzed from the electrolyte matrix resulting in a KOH concentration increase and a water vapor pressure decrease in the matrix. As the water pressure in the electrolyte matrix drops below that in the water feed cavity, water diffuses from the water feed cavity through the hydrogen cavity into the electrolyte matrix in an attempt to reestablish the initial equilibrium. As water diffuses from the water feed cavity it is statically replenished from the feed water tank. The processes of electrolysis, diffusion, and the static replenishment of feed water occur continually as long as power is applied to the cell electrodes.

The electrolysis module is equipped with the voltage, current, and temperature sensors required to monitor its performance.

The FCA consists of seven valves which are mounted on two motor-driven cams. The cams are driven to the required positions to open and close the valves to control the purge gas and feed water flows and water tank fills.

During normal mode operations, valves V2 and V7 (Fig. 39) are open. V2 permits the flow of water from the feed water tank, WT1, while V7 allows the air side of the tank to be pressurized with product oxygen.

The water tank is refilled every 3 hr. During the tank fill sequence, V2 and V7 are closed. V6 opens briefly to vent the air side of the tank to ambient pressure and V1 opens to refill the tank from an external water supply. When V6 and V1 close, V3 opens and facility nitrogen flows in to repressurize the tank. Upon completion of the fill sequence, V3 closes and V2 and V7 reopen. The time required for a tank fill is approximately 2 min.

A nitrogen purge is included in the startup and shutdown sequences. During the purge, V4 and V5 open to allow nitrogen flow through the subsystem oxygen and hydrogen passages.

The FCA is instrumented with valve position indicators and pressure sensors necessary for monitoring its operation.

The PCA consists of two motor driven regulators, an absolute pressure sensor, and a differential pressure sensor. Regulator PR1 controls the hydrogen production pressure, while PR2 controls the oxygen to hydrogen differential pressure. PR1 and PR2 also control the pressurization and depressurization of the SFE during startups and shutdowns.

The PCA is equipped with feedback valve position indicators which, with the pressure and differential pressure sensors, provide for monitoring of its operation.

The CCA consists of a motor, a pump, an accumulator, and a motor-operated diverter valve. The diverter valve controls the ratio of flow through the heat exchanger HX1 to flow through the bypass in order to control the temperature of the feed water. The accumulator AC1 accommodates thermal expansion and contraction of the feed water.

The CCA is instrumented with pressure and temperature sensors and the valve position indicator required to monitor its performance.

The Feed Water Tank (WT1) is a metal bellows tank which supplies static water replenishment to the electrolysis module. The tank is refilled every 3 hr as previously explained. The sensors which provide for monitoring of the tank are included in the FCA.

The startup, shutdown, and other mode transition sequences are software controlled. Any out of range sensor reading will cause an automatic shutdown of the subsystem.

### **5.3.2 Discussion of Results**

#### **5.3.2.1 General**

The SFE was powered up and the transition from shutdown mode to normal mode was begun at 1:10 hr. The mode transition was proceeding nominally when 2:44 hr into the test the communication link between the SFE controller and the performance diagnostic unit was lost. Facility instrumentation indicated that the SFE was functioning and that it reached normal mode at 1:48 hr into the test. At 4:00 hr a transition from normal mode to shutdown was initiated. The SFE was shut down to allow for trouble shooting and repair of the communication link. The repair was complete and the subsystem was restarted at 7:26 hr. Normal mode conditions were achieved at 8:08 hr, and the SFE continued to operate in the normal mode without further anomalies for the remainder of the test. Throughout the test, post-treated product water from the TIMES was input to the SFE water supply tank.

The hydrogen sensor in the SFE oxygen outlet line, FH07, was not operational during the integrated test due to the difficulty in obtaining an appropriate calibration mixture. To assure safe operation of the subsystem, a facility combustible gas sensor, FG01, was connected to the oxygen outlet. Since FG01 was calibrated at its alarm level of 25000 ppm, it is not extremely accurate at low concentrations of combustible gases such as might occur in the SFE oxygen outlet. The FG01 output indicates that the hydrogen concentration in the product oxygen was well below the alarm level. However, the measurement readings cannot be used to quantify hydrogen in the product oxygen. The oxygen sensor in the hydrogen outlet line shows that the oxygen concentration in the product hydrogen was less than 150 ppm during normal mode operations.

The data link from the SFE controller to the performance diagnostic unit and the SCATS was not operational from 2:44 hr to 7:26 hr. Therefore, the plots of SFE subsystem measurements (measurement numbers beginning with "W") do not represent actual subsystem conditions during that time although facility measurements (measurement numbers beginning with "F") continued to record data during this interval.

#### **5.3.2.2 Discussion of Individual Measurements**

##### **5.3.2.2.1 Cell Current – WI01**

The SFE oxygen production rate is a function of the current applied to the cell electrodes. For a three-man metabolic production rate the required current is 29.2 A. During normal mode operations the applied current was controlled to this value as shown by WI01 (Fig. 40).

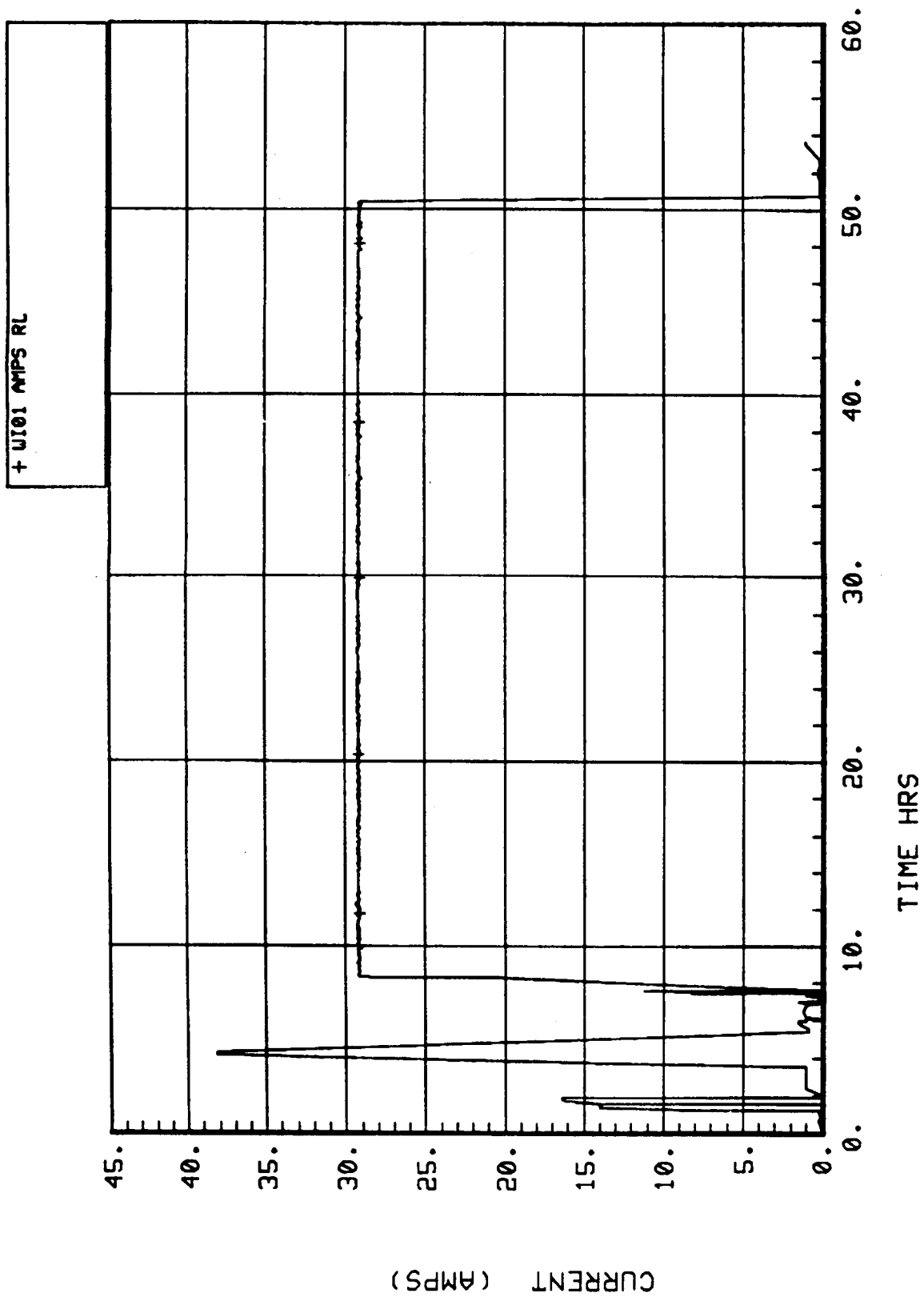


Figure 40. SFE subsystem cell current WI01.

#### **5.3.2.2.2 Cell Voltage – WV13**

Cell voltage is a function of both current and temperature. Measurement WV13 (Fig. 41) represents the total voltage for the twelve cells which are connected electrically in series. During normal mode operations, the total voltage ranged from 19.8 V to 20.6 V. This corresponds to an average cell voltage range of 1.65 V to 1.72 V. Approximately 49 hr into the test, the cell 1 voltage reached the high warning level of 1.75 V. The subsystem temperature at that time was 128°F. The subsystem controller responded to the low temperature by increasing the flow through the CCA heat exchanger bypass. As the temperature rose into the control band,  $133 \pm 2^\circ\text{F}$ , the cell 1 voltage dropped back into the nominal range.

#### **5.3.2.2.3 SFE Operating and Delta Pressures – WP01 and WP02**

WP01 and WP02 (Figs. 42 and 43) are measurements of the subsystem operating pressure and the oxygen to hydrogen differential pressure, respectively. The PCA regulators, PR1 and PR2, are driven to the positions required to control the subsystem operating pressure to 165 psig and the oxygen to hydrogen differential pressure to approximately 2 psid. The PCA functioned as expected throughout the test as shown by plots of WP01 and WP02.

#### **5.3.2.2.4 Feed Water Tank Delta Pressure – WP04**

The spring-loaded bellows in the feed water tank maintains the tank differential pressure, WP04, at approximately 2 to 3 psid (Fig. 44). The cyclic nature of the WP04 reading is due to the periodic tank refills.

#### **5.3.2.2.5 SFE Operating Temperature – WT01**

The CCA diverter valve is driven to the position required to control the SFE operating temperature to approximately 133°F. The plot of measurement WT01 (Fig. 45) shows that the CCA functioned nominally throughout the test.

#### **5.3.2.2.6 Hydrogen and Oxygen Output Flow Rates – FF04 and FF05**

The SFE transition from shutdown to normal mode was begun approximately 1 hr into the test. Plots of FF04 and FF05 (Figs. 46 and 47), the hydrogen and oxygen outputs flowrates, clearly show the variations in flow during the startup and shutdown sequences. The communications link was repaired and the SFE restarted at 6.8 hr. The subsystem achieved normal mode operation at 8 hr. The output flowrates were as expected throughout the test. The drop in hydrogen flow at approximately 27 hr coincided with hydrogen sampling. The hydrogen sample port is upstream of flowmeter FF04.

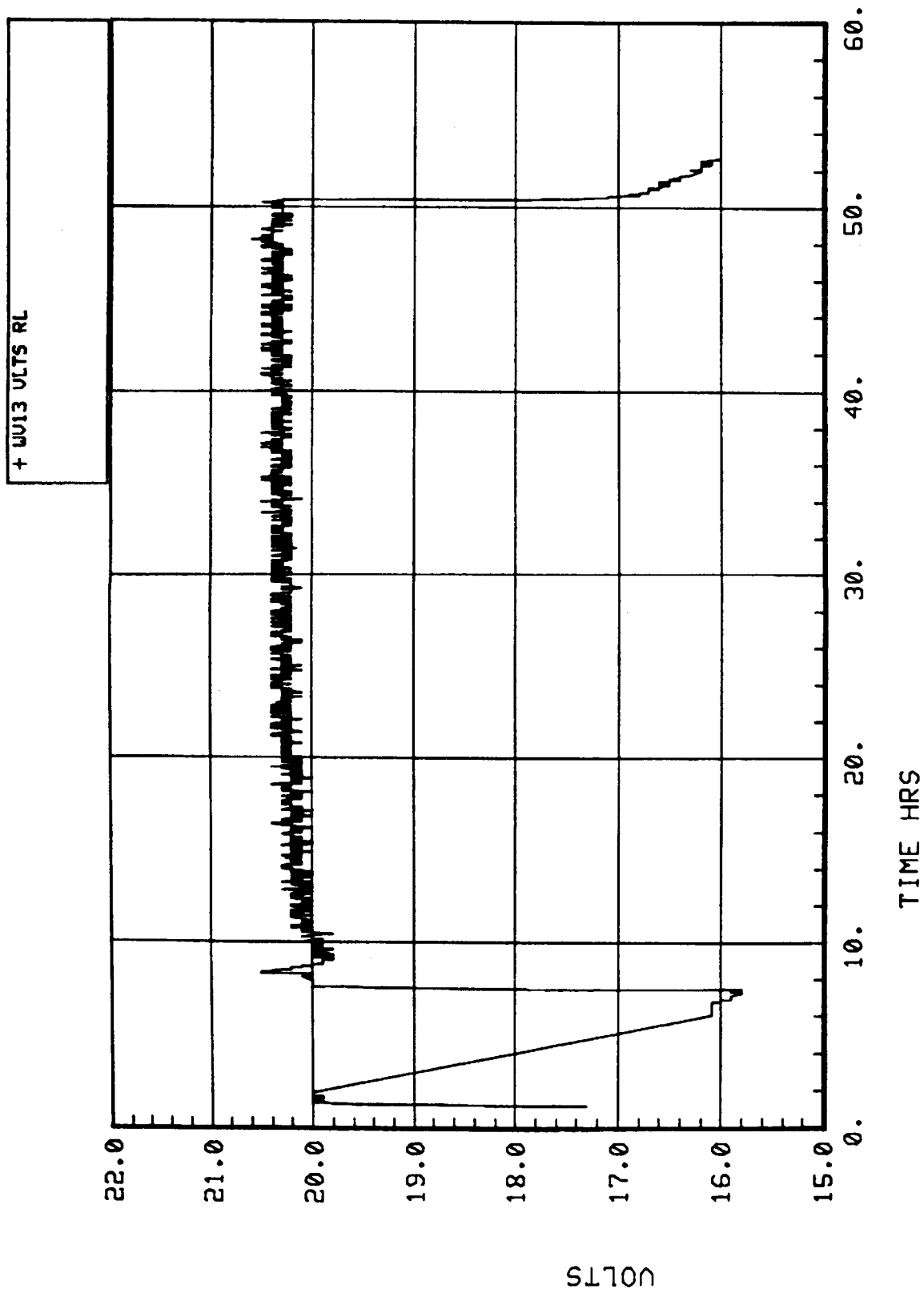


Figure 41. SFE subsystem cell voltage WV13.



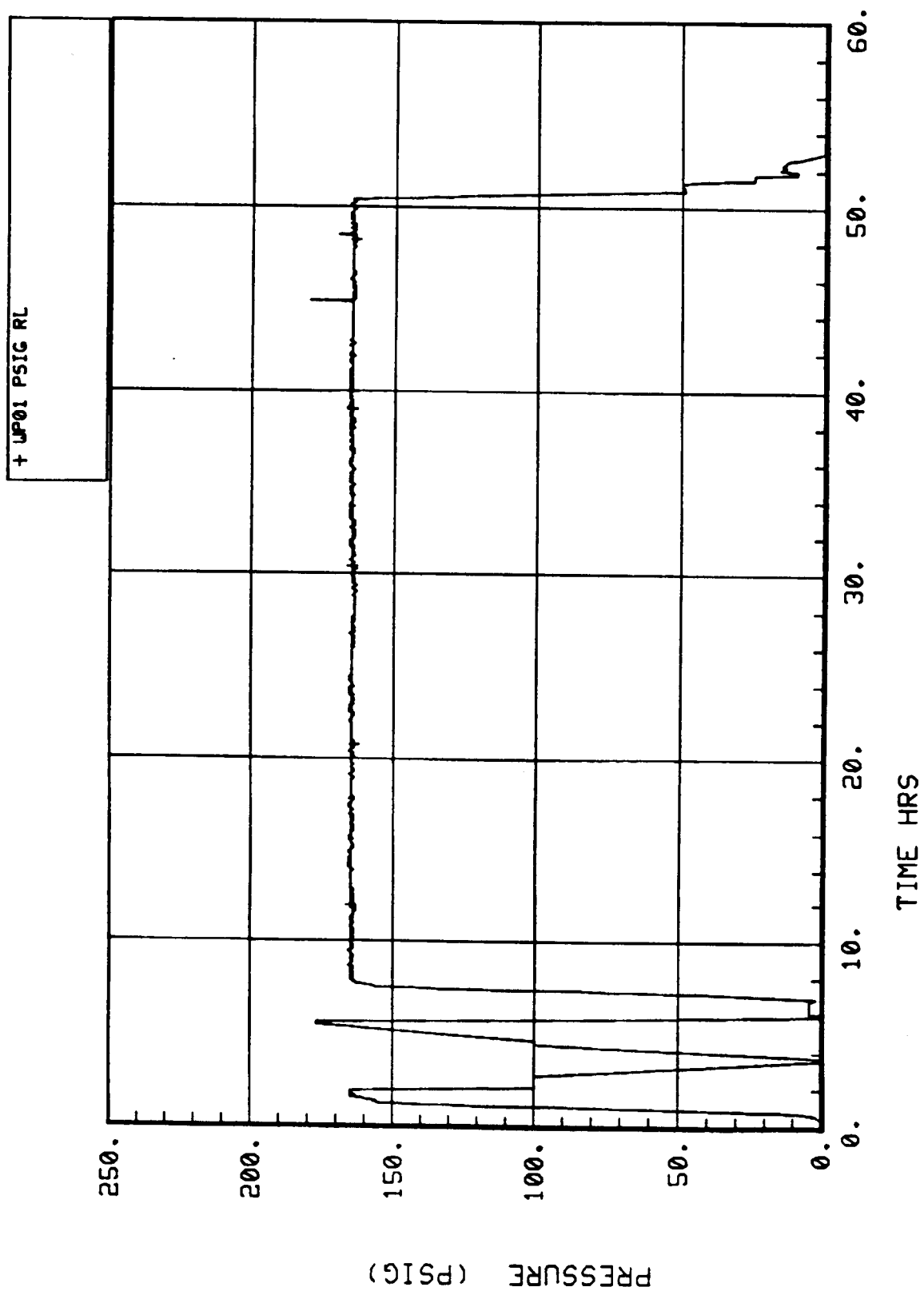


Figure 42. SFE subsystem operating pressure WP01.

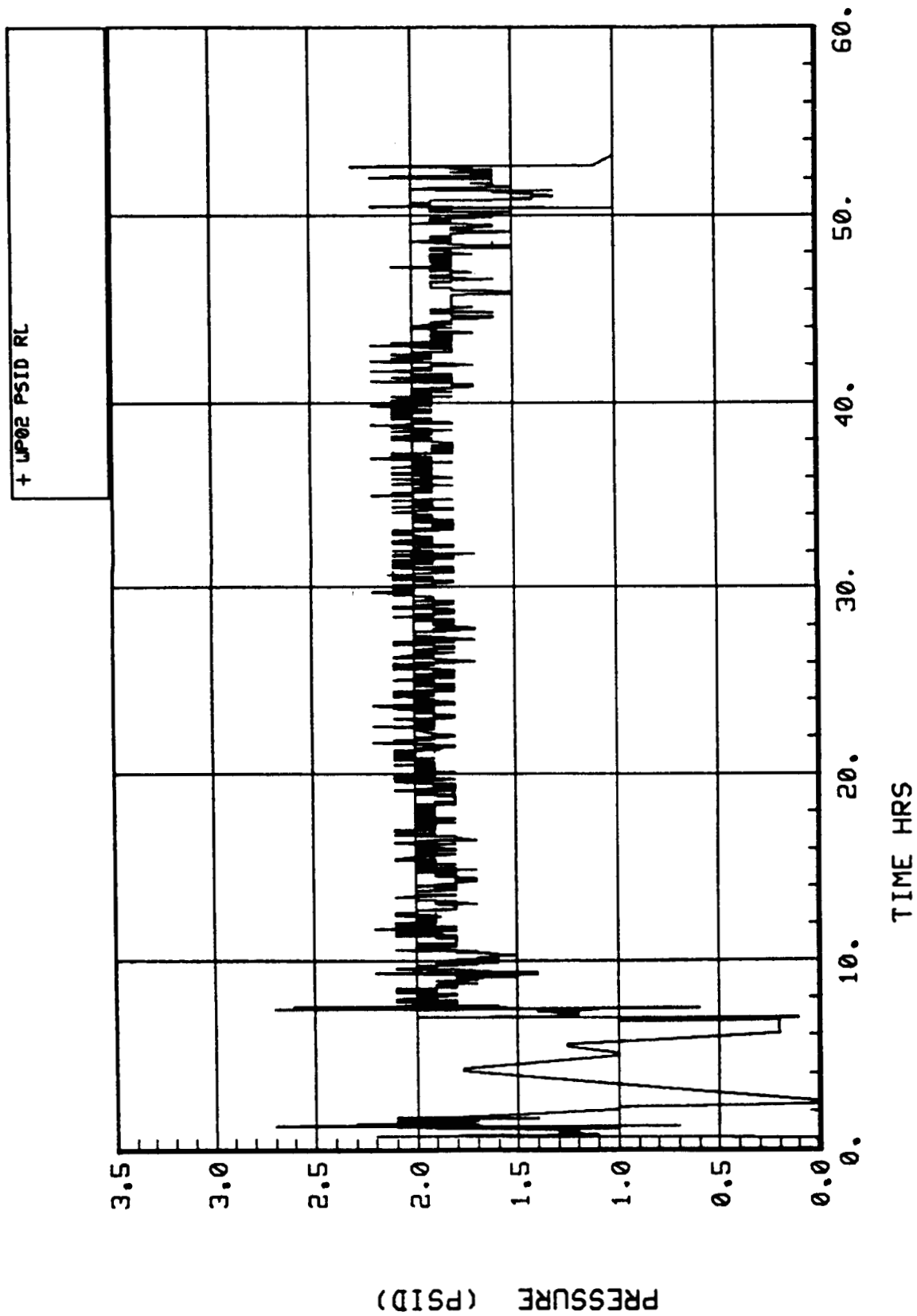


Figure 43. SFE subsystem delta press WP02.

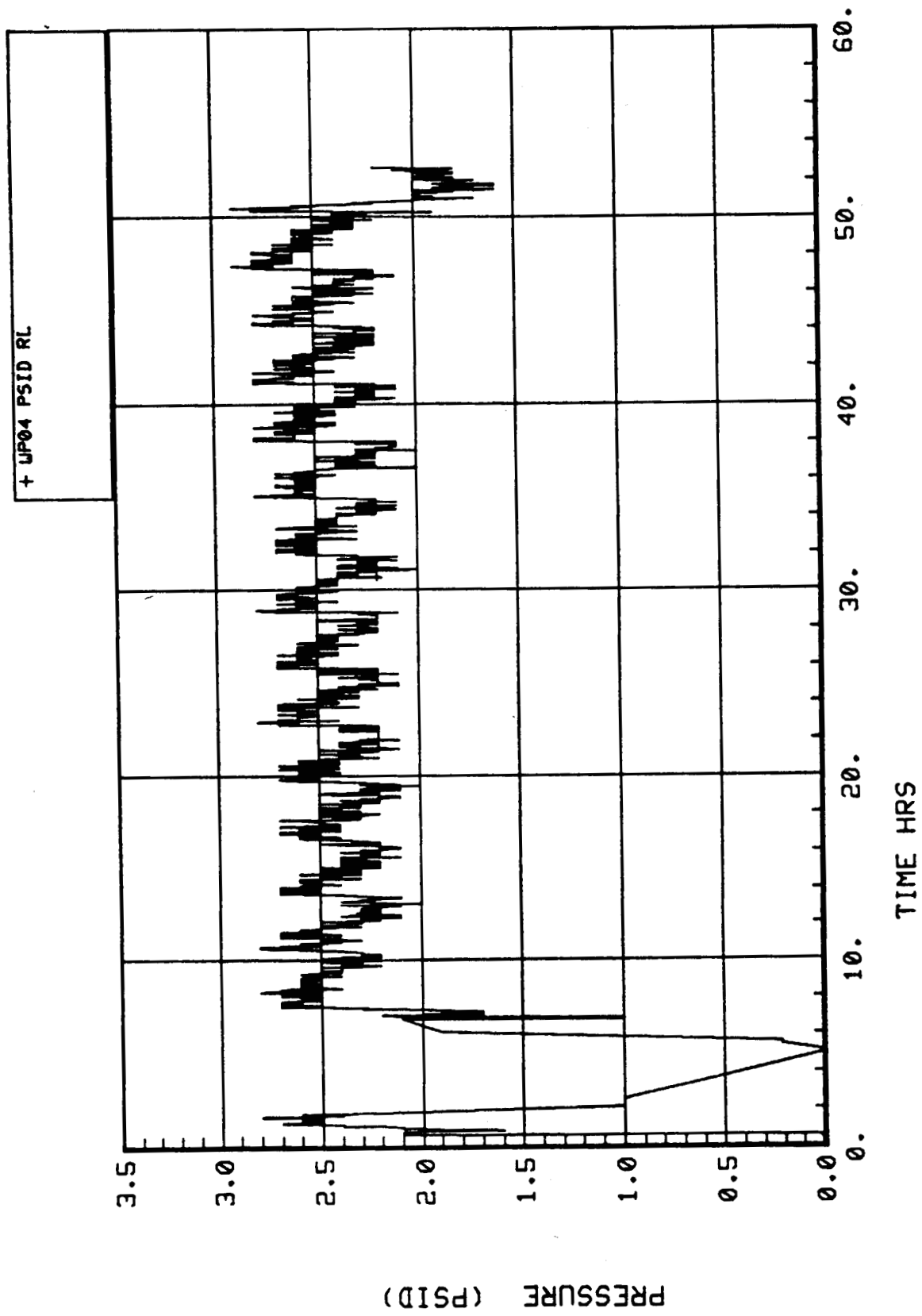


Figure 44. SFE subsystem H<sub>2</sub>O tank pressure WP04.

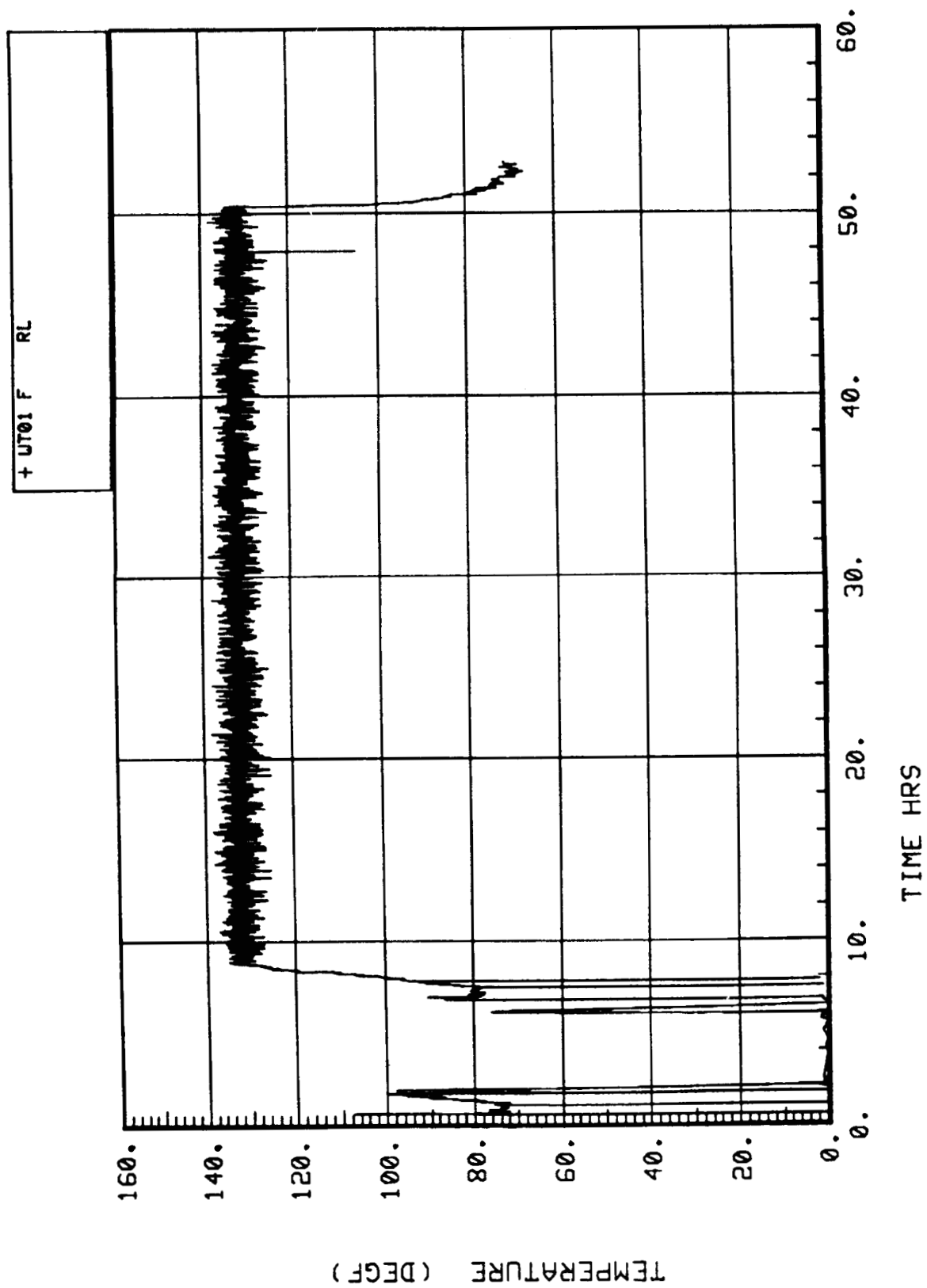


Figure 45. SFE subsystem operating temperature WT01.

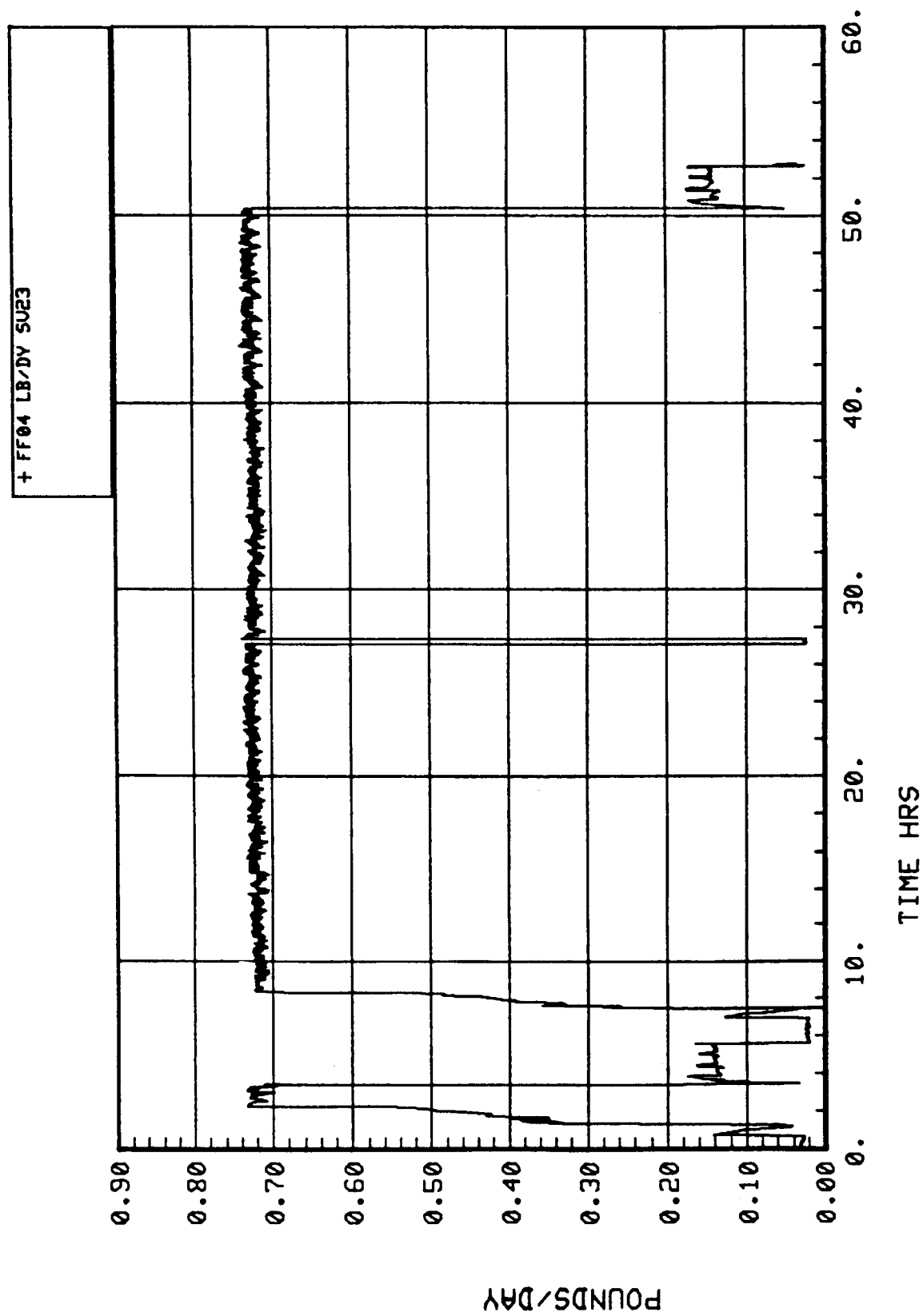


Figure 46. SFE subsystem H<sub>2</sub> flow FF04.

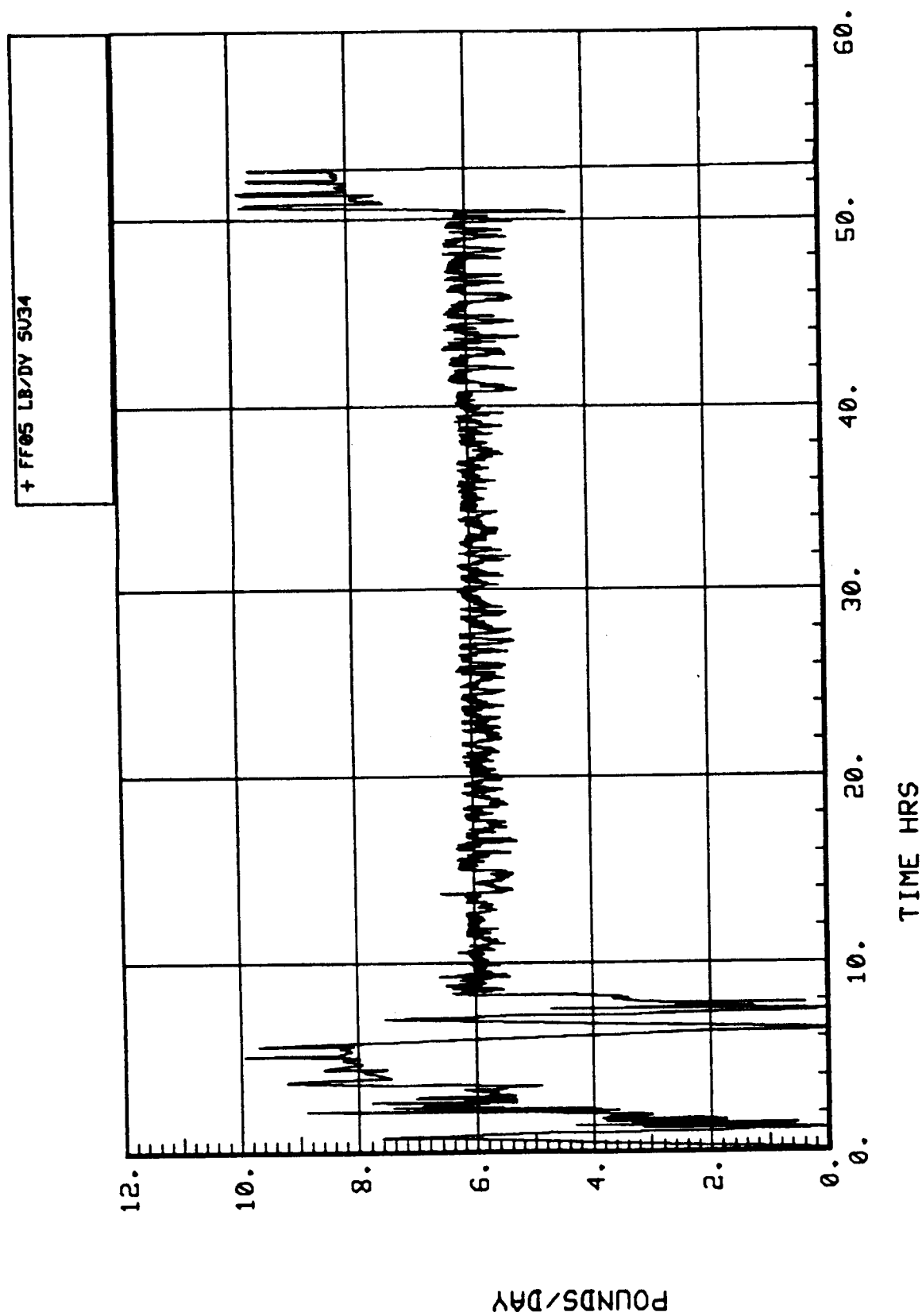


Figure 47. SFE subsystem O<sub>2</sub> flow FF05.

#### **5.3.2.2.7 Hydrogen and Oxygen Outlet Pressures – FP03 and FP04**

The hydrogen and oxygen outlet pressures were measured by FP03 and FP04 (Figs. 48 and 49), respectively. Hydrogen flowed from the SFE to the Sabatier. This flow was restricted by metering valve MV1 which maintained a slight back pressure on the hydrogen outlet line. During this test the hydrogen outlet pressure was approximately 29 psig except during sampling when the pressure dropped to ambient. The oxygen outlet flow was relatively unrestricted and the pressure ranged from 0.2 to 0.37 psig.

#### **5.3.3 Recommendations/Lessons Learned**

Performance was very close to theoretical for the SFE subsystem. It is recommended that dry bulb temperature sensors be added to the hydrogen/oxygen output lines to facilitate computation of output relative humidity. Modifications may also be required to the PDU related to the communication failure which occurred during the test.

### **5.4 Four-Bed Molecular Sieve (4BMS)**

#### **5.4.1 Subsystem Description**

The 4BMS was used to remove CO<sub>2</sub> from the module simulator air and concentrate it for processing by the Sabatier CO<sub>2</sub> reduction subsystem. The basic concept of the 4BMS is quite simple: a mixed air stream (including CO<sub>2</sub>) flows through a sorbent material and the CO<sub>2</sub> is selectively adsorbed while the remaining air flows through. Adsorption is the physical trapping of individual molecules in voids in the sorbent structure and does not result in a physical or chemical change of the sorbent itself (distinct from the process of absorption which involves a chemical reaction or a physical change or both in the sorbent material). In addition to the molecular size, the polarity of the molecules and the vapor pressure are important factors in selecting molecules for adsorption.

For the 4BMS, the CO<sub>2</sub> sorbent material used was a synthetic zeolite which was selected for its superior ability to adsorb CO<sub>2</sub>. The designation for the CO<sub>2</sub> sorbent is Zeolite 5A. Due to the preference of Zeolite 5A for water vapor over CO<sub>2</sub>, it is necessary to first dry the air. The desiccants used to do this are silica gel and another type of zeolite, designated Zeolite 13X. The sorbents are in the form of pellets approximately 1/8-in. long by 1/16-in. in diameter. During operation, the sorbents alternately adsorb and desorb the water vapor and CO<sub>2</sub>, which requires two beds each of desiccant and CO<sub>2</sub> sorbent to perform CO<sub>2</sub> removal in an essentially continuous manner. The cycling is controlled by a timer which causes valve positions to reconfigure at each mode change.

A schematic of the 4BMS is shown in Figure 50. The flowpath of the air through the 4BMS takes it first through a two-layer desiccant bed. The first layer is silica gel which can adsorb water vapor readily at higher relative humidities but its capacity falls off at relative humidities less than 50 percent. The second layer is Zeolite 13X which has a higher capacity than silica gel at relative humidities less than 35 percent. By having a two-layer bed of these desiccants, essentially

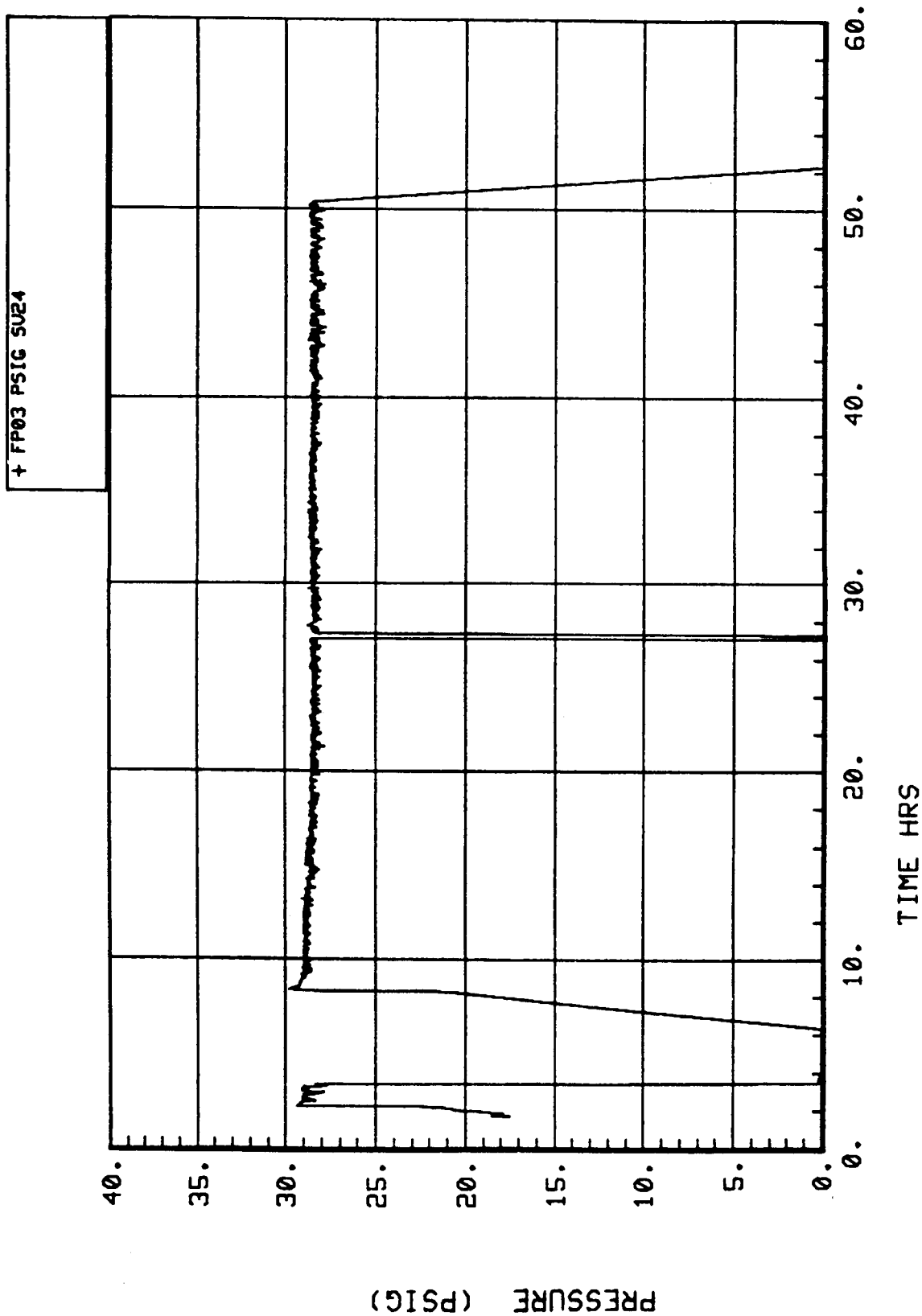


Figure 48. SFE subsystem H<sub>2</sub> outlet pressure FP03.



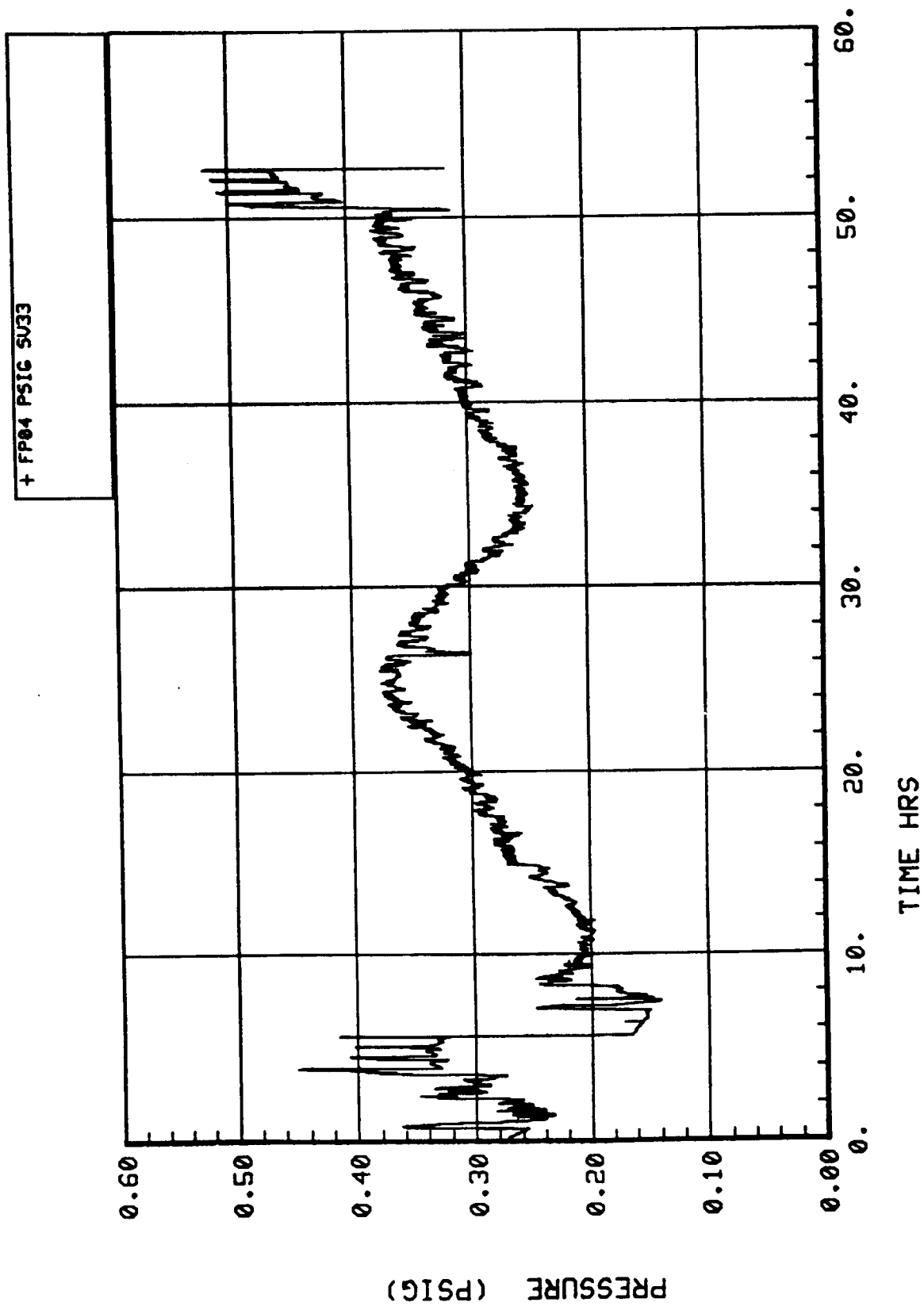


Figure 49. SFE subsystem O<sub>2</sub> outlet pressure FP04.

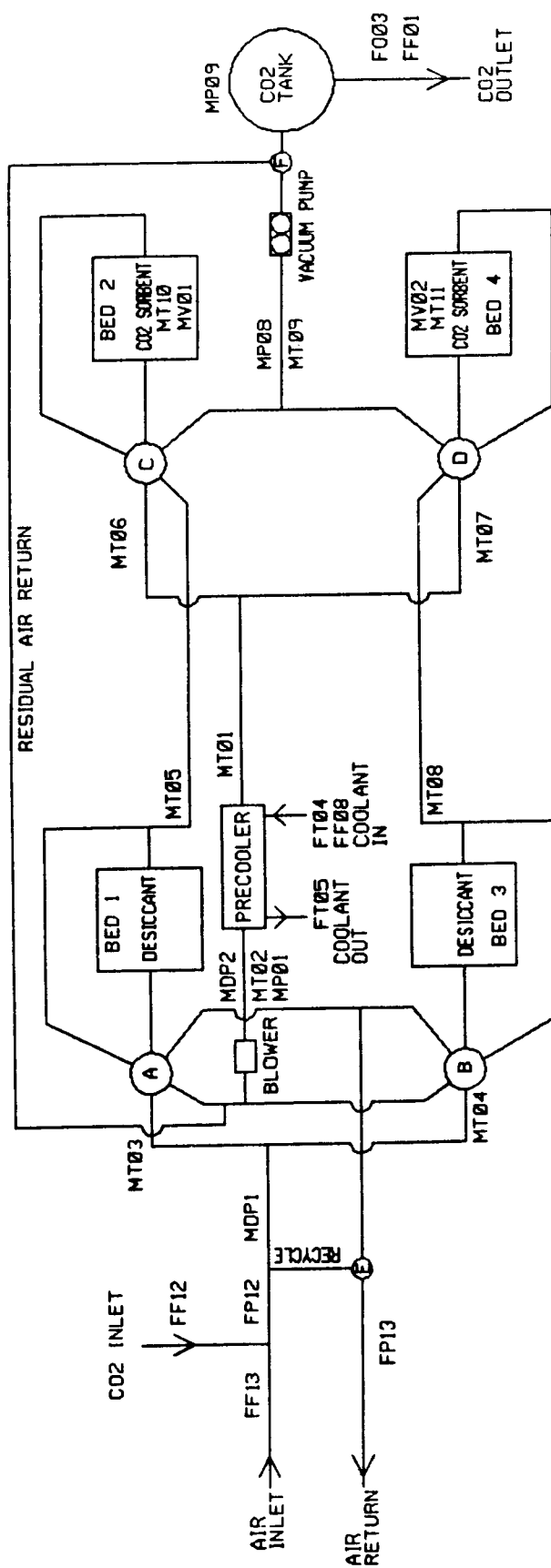


Figure 50. Molecular sieve subsystem schematic.

all of the water vapor can be removed. The adsorption process results in a temperature rise at the air stream and there is also a temperature rise across the blower. The blower is located downstream of the desiccant bed so that the temperature rise does not cause a drop in the relative humidity of the incoming air. Downstream of the blower, the precooler reduces the temperature of the air stream to temperatures more conducive to CO<sub>2</sub> adsorption (from about 190° to 70°F). The dry, cool air then flows through a CO<sub>2</sub> sorbent bed, cooling the bed (heated during the previous desorb half-cycle) to a temperature where much of the CO<sub>2</sub> is removed from the air stream. The air is next directed through the second desiccant bed to desorb the water that was adsorbed during the previous half-cycle. To improve performance, at the beginning of each adsorb half-cycle, the outlet air is recycled to the inlet. After 11 min the desorbing desiccant bed was heated (due to residual heat in the now adsorbing CO<sub>2</sub> sorbent bed) enough to begin desorbing water vapor so the recycle valve switches to end recycle. The outlet air has the same average moisture content as the inlet air.

While one CO<sub>2</sub> sorbent bed is adsorbing CO<sub>2</sub> the other is desorbing CO<sub>2</sub> for storage in the accumulator tank prior to delivery to the Sabatier. During desorption, the residual air in the canister is pumped back to the duct upstream of the blower. This is done for 2 min. Then the heater activates to raise the bed temperature to about 400°F which, in combination with the vacuum pump reducing the pressure to about 0.5 psia, releases the CO<sub>2</sub> from the zeolite. After about 55 min the desorption is complete and the next half-cycle begins. (See Fig. 51 for the operating modes.)

The subsystem was constructed from Skylab hardware (canisters and heaters, five-way valves) and commercially available components (blower, vacuum pumps, CO<sub>2</sub> holding tank, controller). As a result, the subsystem was not optimized with regard to weight, volume, or power usage.

The 4BMS was installed so that it could be operated independently (and vent CO<sub>2</sub>) or integrated with the Sabatier for CO<sub>2</sub> reduction. The subsystem as installed included a CO<sub>2</sub> liquefaction capability, which was not used for this test program. During operation, air from the THC heat exchanger was ducted directly to the inlet of the 4BMS. This duct contained a flow meter, a port for injection of CO<sub>2</sub>, and a connection to a CO<sub>2</sub> partial pressure sensor. The CO<sub>2</sub> supply line contained a flow meter and a metering valve for regulating the CO<sub>2</sub> flow. As the air flowed through the subsystem, temperature measurements were made at various locations (e.g., inlet, upstream and downstream of the precooler, downstream of the sorbent beds) and, at the air exit, the CO<sub>2</sub> partial pressure was again measured. The air exited into the volume of the simulator.

The desorbed CO<sub>2</sub> was pumped to a storage tank (part of the CO<sub>2</sub> liquefaction unit) from where the CO<sub>2</sub> could be regulated to the Sabatier or vented. An O<sub>2</sub> sensor in the CO<sub>2</sub> outlet line was used to measure the percentage of O<sub>2</sub> (an indication of the amount of air present in the CO<sub>2</sub>).

The five-way valves, recycle valve, and CO<sub>2</sub> outlet-flow control valve are pneumatic type and pressurized nitrogen was supplied to actuate them.

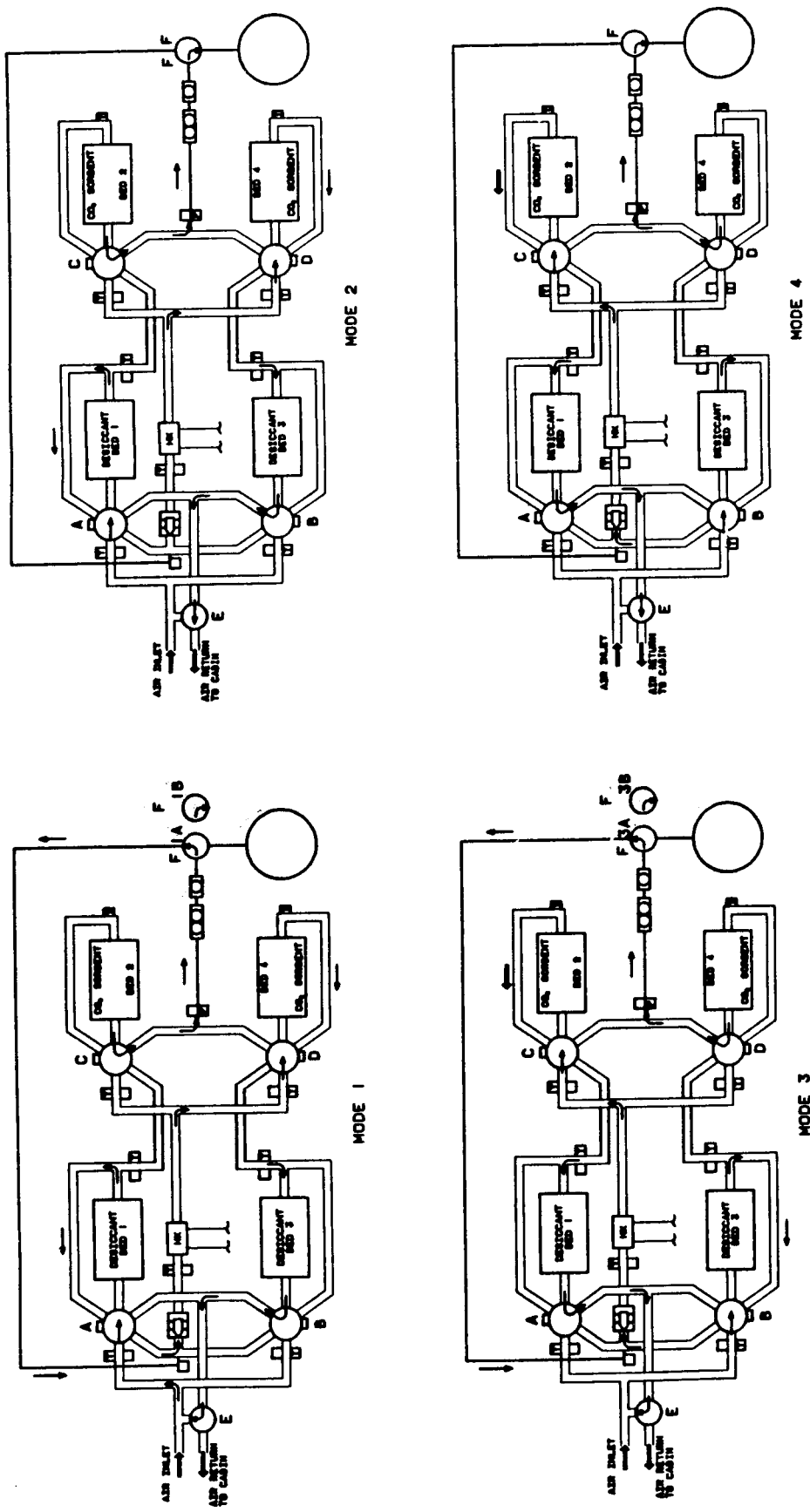


Figure 51. Molecular sieve subsystem operational schematic.

MINUTES	CYCLE 1	0	9	11	56	56	67	115	
	CYCLE 2	0	2	10	57	60	67	111	
	CYCLE 3	0	2	11	58	57	66	110	
CYCLE MODE		1A	1B	2	3A	3B	4		
DESICCANT	BED 1	----- ADSORB -----		----- DESORB -----					
		----- DESORB -----		----- ADSORB -----					
	BED 3	----- DESORB -----		----- ADSORB -----					
	CO <sub>2</sub> SORBENT	BED 2 HEATER	⚠ ----- DESORB -----		----- ADSORB -----				
			OFF	ON	ON	OFF	OFF	OFF	
BED 4 HEATER		----- ADSORB -----		⚠ ----- DESORB -----					
		OFF	OFF	OFF	OFF	ON	ON		
COMPONENT DESCRIPTION		POSITION							
VALVE A		2	2	2	1	1	1		
VALVE B		1	1	1	2	2	2		
VALVE C		1	1	1	2	2	2		
VALVE D		2	2	2	1	1	1		
VALVE E		4	4	3	4	4	3		
VALVE F		5	6	6	5	6	6		
CO <sub>2</sub> COMPRESSOR		ON	ON	ON	ON	ON	ON		
CO <sub>2</sub> HOLDING TANK		CHARGING		TANK		CHARGING		TANK	
H.P. COMPRESSOR		OFF	OFF	OFF	OFF	OFF	OFF		

VALVE	POSITION	DESCRIPTION
A.B.C.D	1	DESICCANT BED TO CABIN RETURN/CO <sub>2</sub> BED TO COMPRESSOR
A.B.C.D	2	AIR INLET TO DESICCANT BED/CO <sub>2</sub> BED OUTLET TO DESICCANT
E	3	OUTLET TO CABIN
E	4	RECYCLE OUTLET TO INLET
F	5	RESIDUAL GAS REMOVAL
F	6	CO <sub>2</sub> TO HOLDING TANK
△		= RESIDUAL GAS REMOVAL MODE

CDM-10474

Figure 51. (Concluded)

## **5.4.2 Discussion of Results**

### **5.4.2.1 General**

The 4BMS operated for 48 hr during which time measurements from 27 sensors were recorded. Plots of these measurements were made and are discussed below. The average CO<sub>2</sub> removal efficiency was 35.9 percent, somewhat lower than expected, at a rate between 3.96 and 4.69 lb/day (1.80 to 2.13-man load). Analyses of samples of the outlet CO<sub>2</sub> are given in Section 6.0 and show that the composition was roughly 85 percent CO<sub>2</sub>, 9 percent N<sub>2</sub>, and 1.5 percent O<sub>2</sub>, with no detectable quantities of any other compound. An excess of N<sub>2</sub> is indicated (greater than the 4:1 N<sub>2</sub> to O<sub>2</sub> ratio in air) which may be due to analysis uncertainties or leakage in the five-way valves. The measured O<sub>2</sub> level in the outlet reading was about 0.7 percent (the tank was initially evacuated and filled with bottled CO<sub>2</sub>) and rose to 2.5 percent by the end of the test. Since the allowable limit for O<sub>2</sub> and CO<sub>2</sub> is 3.0 percent, some type of correction will be needed before longer testing (this is discussed further in Section 5.4.3).

### **5.4.2.2 Discussion of Individual Measurements**

#### **5.4.2.2.1 Air Temperature of the Inlet Air to Bed 1 – MT03**

The Molecular Sieve bed 1 inlet air temperature is shown in Figure 52. There are two obvious patterns shown in this plot: (1) a cyclic variation that ranges from approximately 67°F up to approximately 95°F, and (2) a mild undulation that completes two cycles over the course of the test. The first pattern is related to the cyclic adsorb/desorb operation of the 4BMS and is due to the heat being removed from bed 2 during adsorption and conducted from the air stream through valve A. The temperature then drops as Mode 1 begins, since air was again flowing past the temperature sensor. The second pattern is due to changes in the ambient air temperature associated with the day/night cycle. These patterns are evident in essentially all of the temperature measurements and are characteristic of operation inside the module simulator.

Also present is a short spike on the downward slope of each of the cyclic variations. This occurs just prior to the end of recycle (Mode 1B) as heat from the adsorbing CO<sub>2</sub> sorbent bed (which is cooling from the previous desorption) reaches the inlet. Valve E then switches as Mode 2 begins and the temperature drops.

#### **5.4.2.2.2 Air Temperature of the Inlet Air to Bed 3 – MT04**

Figure 53 contains a plot of the Molecular Sieve bed 3 inlet air temperature. This plot is very similar to MT03, except that it is for the alternate half-cycle. The differences are due to the different location of the sensor and the slight differences in the temperatures reached by the CO<sub>2</sub> sorbent beds (discussed below, MT10 and MT11).

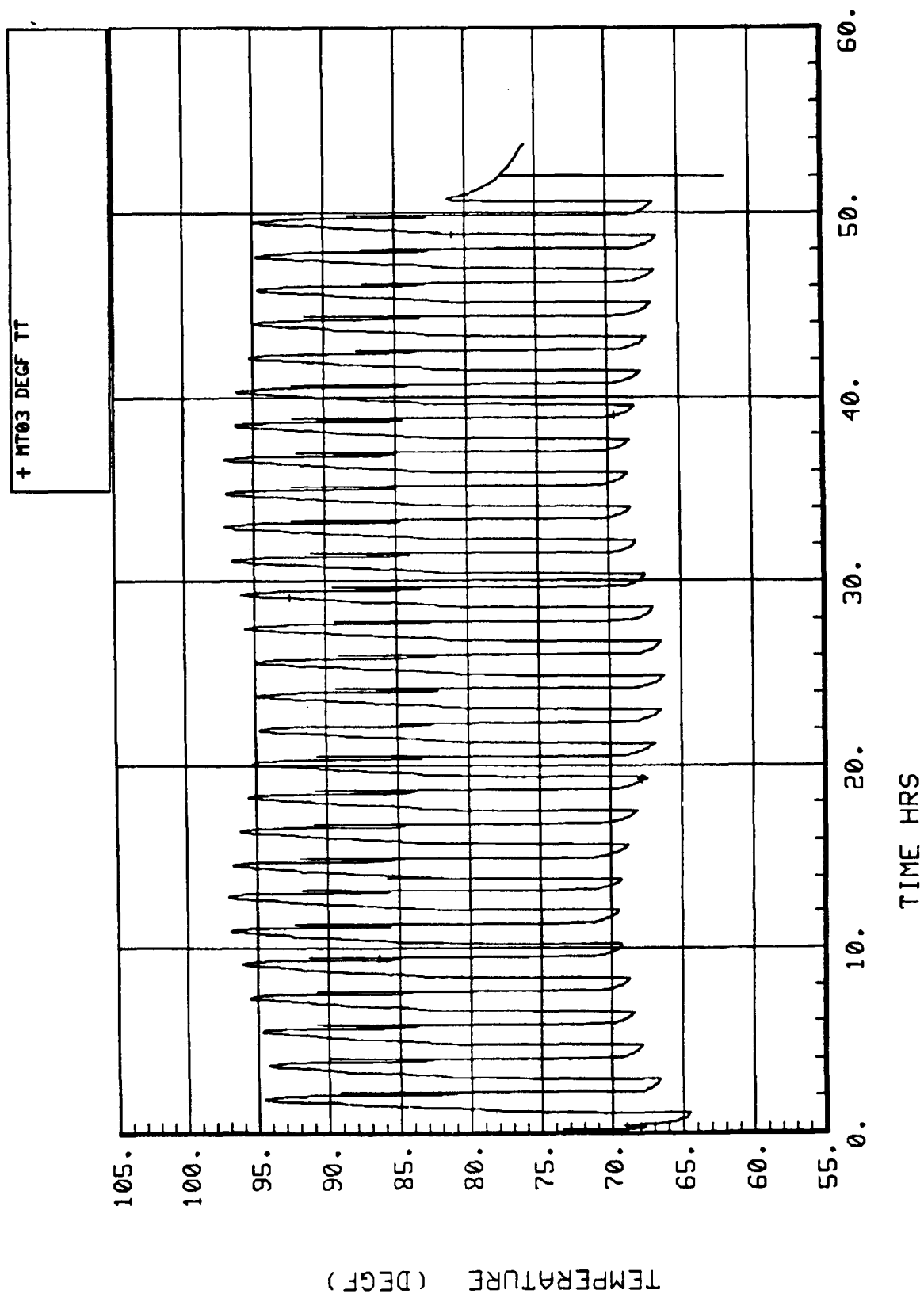


Figure 52. Molecular sieve subsystem bed 1 inlet air temperature MT03.

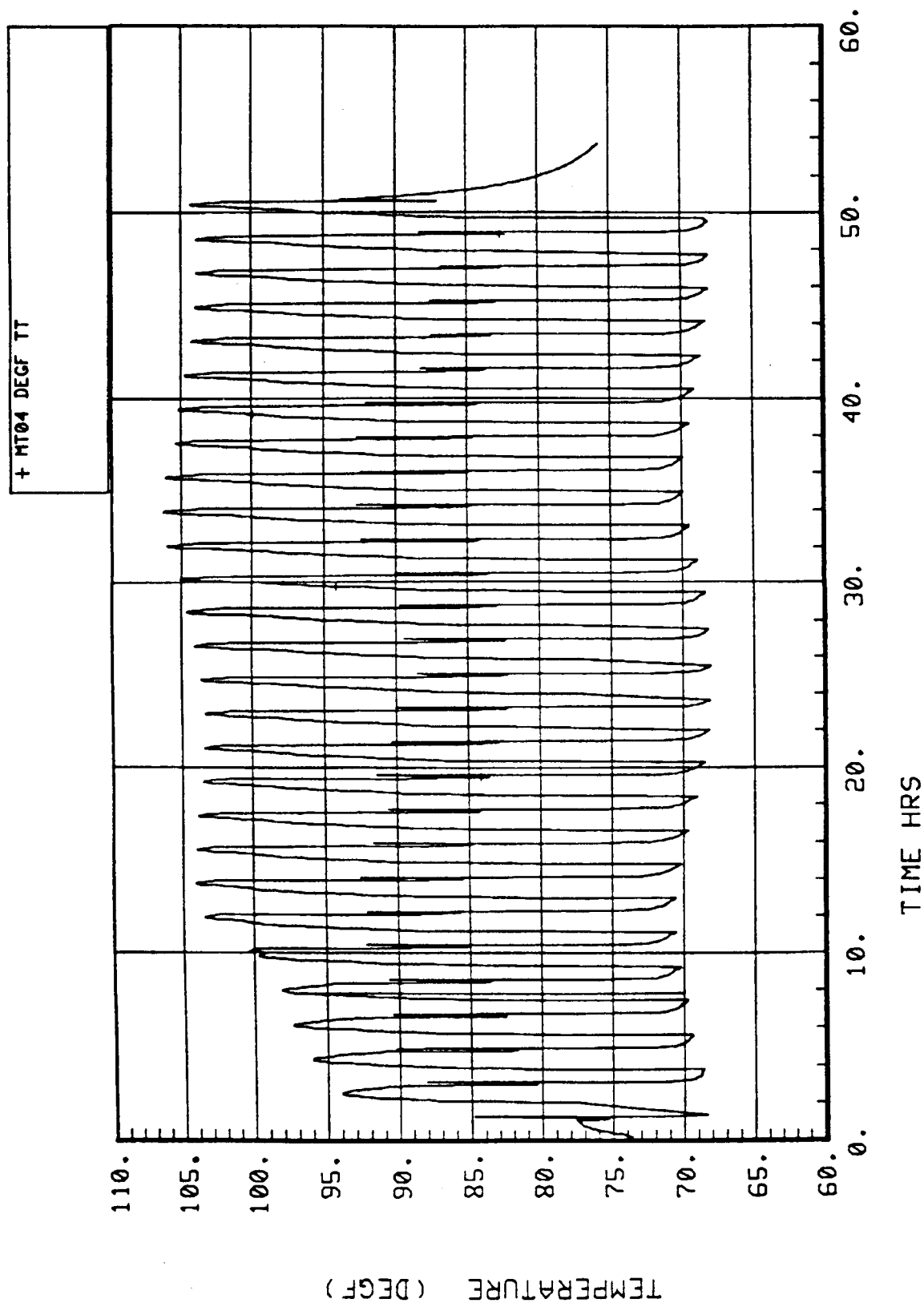


Figure 53. Molecular sieve subsystem bed 3 inlet air temperature MT04.



#### **5.4.2.2.3 Air Temperature Upstream of the Subsystem Precooler – MT02 (Blower Outlet Temperature)**

Measurement MT02 is shown in Figure 54. The air temperature at this location ranges from about 178° to 212°F. Again the cyclic operation and the day/night cycles are apparent. The number of peaks corresponds to the number of half-cycles since the air from each desiccant bed flows through the precooler.

#### **5.4.2.2.4 Air Temperature Downstream of the Subsystem Precooler – MT01**

Measurement MT01 is shown in Figure 55. At this location the temperature ranges from about 64° to 74°F indicating that the precooler is cooling the air as intended. However, the plot also indicates that leakage occurred through valve A during modes 1 and 2, which allowed some incoming air to bypass bed 1 (where a temperature rise occurs due to adsorption heating) and, therefore, have a cooler temperature. Without this leakage the lower temperature would be approximately 68°F.

#### **5.4.2.2.5 Air Temperature into Bed 2 – MT06**

The Molecular Sieve bed 2 inlet air temperature is shown for a single cycle in Figure 56. At this location the temperature ranges from approximately 65° to 88°F, similar to the temperatures at MT01. The increase in the upper temperature (compared with MT01) is due to the proximity of the sensor to the valve C which conducts heat from the desorbing bed 2. The temperature increases throughout mode 2 when bed 2 is heated for CO<sub>2</sub> desorption. As a result of the heat conduction, this measurement is not necessarily an accurate indication of the air temperature.

#### **5.4.2.2.6 Air Temperature into Bed 4 – MT07**

The temperature at MT07 (Fig. 57) ranges from approximately 70° to 105°F, again similar to the temperatures at MT01. The comments for MT06 on the effects of heat conduction on the measurement accuracy apply for this sensor also.

#### **5.4.2.2.7 Sorbent Bed 2 Temperature – MT10**

The temperatures in sorbent bed 2 (Fig. 58) vary from approximately 70° to 400°F, as the bed cycles through CO<sub>2</sub> adsorption and desorption. The heater was on during modes 1B and 2 and upon reaching 400°F maintained that temperature until the end of mode 2.

#### **5.4.2.2.8 Sorbent Bed 4 Temperature – MT11**

The temperature in bed 4 (Fig. 59) varies from approximately 70° to 410°F. The temperature controller for this bed was set slightly higher than for bed 2. The heater was on during modes 3B and 4 and upon reaching 410°F maintained that temperature until the end of mode 4.

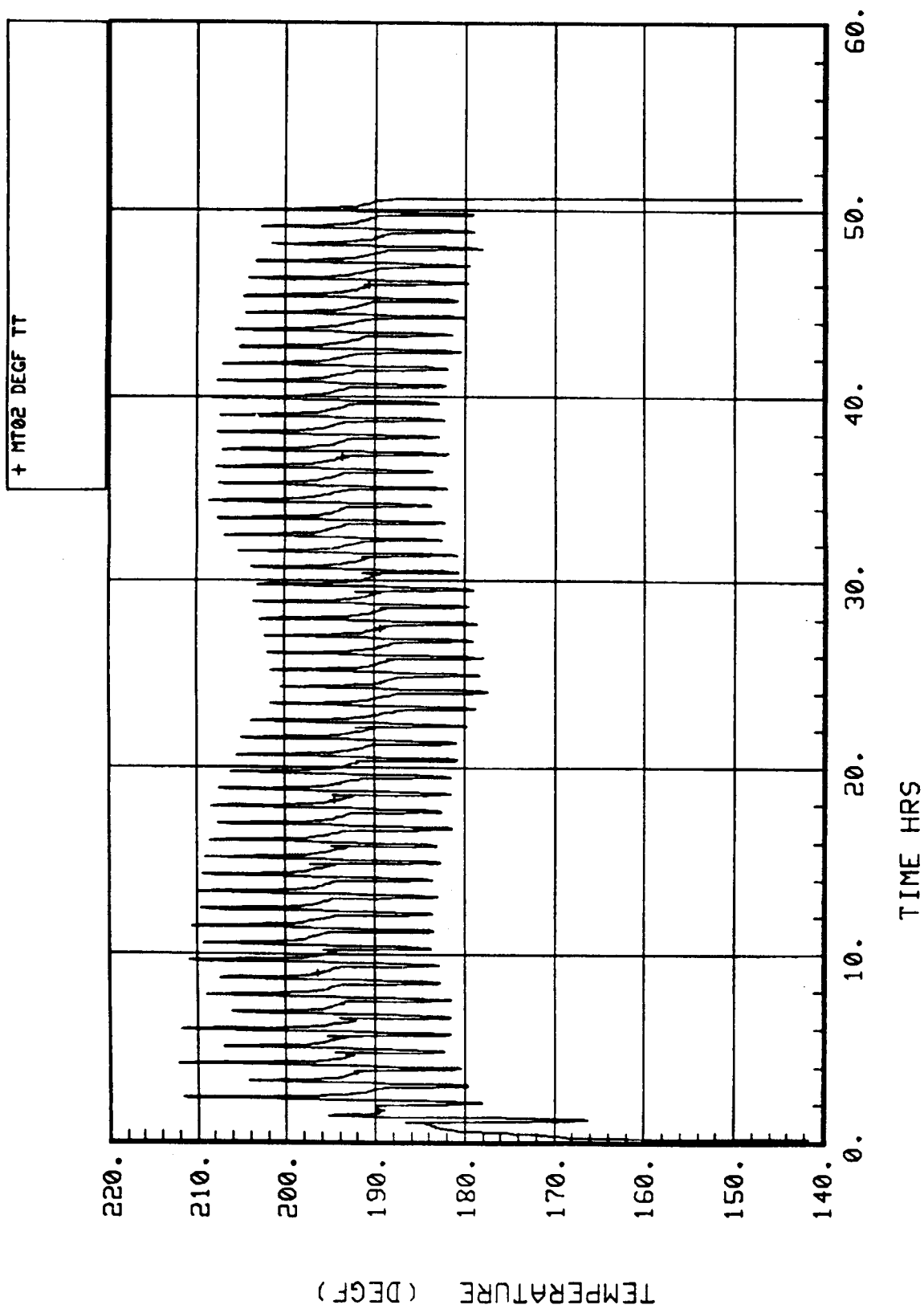


Figure 54. Molecular sieve subsystem blower outlet temperature MT02.

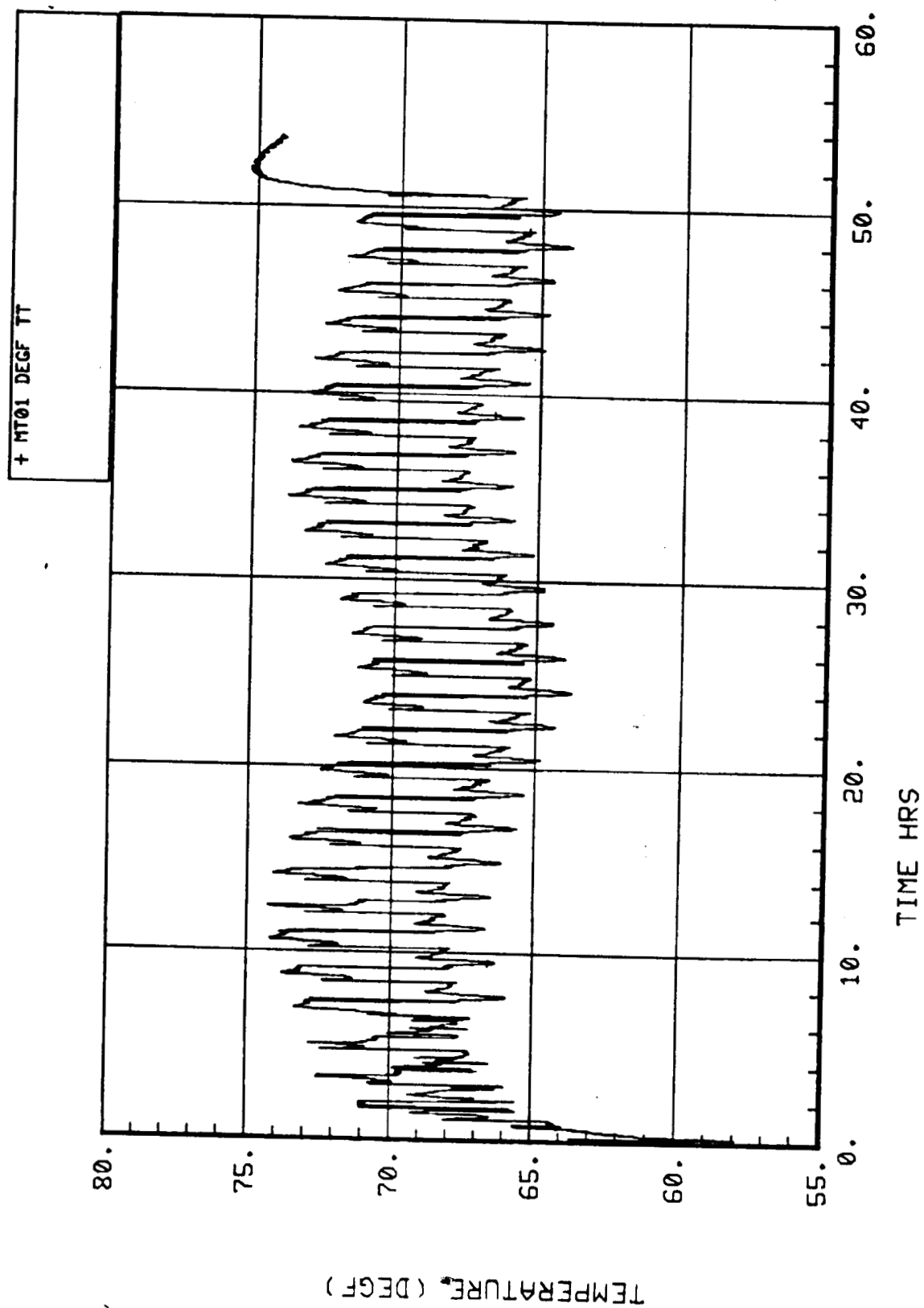


Figure 55. Molecular sieve subsystem HX air outlet temperature MT01.

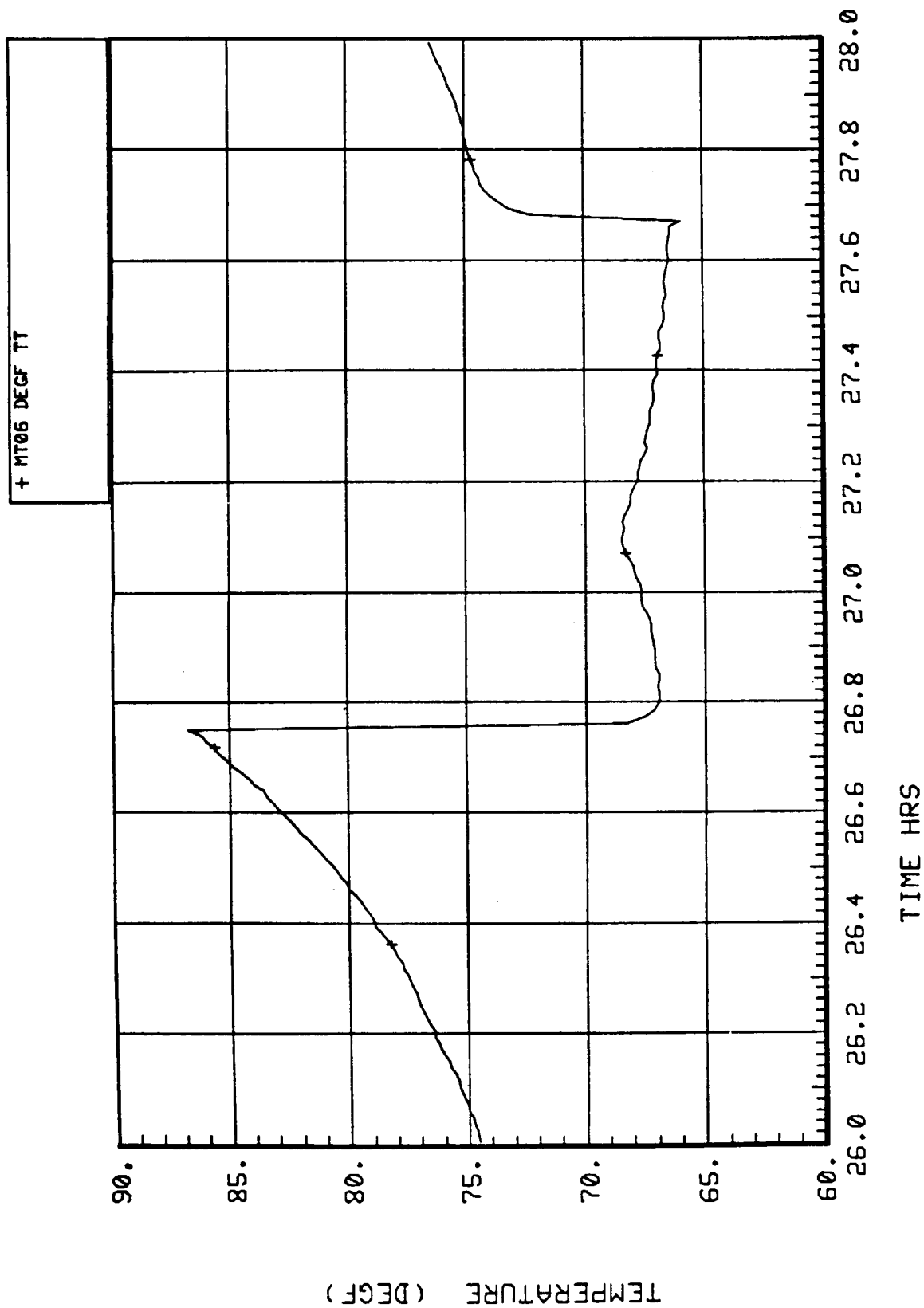


Figure 56. Molecular sieve subsystem bed 2 inlet air temperature MT06.

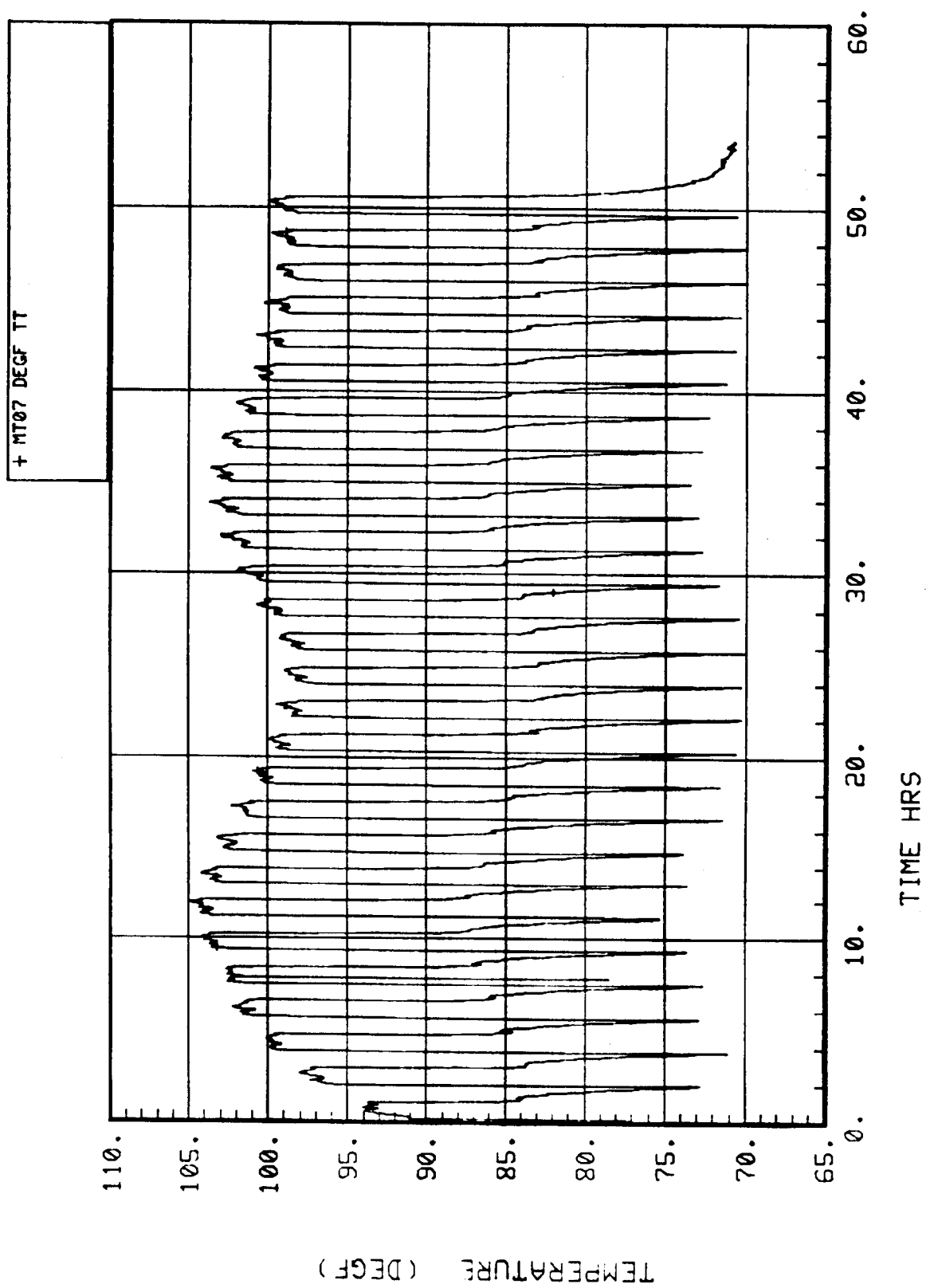


Figure 57. Molecular sieve subsystem bed 4 inlet air temperature MT07.

c. 2

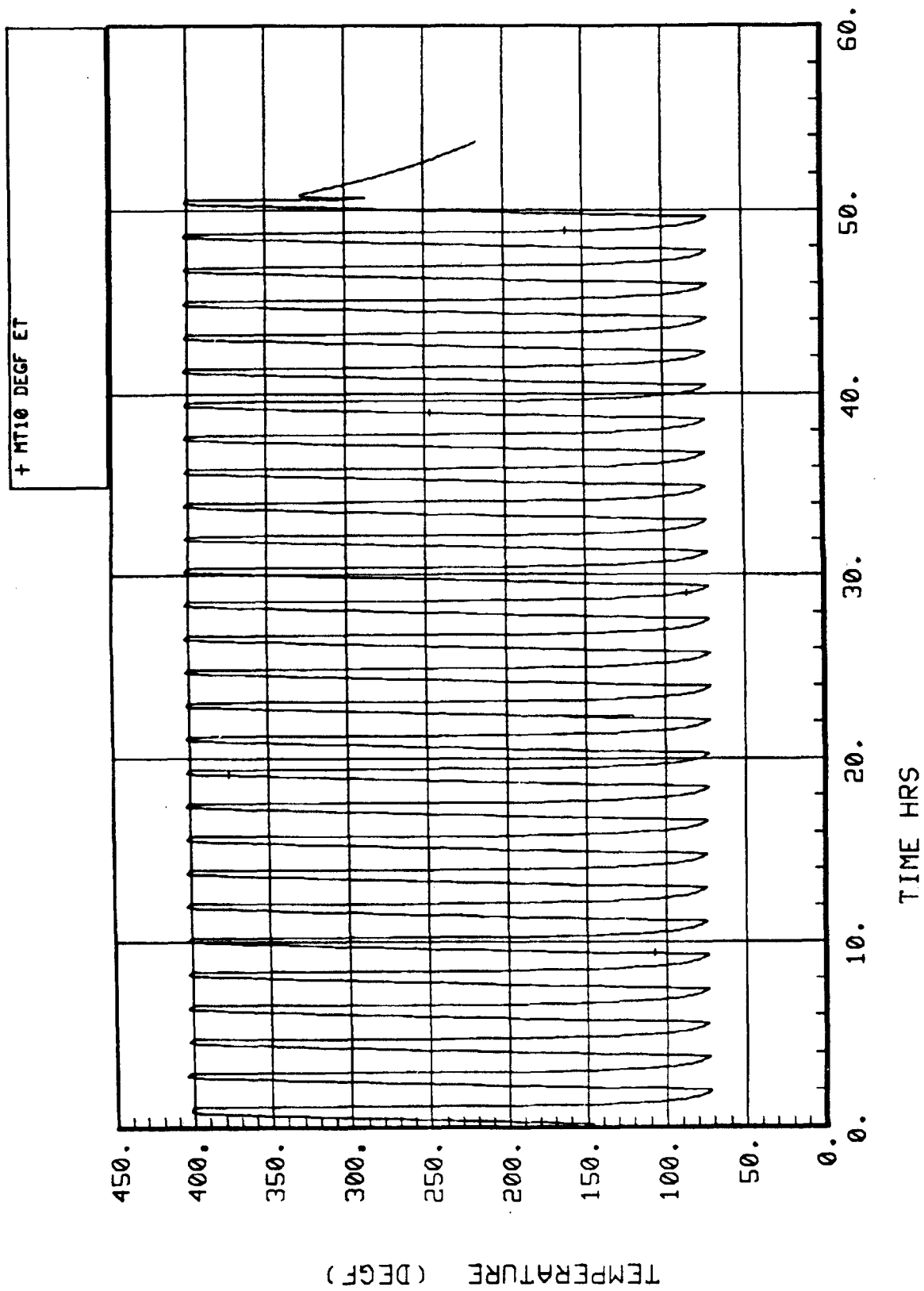


Figure 58. Molecular sieve subsystem sorbent bed 2 temperature MT10.

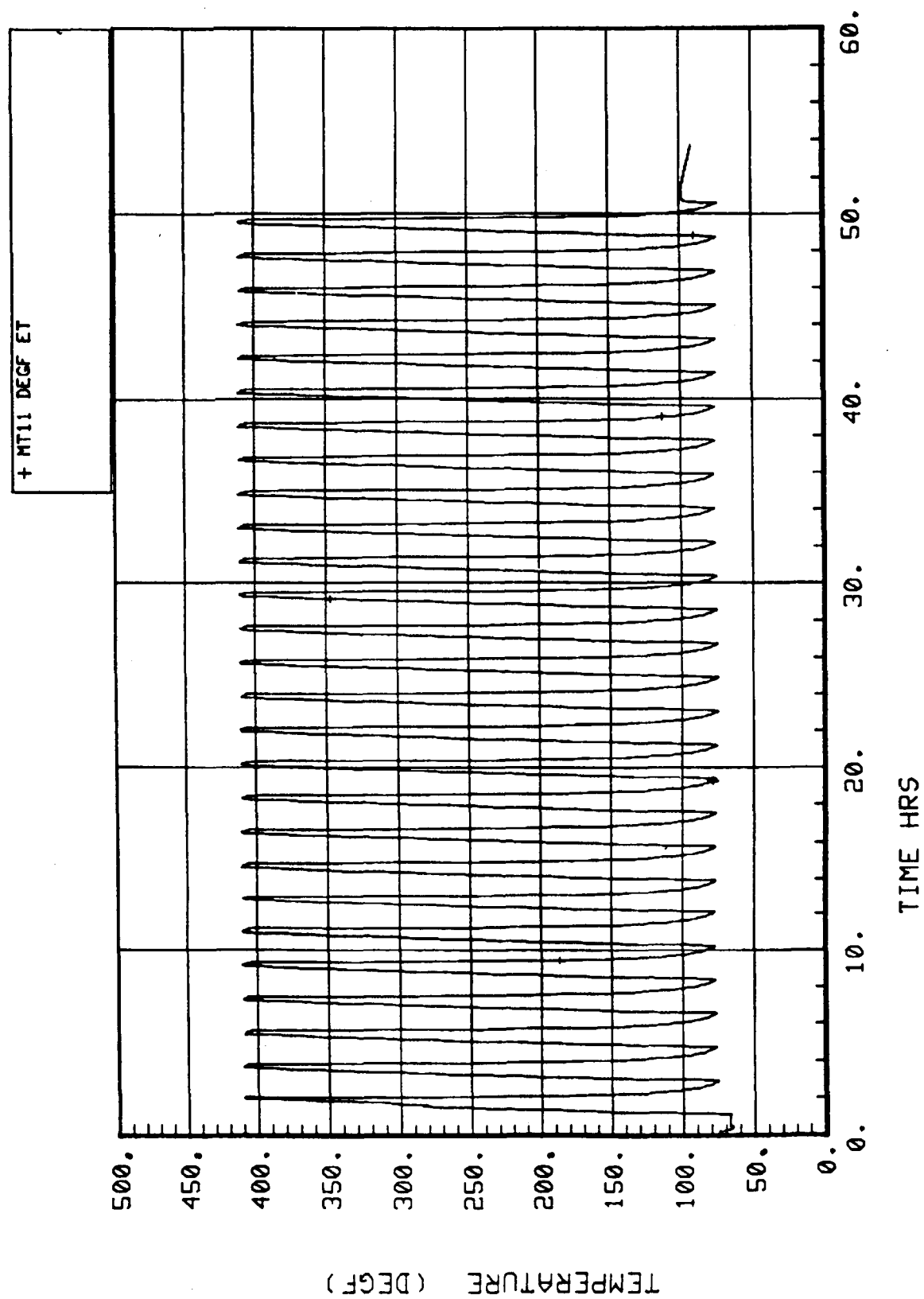


Figure 59. Molecular sieve subsystem sorbent bed 4 temperature MT11.

#### **5.4.2.2.9 Temperature of Air Entering Desiccant Bed 1 During Desorption – MT05**

The desiccant bed 1 inlet air temperature during desorption is shown for a single cycle in Figure 60. At this location the air temperature varies from approximately 80° to 310°F. The plot shows both large and small peaks which correspond with the cycle mode changes. The large peak occurs when the bed is being desorbed of water and has hot air from bed 2 (which had just been desorbed of CO<sub>2</sub> and is being cooled for adsorption) flowing through it. The smaller peak occurs during mode 2 when heat due to adsorption of water vapor reached MT05 even though air was not flowing past the sensor at that time.

#### **5.4.2.2.10 Temperature of Air Entering Desiccant Bed 3 During Desorption – MT08**

The desiccant bed 3 inlet air temperature is shown in Figure 61. The measurement is similar to MT05 except that it is for the alternate half-cycle.

#### **5.4.2.2.11 Temperature of the Desorption Flow from the Sorbent Beds – MT09**

The temperature at MT09 (Fig. 62) varies from approximately 85° to 125°F. The flow at this location initially consists of residual air as the bed pressure is reduced and then the desorbed CO<sub>2</sub>. The heat from the desorbing bed causes a temperature rise; however, due to the reduced pressure (about 1 psia) and the heat loss through uninsulated valves and ducting upstream of the sensor, the temperature increase is mitigated.

#### **5.4.2.2.12 Inlet Air Dewpoint – MDP1**

The dewpoint of the inlet air (Fig. 63) is approximately 48° to 50°F which, when compared with the facility bulk air dewpoint (FD01), shows that the simulator air conditioning unit is reducing the dewpoint by approximately 10°F. The transient spikes and short duration steps are associated with mode changes that send air from a saturated desiccant bed (upward spikes) or fully desorbed bed (downward spikes) past MDP1.

#### **5.4.2.2.13 Dewpoint of Air Downstream of Desiccant Beds – MDP2**

The dewpoint of the air downstream of the desiccant beds (Fig. 64) ranges from -10° to -42°F, indicating water removal by the desiccant. This is somewhat higher than expected, but over the course of the test this measurement was trending downward. The higher readings at the start of the test probably reflect excessive moisture loading resulting from previous short-term operation periods. The drop in dewpoint shows the recovery capability of the desiccant beds. Later leak checks showed that some leakage was occurring at MDP2 which allowed moist chamber air to enter this section of duct.



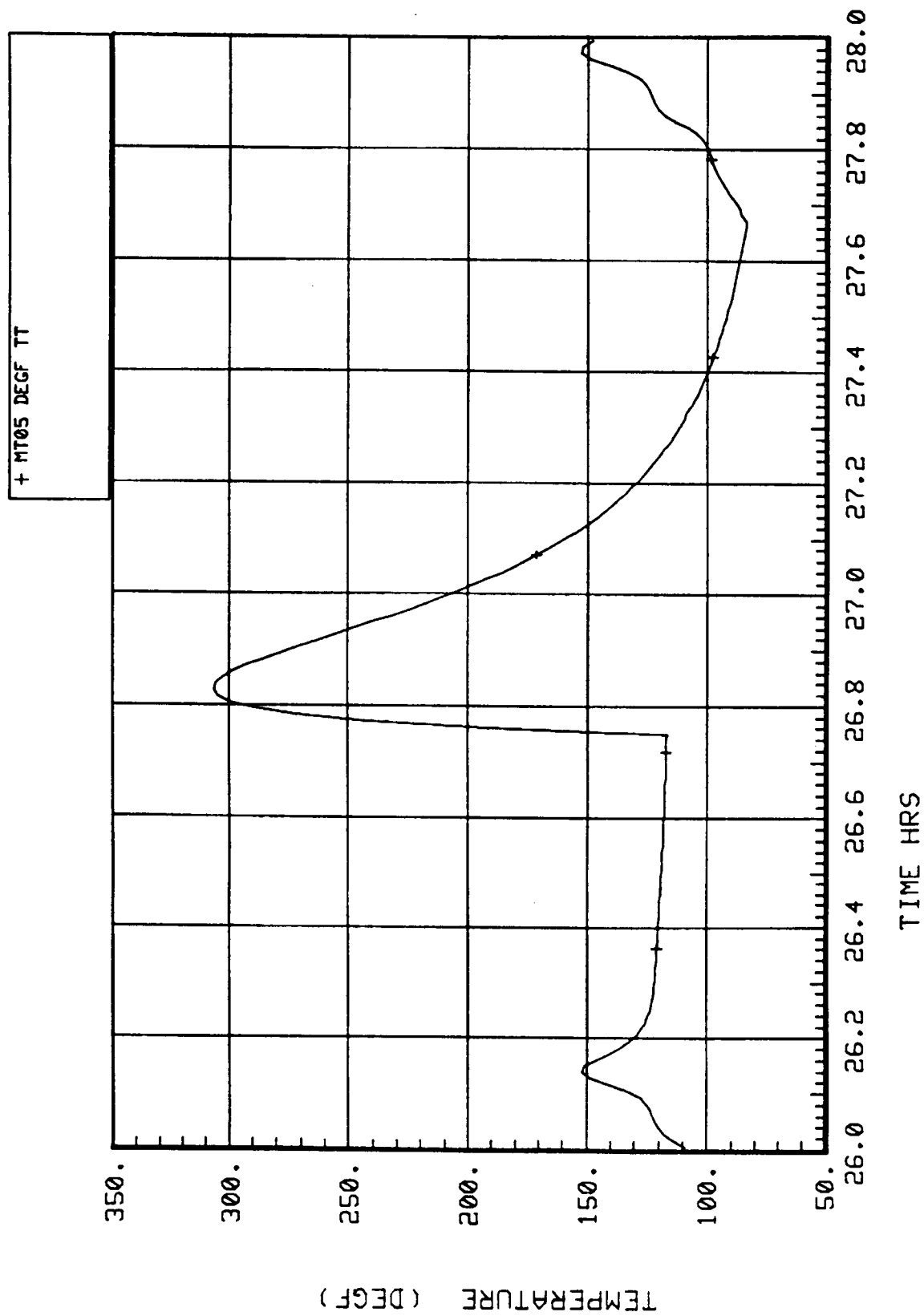


Figure 60. Molecular sieve subsystem desiccant bed 1 in temperature MT05.

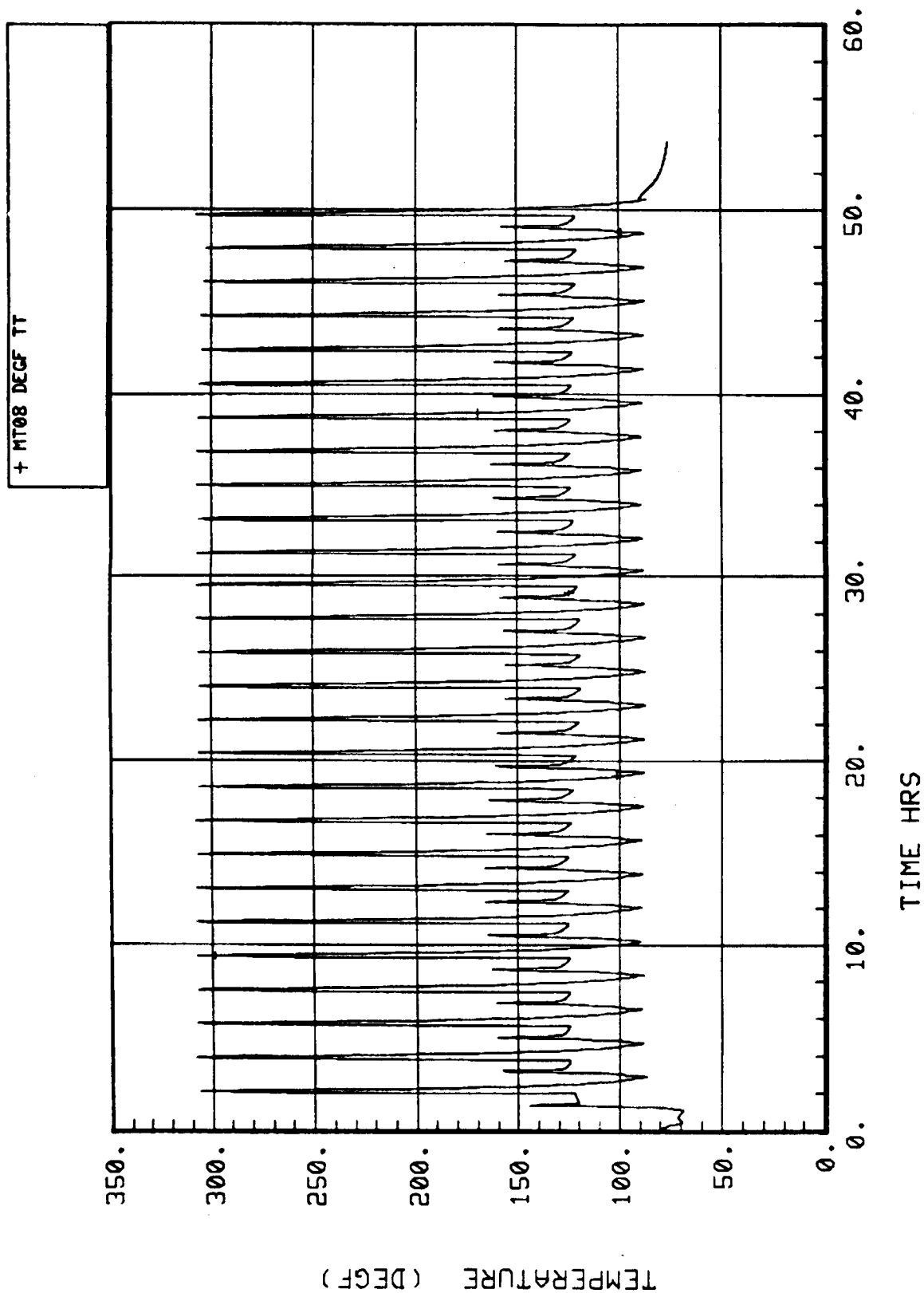


Figure 61. Molecular sieve subsystem desiccant bed 3 in temperature MT08.

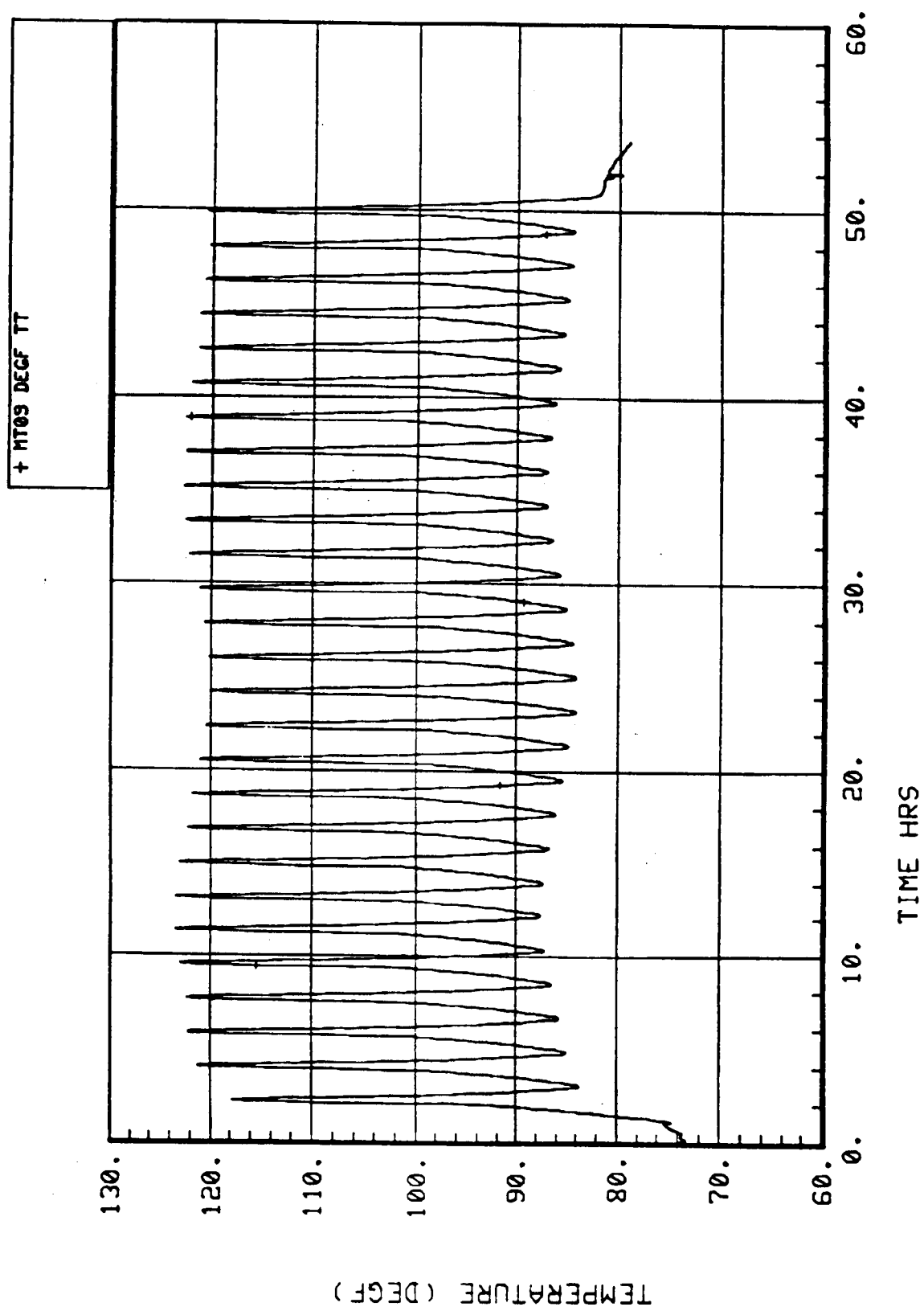


Figure 62. Molecular sieve subsystem desorption flow temperature MT09.

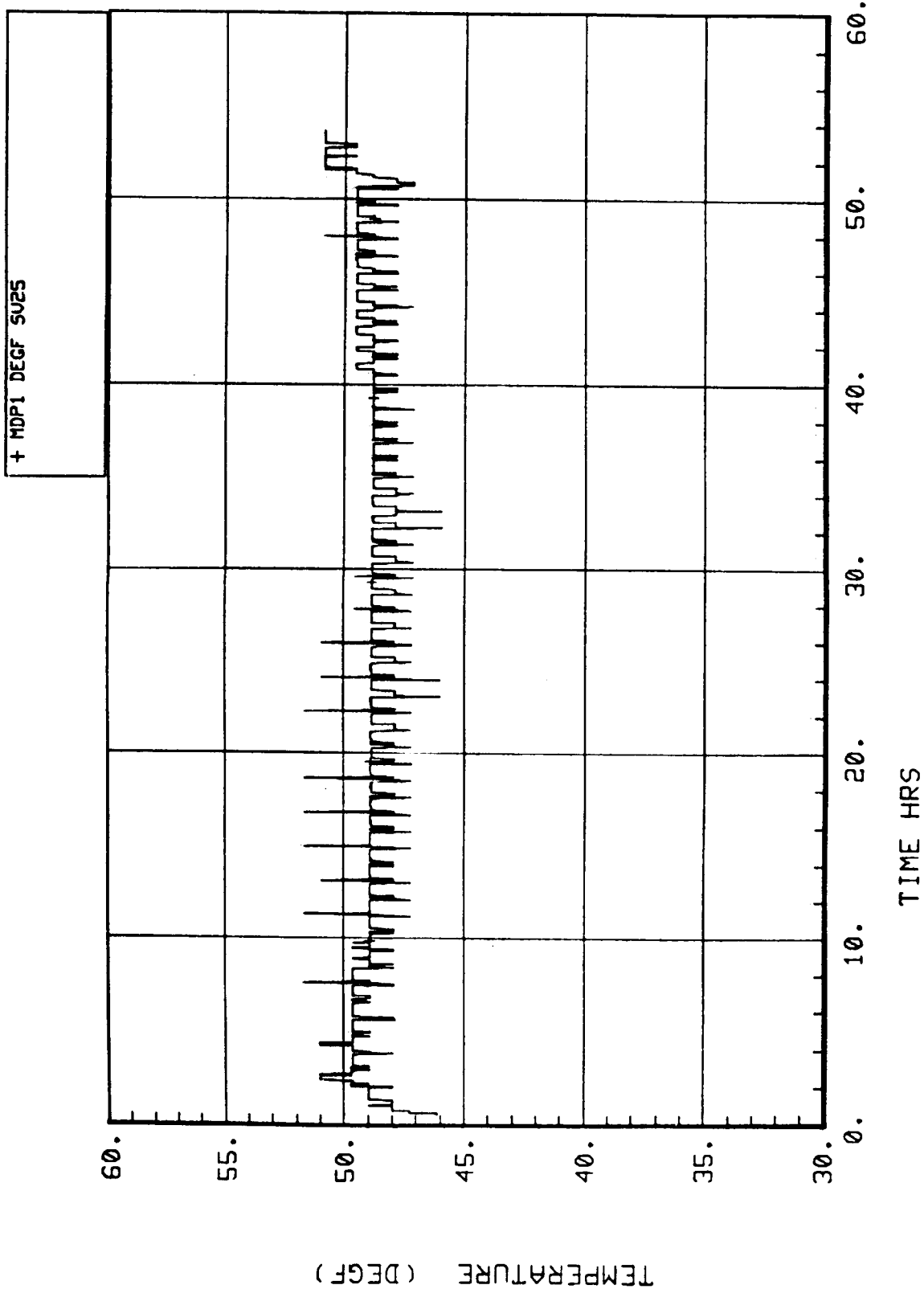


Figure 63. Molecular sieve subsystem inlet air dewpoint MDP1.

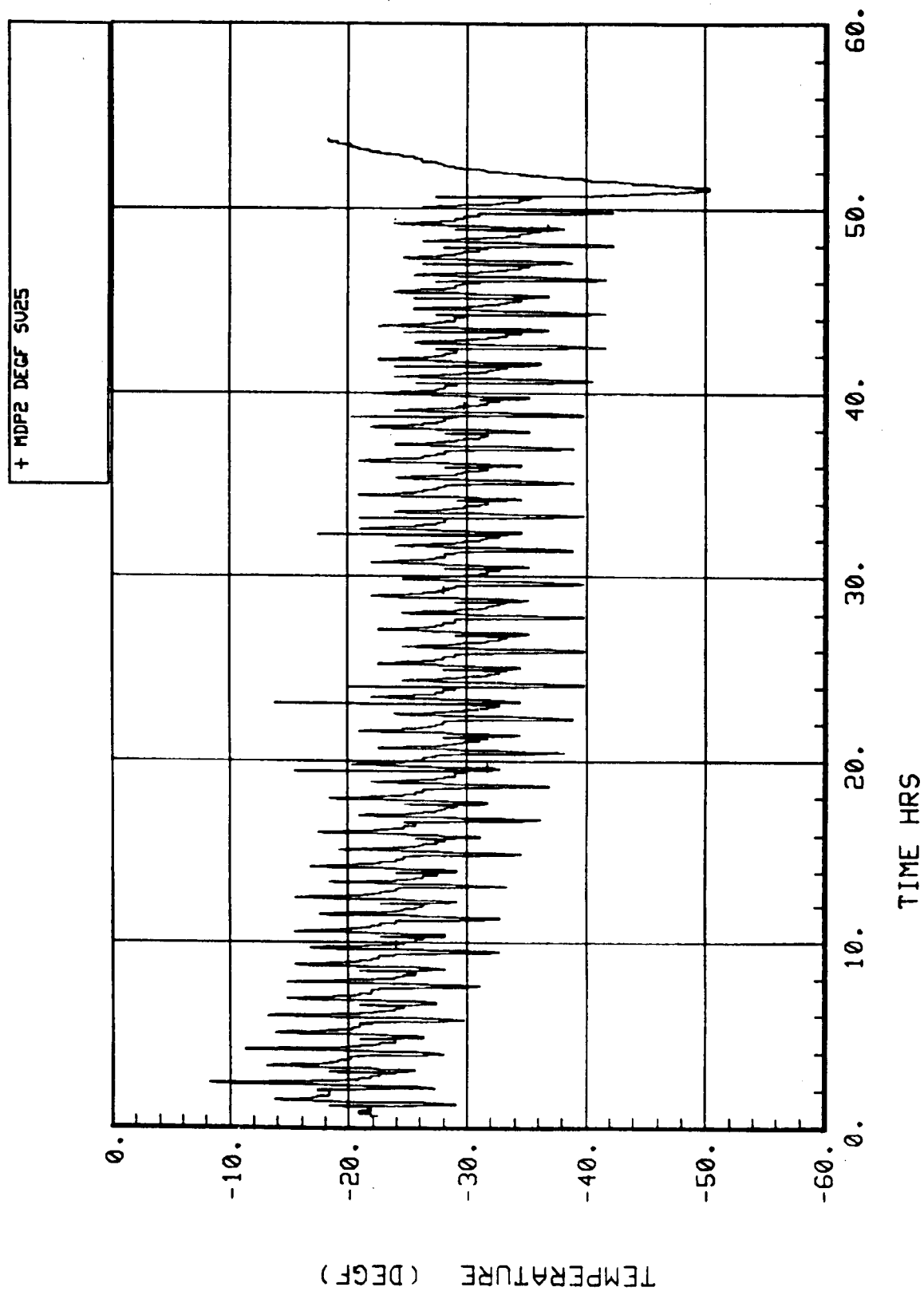


Figure 64. Molecular sieve subsystem desiccant bed dewpoint outlet MDP2.

#### **5.4.2.2.14 Precooler Coolant Inlet Temperature – FT04**

The coolant inlet temperature (Fig. 65) ranges from approximately 45° to 48°F. The day/night variation is apparent as is the variation corresponding to the cycle mode changes (a peak occurs during every half-cycle).

#### **5.4.2.2.15 Precooler Coolant Outlet Temperature – FT05**

The coolant outlet temperature (Fig. 66) ranges from approximately 45° to 55°F. The day/night variation and cycle mode changes are again readily apparent. The temperature rise of the coolant was about 3°F.

#### **5.4.2.2.16 Coolant Flow Rate – FF08**

The coolant flow rate (Fig. 67) was maintained at just under 1.1 gallons per minute for the duration of the test.

#### **5.4.2.2.17 Inlet Air Flow Rate – FF13**

The inlet air flow rate (Fig. 68) was usually in the 84 to 88 lb/hr range. During the recycle portion (11 min) of each half-cycle, however, the air was circulated internally and inlet air flow past the flow sensor was negligible. A slight (2 to 4 lb/hr) increase in flow is noticeable between modes 2 and 4 for each cycle.

#### **5.4.2.2.18 Inlet CO<sub>2</sub> Flow Rate – FF12**

The inlet CO<sub>2</sub> flow rate (Fig. 69) was initially adjusted to approximately 12.3 lb/day. With this inlet flow rate, however, the outlet flow rate was lower than desired, so at 19 hr the flow was increased to approximately 13.8 lb/day. The effect of doing this can be seen on the plot of MP09. The accumulator pressure was leveling off with an average 15 psig when the CO<sub>2</sub> inlet flow was increased. The pressure then increased and leveled off with an average pressure of approximately 17 psig.

#### **5.4.2.2.19 CO<sub>2</sub> Outlet Flow Rate – FF01**

The Molecular Sieve carbon dioxide outlet flow rate is shown in Figure 70. The delivery rate of CO<sub>2</sub> to the Sabatier ranged from approximately 3.9 to 4.8 lb/day. The variations coincide with the cycle mode changes, with peaks occurring during desorption of the CO<sub>2</sub> sorbent beds when pressure in the tank was building up. Two events which are evident in this plot are the shutdowns of the Sabatier, due to a communication failure approximately 8 hr into the test and after taking samples of outlet gases at approximately 28 hr, during which the CO<sub>2</sub> outlet flow was stopped.

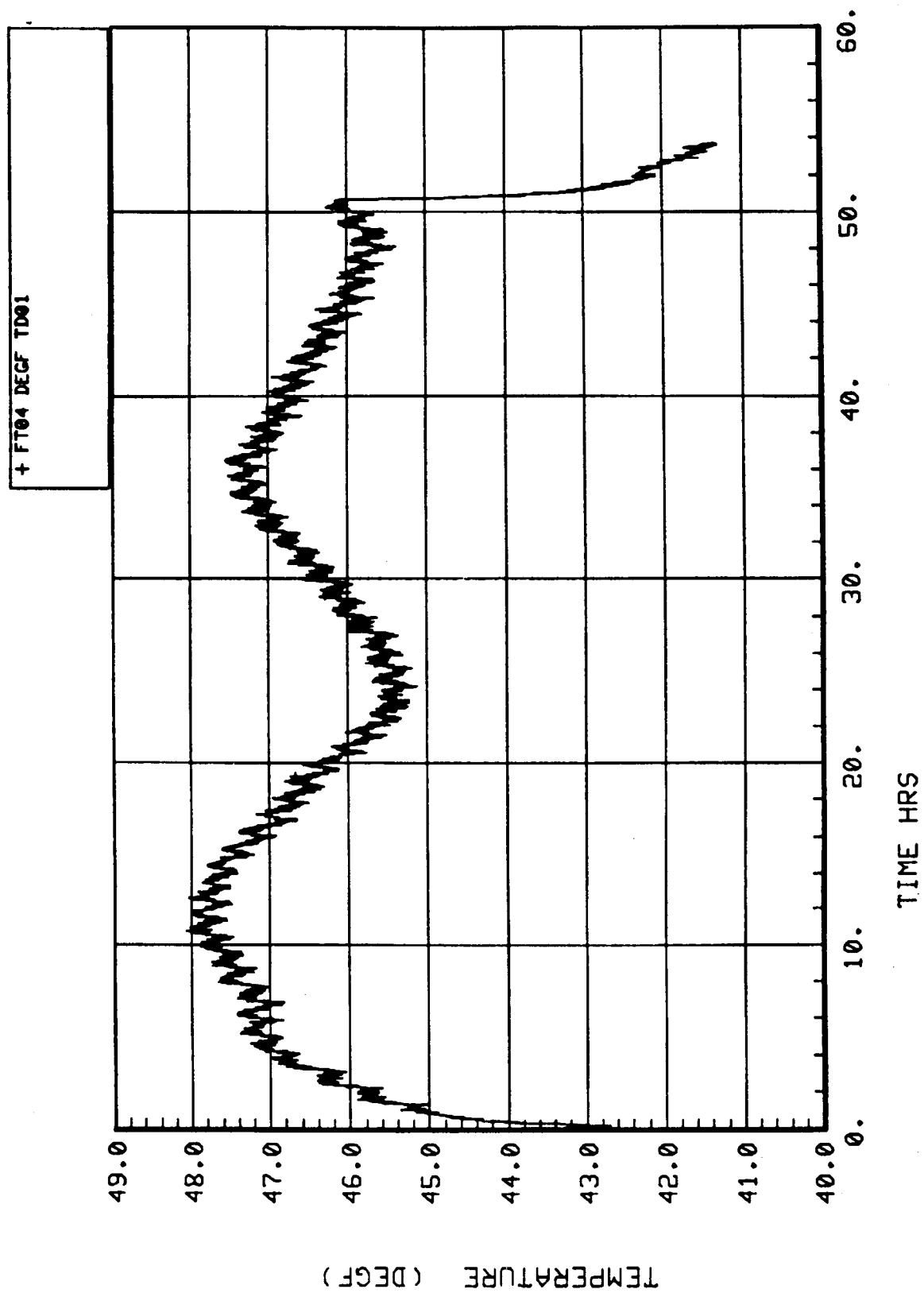


Figure 65. Molecular sieve subsystem coolant inlet temperature FT04.

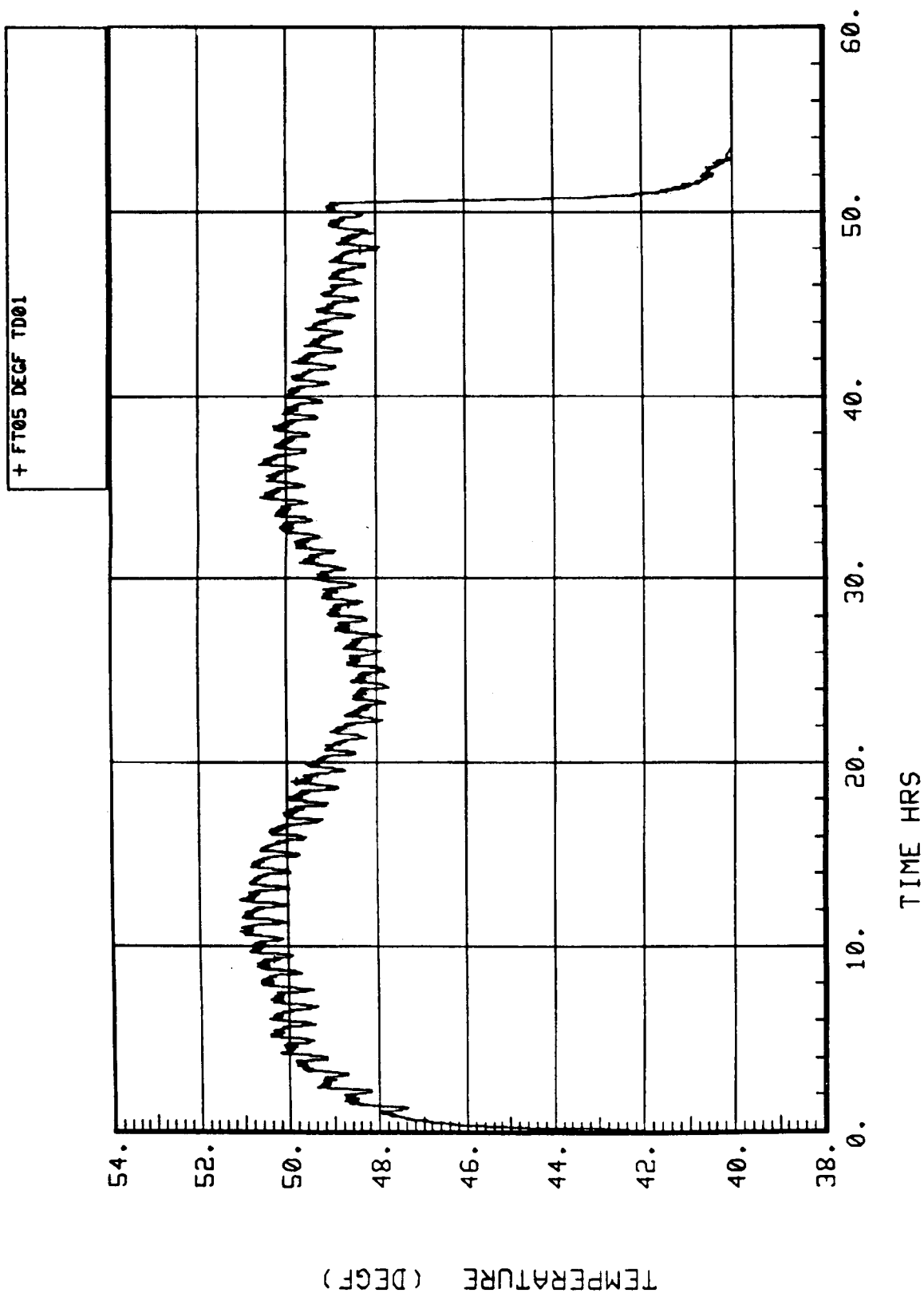


Figure 66. Molecular sieve subsystem coolant outlet temperature FT05.



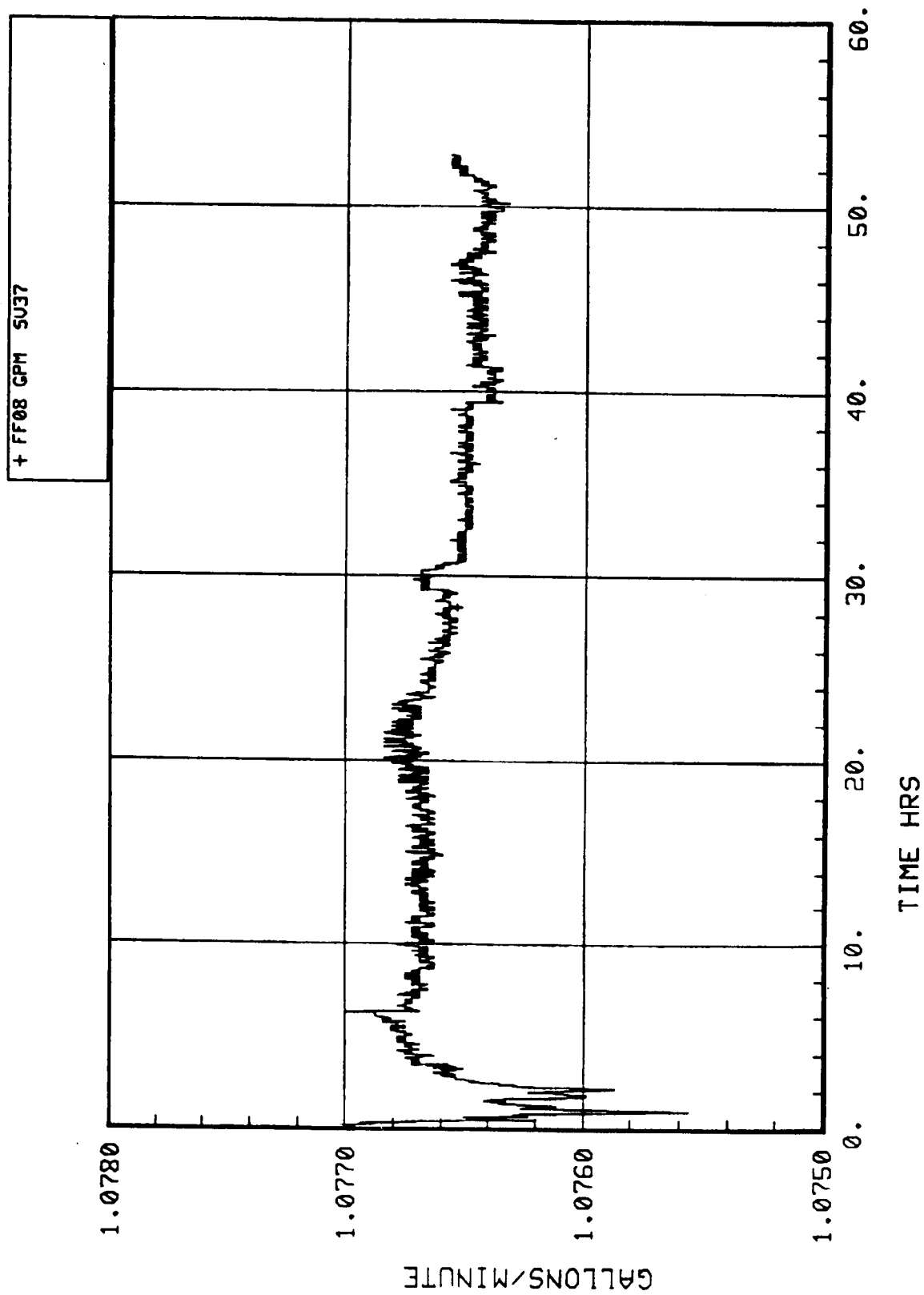


Figure 67. Molecular sieve subsystem coolant flowrate FF08.

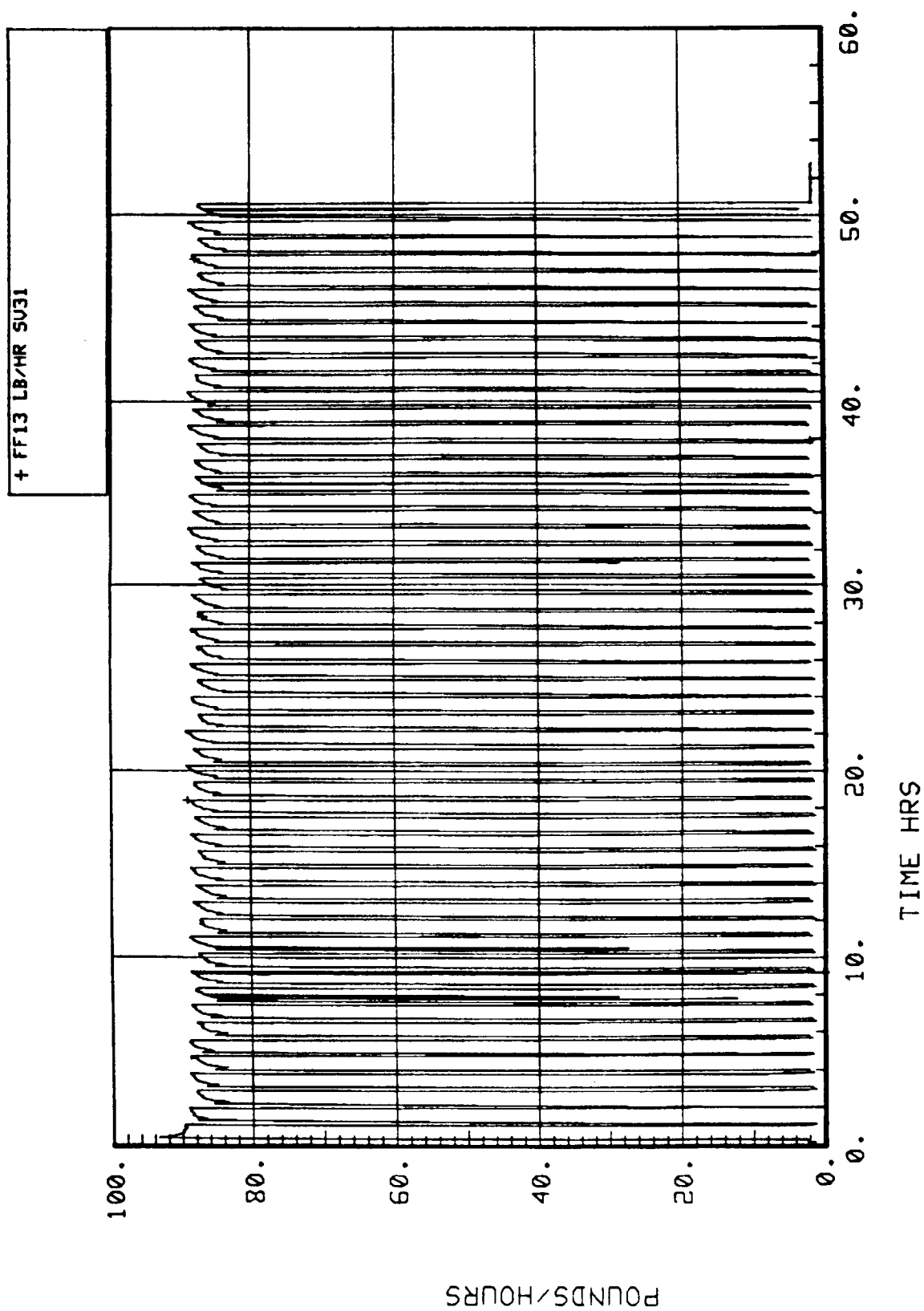


Figure 68. Molecular sieve subsystem inlet air flowrate FF13.

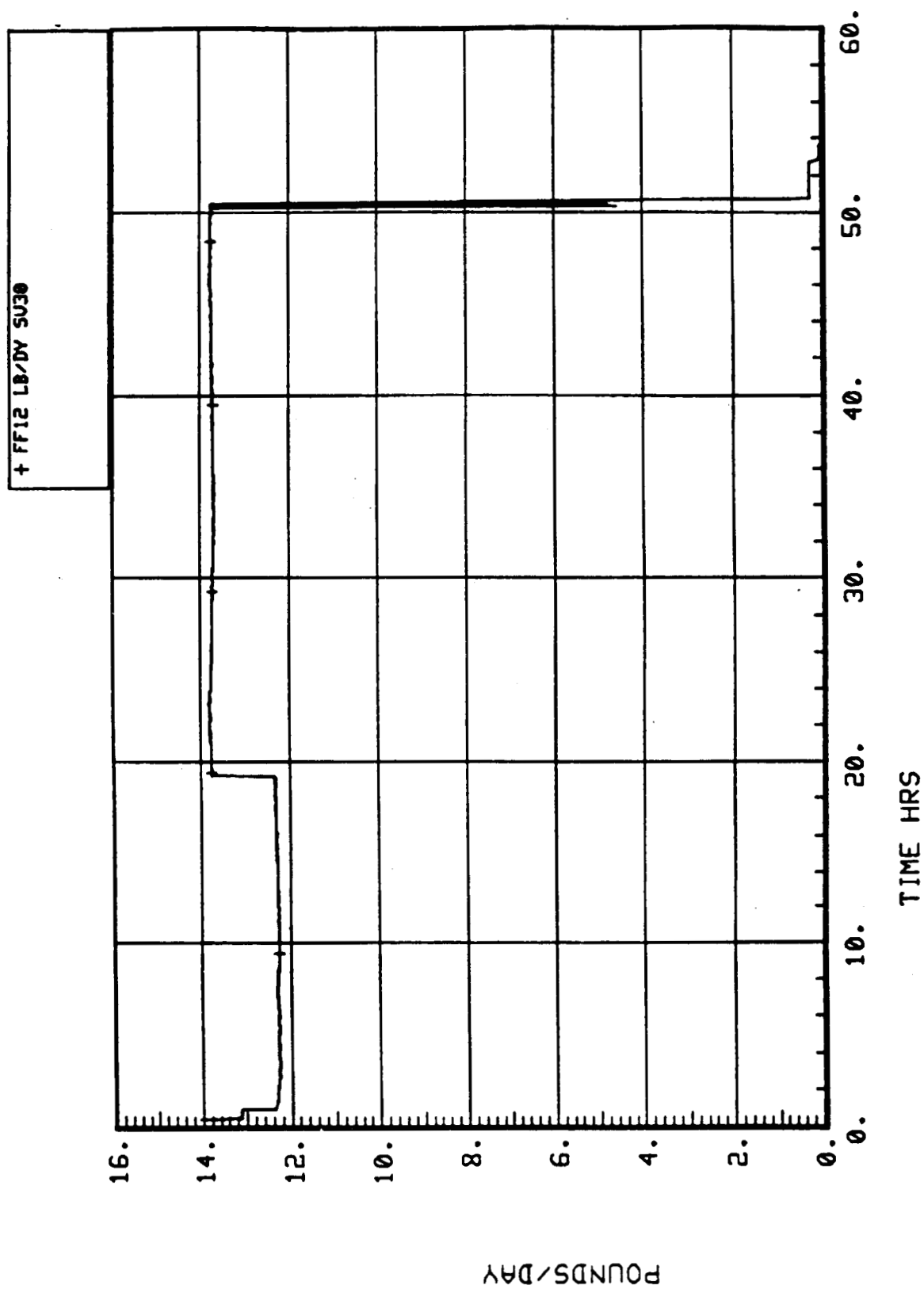


Figure 69. Molecular sieve subsystem inlet CO<sub>2</sub> flowrate FF12.

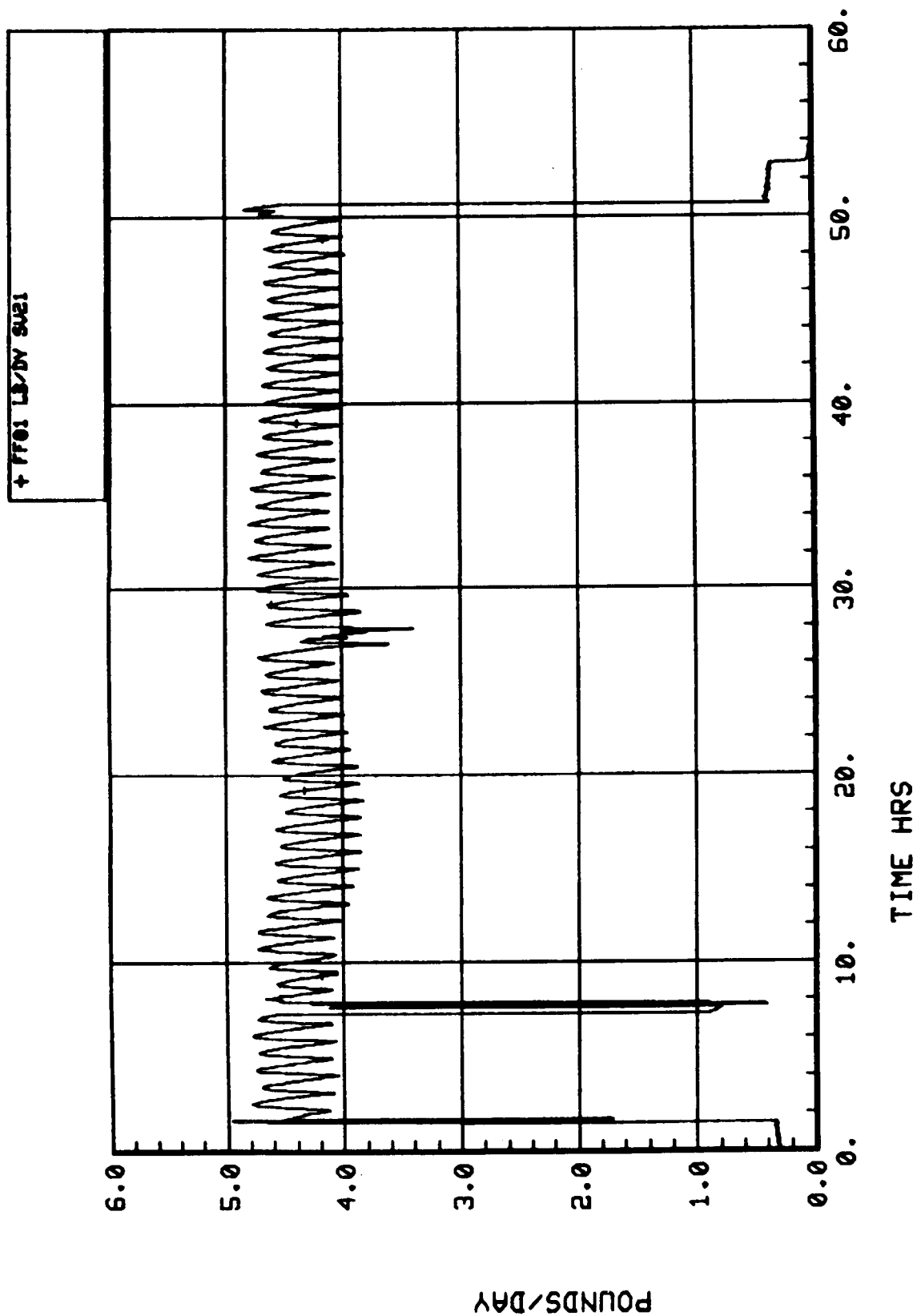


Figure 70. Molecular sieve subsystem outlet CO<sub>2</sub> flowrate FF01.

#### **5.4.2.2.20 Percentage of O<sub>2</sub> in the CO<sub>2</sub> Outlet – FO03**

The plot of O<sub>2</sub> percentage in the CO<sub>2</sub> outlet stream (Fig. 71) shows a general increase which ranges from approximately 0.75 percent at the beginning of the test to 2.45 percent near the end. The CO<sub>2</sub> accumulator tank was initially evacuated and filled with CO<sub>2</sub> from a supply bottle and the increasing CO<sub>2</sub> trend indicates a persistent ingress of air (20 percent O<sub>2</sub> content) throughout the test period. The cyclic peaks (of approximately 0.5 percent) correspond with the mode changes and indicate two possible causes of the overall increase: (1) during desorption the duration of modes 1A and 3A may be too short, allowing residual air to enter the CO<sub>2</sub> accumulator tank; and (2) leakage may be occurring through the five-way valves or associated ducting, with more leakage during modes 3 and 4 than modes 1 and 2. At approximately 8 hr and 28 hr into the test the indicated O<sub>2</sub> percentage drops sharply. These drops also coincide with the two times when the Sabatier subsystem shut down and stopped the flow of CO<sub>2</sub>. The shutdown resulted in flow rate and pressure changes and the change in O<sub>2</sub> percentage reading indicates that the O<sub>2</sub> sensor is flow rate and/or pressure sensitive. Due to this sensitivity, this reading cannot be accepted as absolutely accurate unless these factors are considered.

#### **5.4.2.2.21 Inlet Air CO<sub>2</sub> Partial Pressure – FP12**

The CO<sub>2</sub> inlet flow rate (Fig. 72) was initially set to provide a CO<sub>2</sub> partial pressure of approximately 3.1 mmHg. This was increased after approximately 19 hours and the partial pressure rose to approximately 3.5 mmHg. The sawtooth profile and the peaks are related to air flow changes resulting from mode cycling. The CO<sub>2</sub> was injected at a constant rate into the inlet air, however, during the recycle modes (1 and 3) the amount of air drawn in from the facility air conditioning system was minimal and during mode 1 the concentration of CO<sub>2</sub> increased accordingly. During mode 3, downward spikes occurred which are not presently understood.

#### **5.4.2.2.22 Outlet Air CO<sub>2</sub> Partial Pressure – FP13**

The CO<sub>2</sub> partial pressure (Fig. 73) in the outlet air stream averaged approximately 1.8 mmHg initially and increased to just under 2.0 mmHg after the inlet CO<sub>2</sub> flow was increased at 19 hr into the test. The plot profile shows the effects of mode changes. During mode 1 or 3 (recycle) FP13 is exposed to ambient air the pCO<sub>2</sub> reading drops to 0.6 mmHg (0.079 percent). Upon initiation of mode 2 or 4, a partial pressure spike occurs due to the higher concentration of CO<sub>2</sub> which accumulated in the inlet air duct. As mode 2 or 4 proceeds, the outlet pCO<sub>2</sub> drops and then increases as the CO<sub>2</sub> sorbent becomes saturated.

#### **5.4.2.2.23 Blower Outlet Pressure – MP01**

The Molecular Sieve blower outlet pressure is shown in Figure 74. This plot shows cycle changes varying from approximately 2.02 to 2.5 psig. The changes correspond with the half-cycle time and indicate different pressure losses during different modes. The peaks occur at the beginning of modes 1 and 3 and are at least partially due to the residual air being returned upstream of the blower. The pressure during mode 4 is shown to be lower than during mode 2, indicating a smaller pressure drop through bed 4 and its associated valves and ducting.

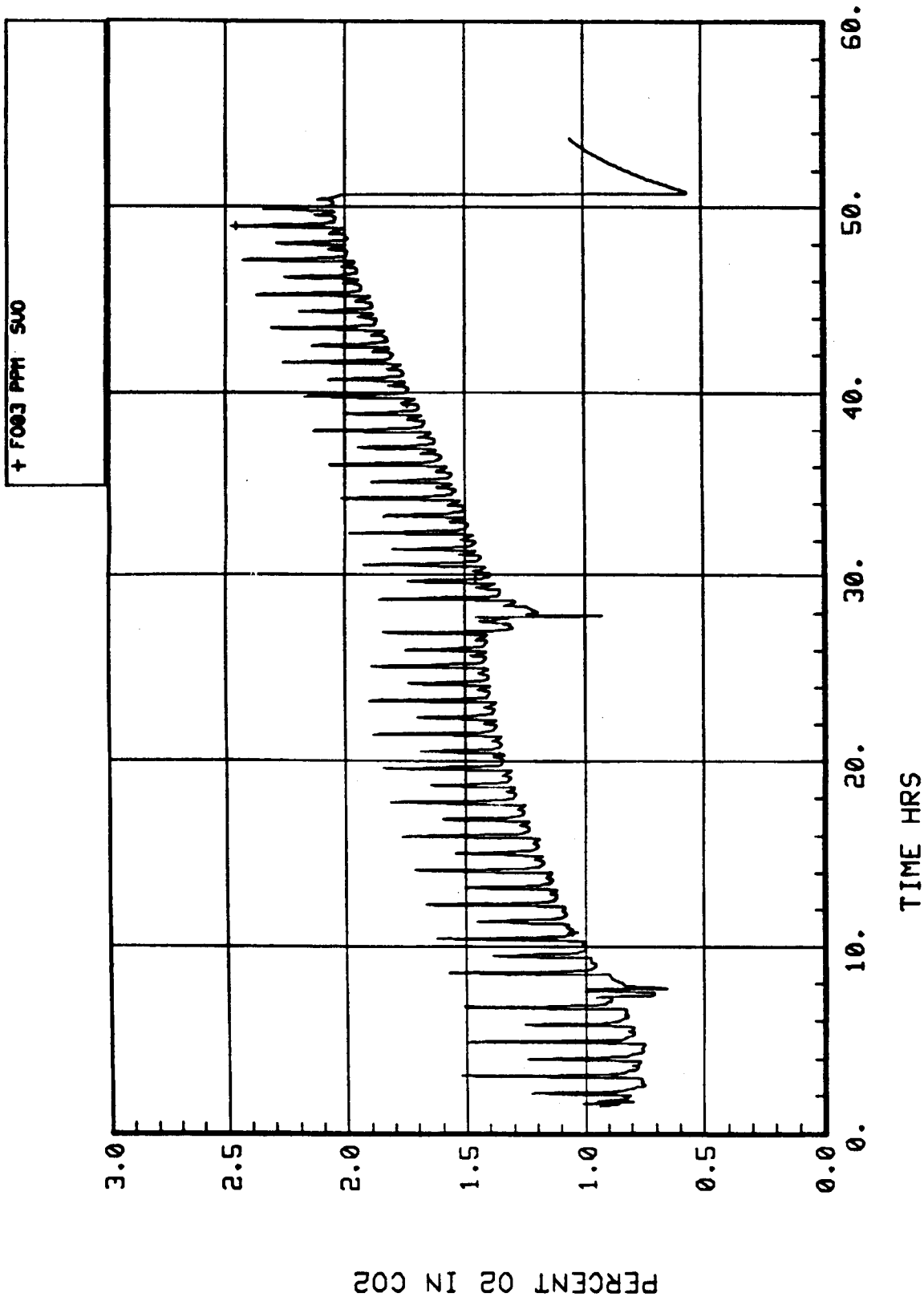


Figure 71. Molecular sieve subsystem O<sub>2</sub> percentage FO03.

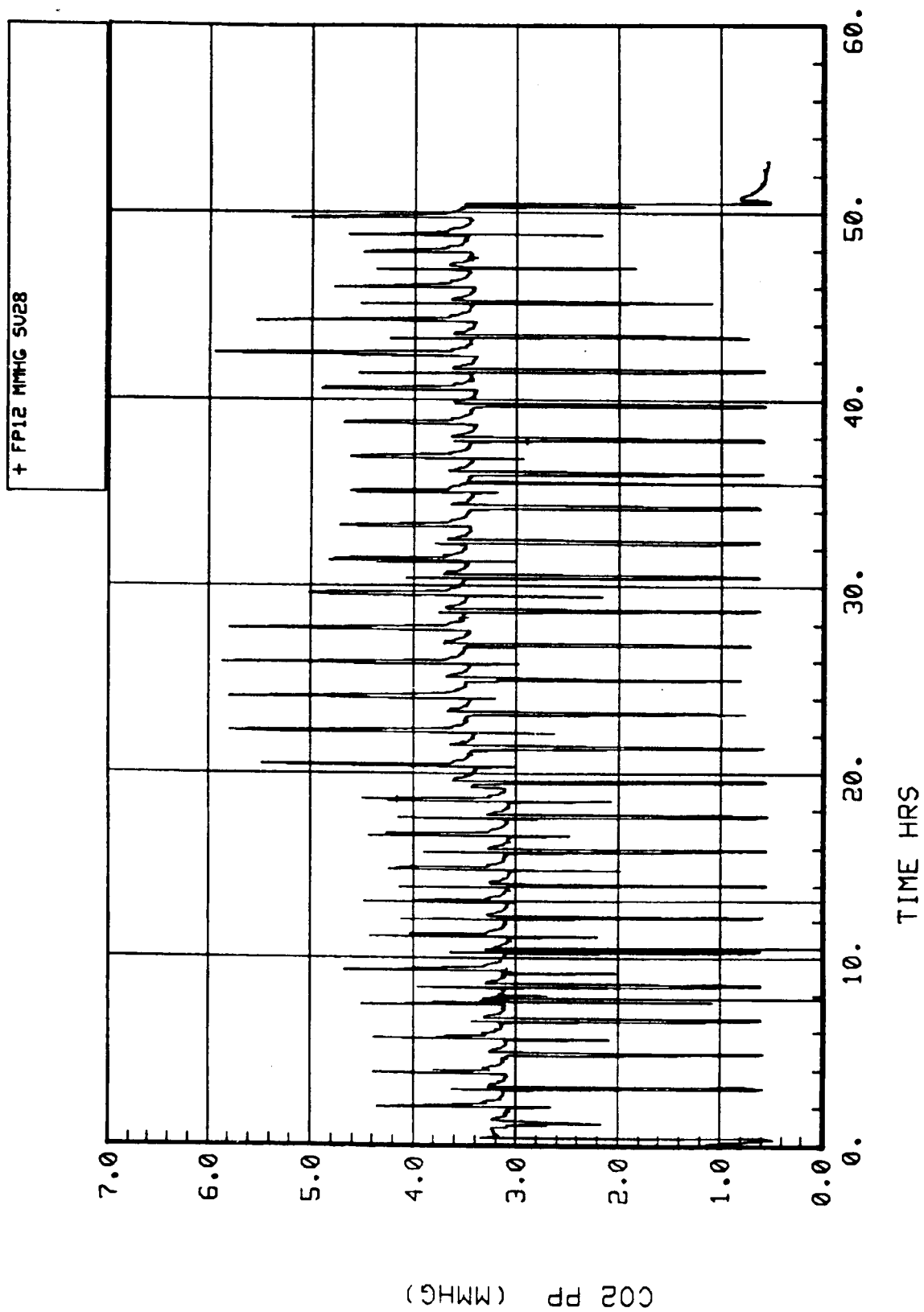


Figure 72. Molecular sieve subsystem inlet CO<sub>2</sub> partial pressure FP12.

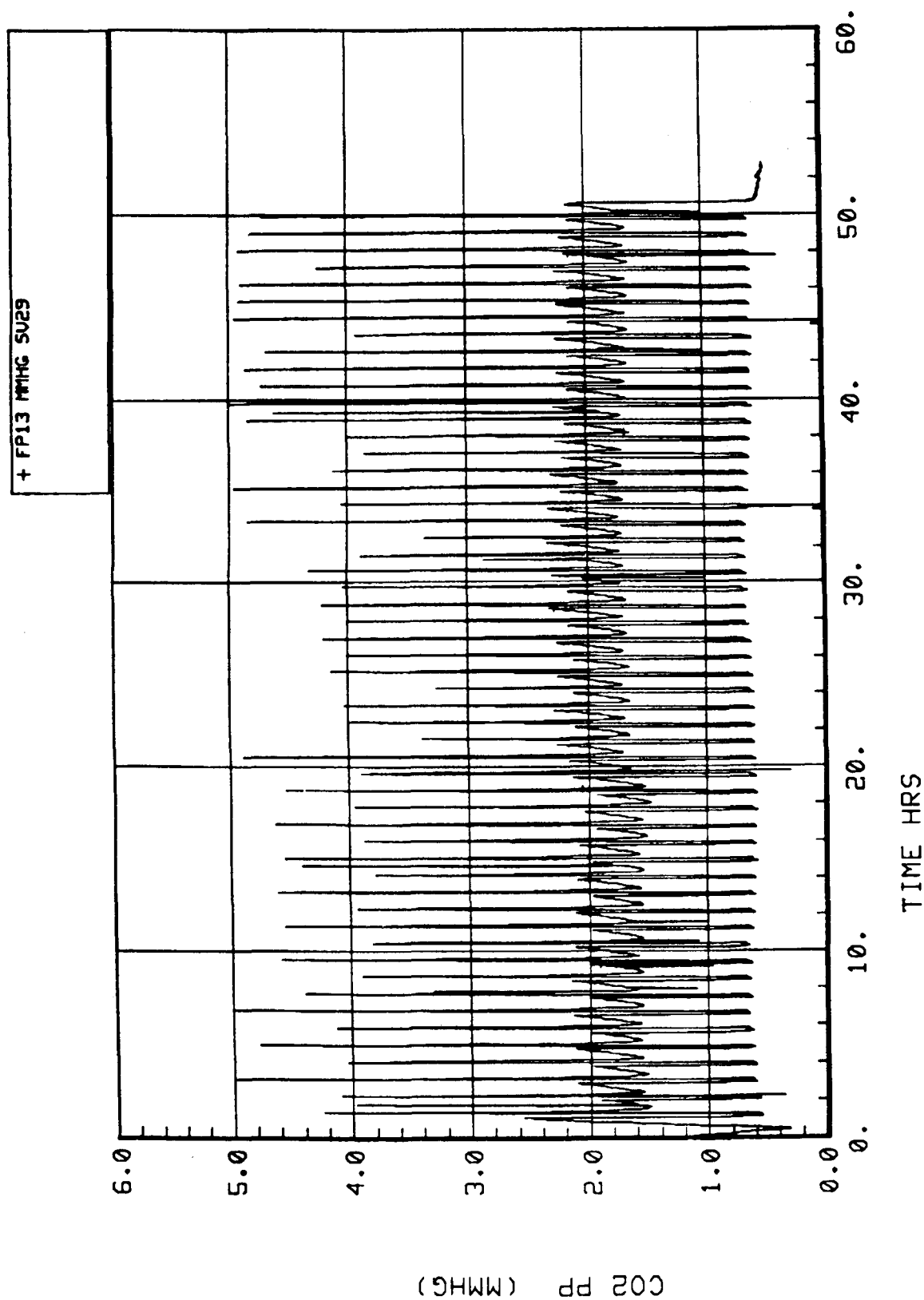


Figure 73. Molecular sieve subsystem outlet CO<sub>2</sub> partial pressure FP13.



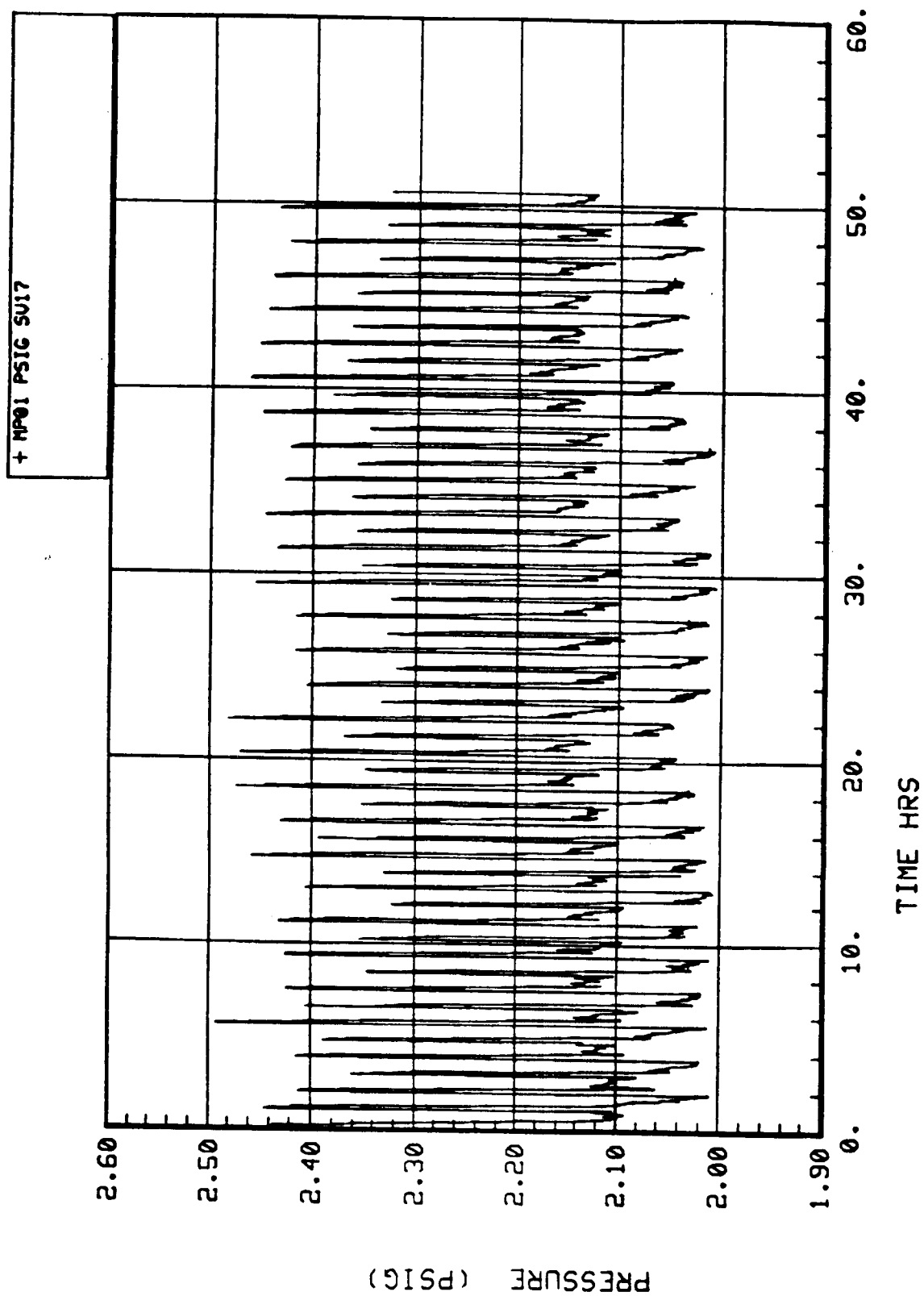


Figure 74. Molecular sieve subsystem fan outlet pressure MP01.

#### **5.4.2.2.24 Desorbing Sorbent Bed Outlet Pressure – MP08**

The Molecular Sieve desorbing sorbent bed outlet pressure is shown in Figure 75. The pressure ranges from approximately 0.8 to 1.5 psia and shows the cyclic changes expected. After 19 hr there is a slight increase which corresponds to an increased amount of CO<sub>2</sub> being adsorbed due to the increased CO<sub>2</sub> injection rate. The peaks correspond with maximum desorption of CO<sub>2</sub> and occur fairly early in modes 2 and 4.

#### **5.4.2.2.25 CO<sub>2</sub> Accumulator Pressure – MP09**

The pressure in the CO<sub>2</sub> accumulator (Fig. 76) ranges from approximately 12 to 19 psig and shows the changes expected due to cyclic desorption of CO<sub>2</sub> with a constant, metered flow rate to the Sabatier. The higher peak at about 8 hr is due to the shutdown of flow to the Sabatier. The drop beginning at 10 hr is not presently understood. The rise beginning at approximately 19 hr is due to increasing the CO<sub>2</sub> injection rate. The drop at approximately 26 hr is due to a sample of the CO<sub>2</sub> being taken for analysis. (The sample line was connected directly to the accumulator tank.) The pressure then returned to the previous range in approximately three cycles.

#### **5.4.2.2.26 Bed 2 and Bed 4 Heater Voltages – MV01 and MV02**

The heater voltage plots (Figs. 77 and 78) show that the voltages to the sorbent bed heaters were either 0 or 26 V, corresponding to the “off” and “on” conditions. Comparison of the two plots shows that the heaters alternated as intended and otherwise operated properly.

### **5.4.3 Recommendations/Lessons Learned**

The results of this test show that the 4BMS does perform its intended function during integrated operation. However, excessive air leakage and heat conduction at various locations resulted in reduced performance and erroneous measurements by some sensors. Sealing the leaks and reducing the effects of heat conduction by modifying the ducts and valves could significantly improve performance and the accuracy of sensor readings.

During review of the test results it became apparent that several changes would need to be made for the following reasons:

Temperature readings at MT06 and MT07 should be near those of MT01, but the upper temperatures were significantly higher. The reason for this is that MT06 and MT07 were located near the five-way valves which conducted heat from the sorbent beds and from the hot air exiting the beds through the ducts to the sensors. Relocation of the sensors is needed to obtain more accurate readings.

The concentration of O<sub>2</sub> in the outlet CO<sub>2</sub> was shown by FO03 to steadily increase as the test proceeded. One possible cause is that not all of the residual air was being pumped out of the sorbent beds by the end of mode 1A or 3A. The duration of the pump down period was 2 min.

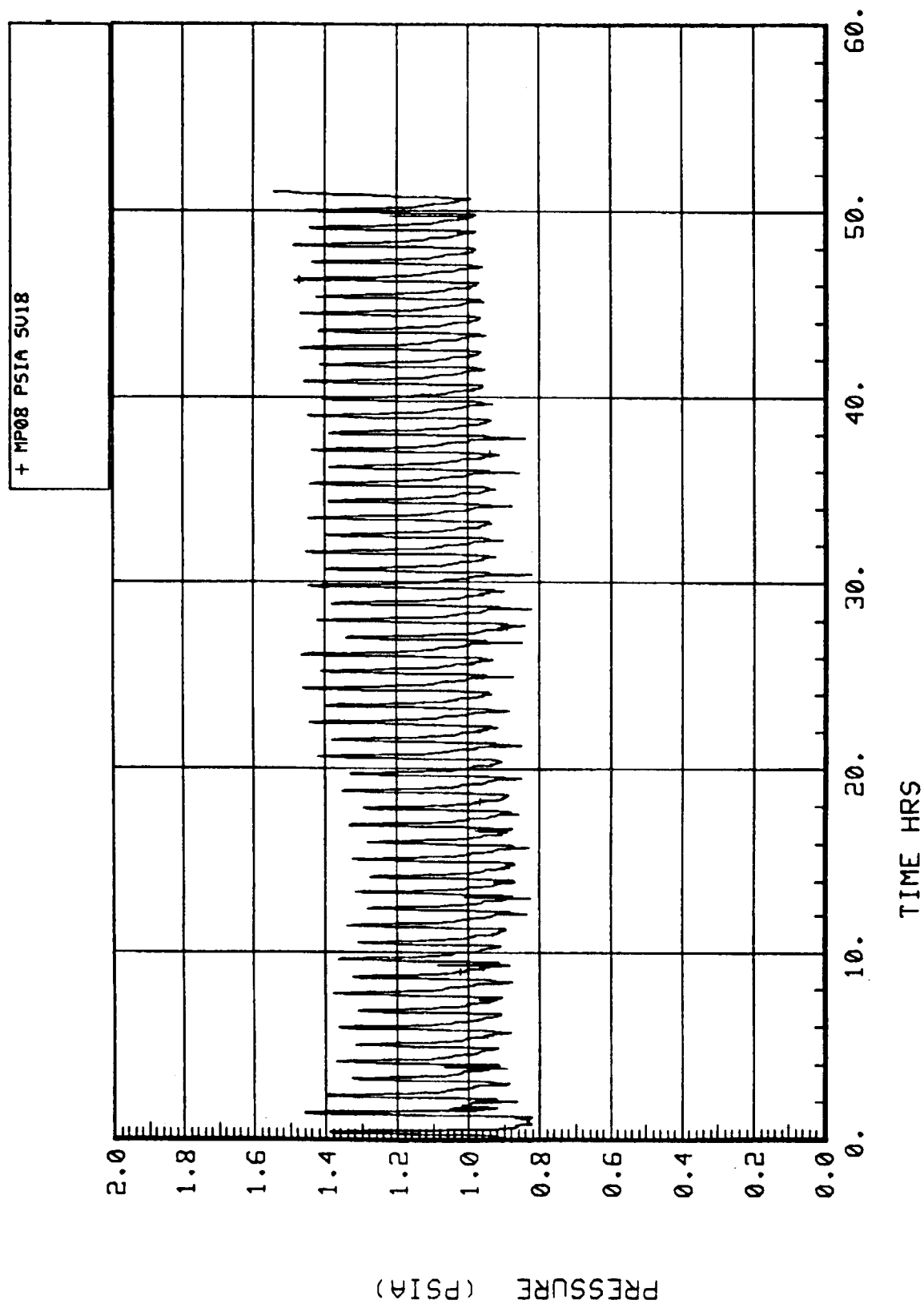


Figure 75. Molecular sieve subsystem sorbent bed outlet pressure MP08.

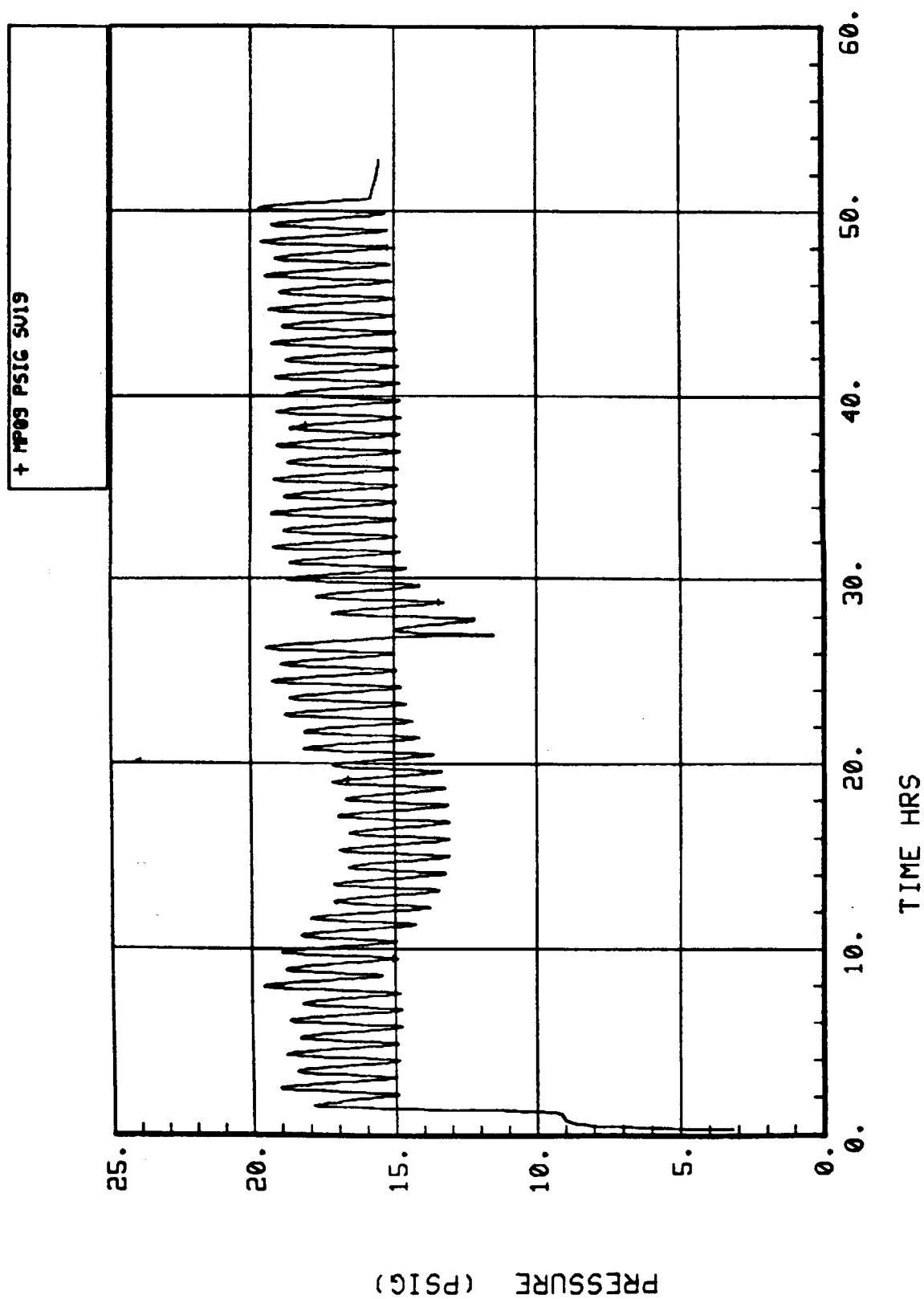


Figure 76. Molecular sieve subsystem CO<sub>2</sub> accumulator pressure MP09.

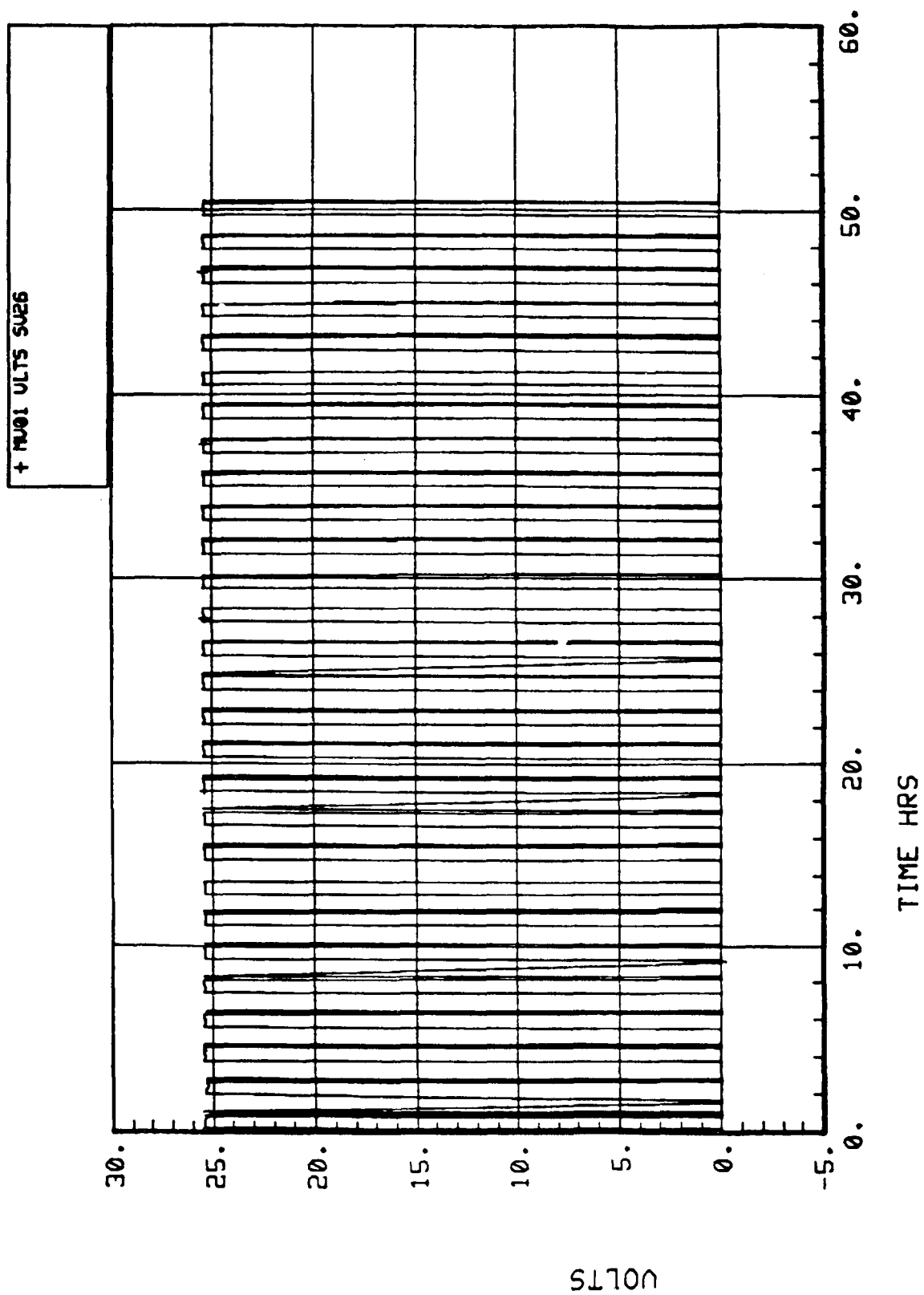


Figure 77. Molecular sieve subsystem bed 2 heater voltage MV01.

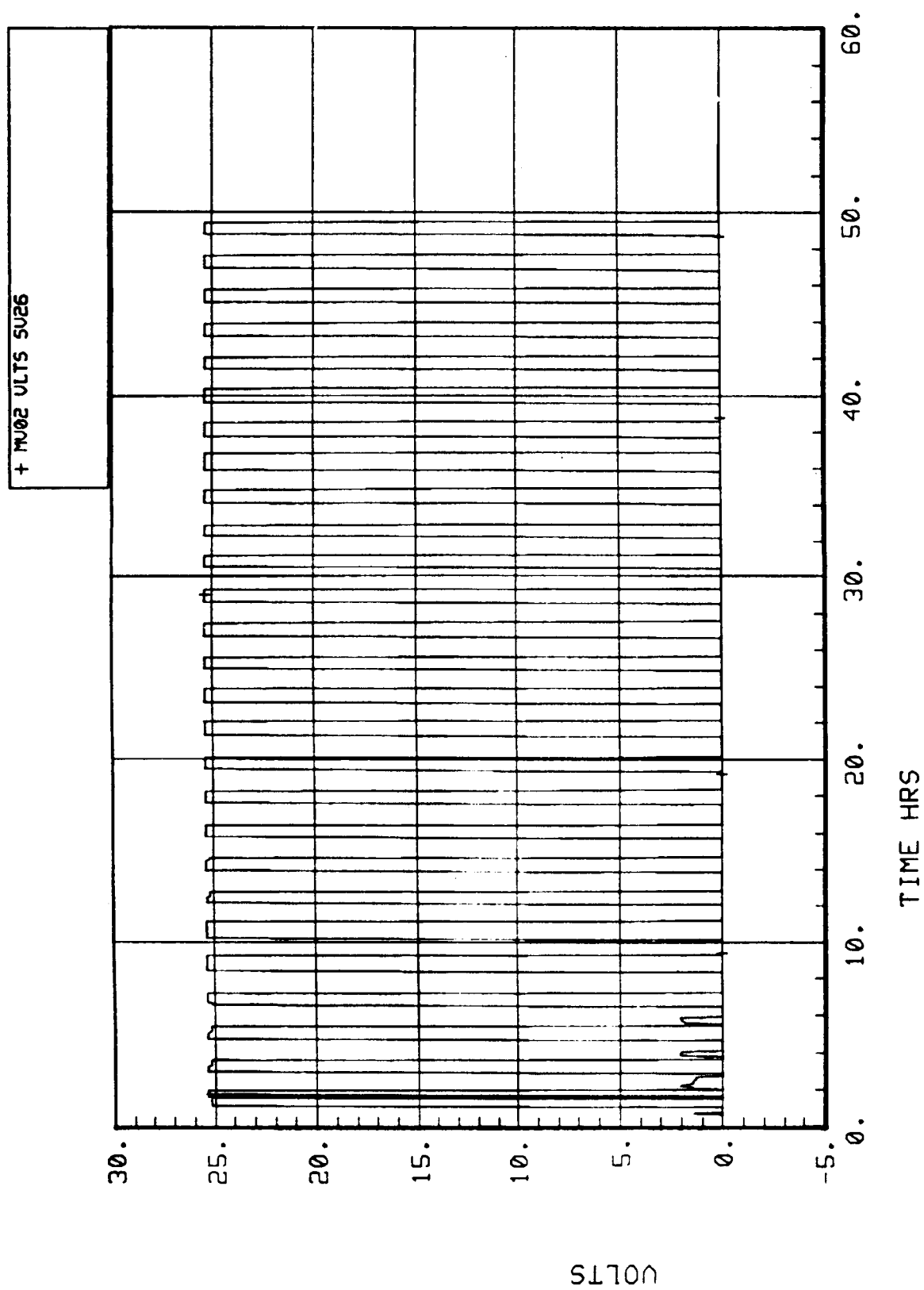


Figure 78. Molecular sieve subsystem bed 4 heater voltage MV02.

Examination of the data indicates that a substantial increase would improve the subsystem performance. Another possible cause is leakage either through valves or connections or both. A leak check done prior to the test indicated very little leakage, but another leak check performed after the test indicated that significant leakage was occurring through valves C and D (Fig. 50). The reason for the disparity is that the valves were not designed for this specific application where hot air (up to 400°F) flows through them. The Skylab Molecular Sieve was desorbed by vacuum only and the valves were not subjected to high temperatures. Repeated exposure to the hot air resulted, over time, in degradation of the seals in the valves. Selection of valves which are suitable for this specific use and changes to the controller to increase the duration of modes 1A and 3A are needed.

The dewpoint measurements at MDP2 were higher than expected. During the leak check performed after the test, it was found that air was leaking around the sensor fitting. While the leakage was small, the effect on the dewpoint was significant. It is important to verify that sensor fittings and duct connections are tight.

In response to these findings, several modifications have been made to the hardware and controller. These are: (1) replacement of the two five-way valves on the CO<sub>2</sub> sorbent beds with six two-way valves and associated ducting modifications, so that hot outlet air does not simultaneously flow through the same valves as the cool inlet air; (2) elimination of MT06 and MT07, since MT01 performs the function of measuring the temperature of the air entering the CO<sub>2</sub> sorbent beds and is a location to get a more accurate reading; and (3) increasing the duration of modes 1A and 3A from 2 min to 7 min to ensure that all of the residual air is removed from the CO<sub>2</sub> sorbent beds.

## **5.5 Trace Contaminant Control Subsystem (TCCS)**

### **5.5.1 Subsystem Description**

The TCCS serves to remove contaminants from the space station cabin which would otherwise build to potentially toxic levels. It consists of a sequence of removal devices each designed to remove a specific type or group of contaminants. A schematic of the TCCS is shown in Figure 79.

Approximately 35 cfm of air is drawn into the inlet duct and passes first through the fixed charcoal bed which contains 48 lb of Barnebey Cheney BD charcoal impregnated with phosphoric acid. The fixed bed controls organic contaminants of high molar volume and ammonia. A differential pressure sensor monitors the pressure drop across the fixed bed fan. After passing through the fixed bed, 25 cfm passes directly to the discharge line. The remaining air is drawn by a fan into the remainder of the system. Another differential pressure sensor monitors the pressure drop across the second fan.

The TCCS has five solenoid valves, CRV-1 through 5. Isolation valves CRV-1 and 2 are normally open, permitting flow into and out of the regenerable charcoal bed. Vacuum valve CRV-3 is normally closed as is vacuum bleed valve CRV-4. The vacuum system which is used in desorption of the regenerable bed has not been used in these tests.

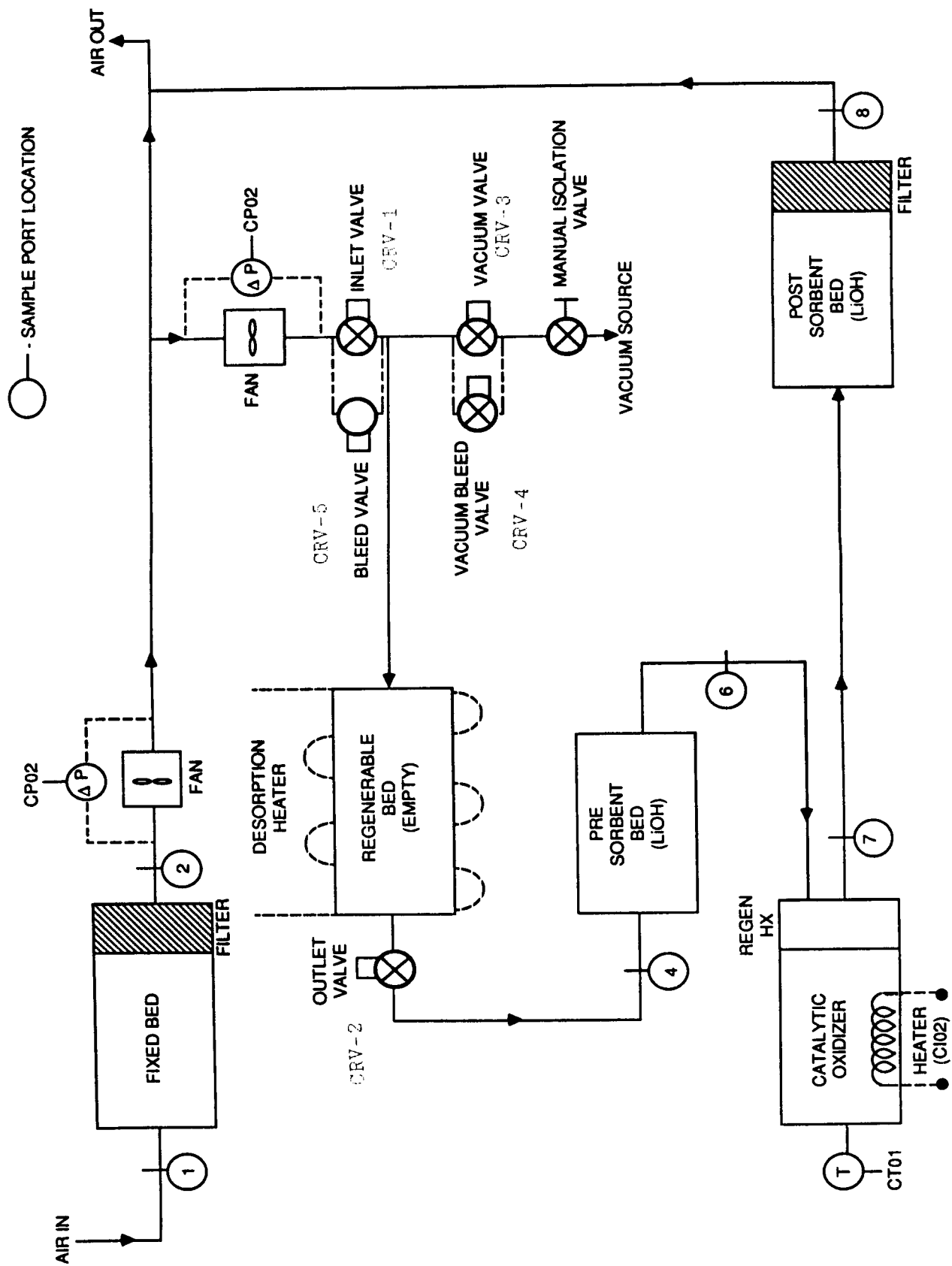


Figure 79. Trace contaminant control subsystem schematic.



Isolation bleed valve CRV-5 is normally closed. All of the air which flows through CRV-1 flows through the empty (not filled with charcoal) regenerable bed and into the pre-sorbent bed to the catalytic oxidizer. The lithium hydroxide in this bed removes acid gases and other potential catalyst poisons.

Next in series is the high temperature catalytic oxidizer equipped with a regenerable heat exchanger. The catalyst bed consists of 900 grams of 1/2 percent palladium deposited on 1/8 in. aluminum pellets. The bed is heated to approximately 680°F; a thermocouple monitors the temperature and initiates an automatic shutdown if it exceeds 950°F. All oxidizable contaminants which were not removed by the charcoal bed (such as methane, carbon monoxide, and hydrogen) are burned at this point. The catalytic oxidizer is well insulated with MIN-K type insulation.

After leaving the catalytic oxidizer, the air is ducted to the post-sorbent bed which contains lithium hydroxide. This bed is designed to remove the toxic products of combustion. The air exiting the post-sorbent bed joins the fixed bed effluent and is discharged to the cabin.

### **5.5.2 Discussion of Results**

The TCCS was operated continuously throughout the duration of the test with no shutdowns. No data plots are included for the several TCCS operational parameters because the data link to the SCATS for this subsystem was not installed at the time of testing. Future tests are planned for this subsystem.

## **6.0 AIR AND WATER SAMPLING RESULTS**

### **6.1 Introduction**

On June 10 and 11, the Martin Marietta Corporation and the Boeing Aerospace Company took water and gas samples during the SIT for chemical analysis. Each contractor took water samples from the following: (1) the TIMES post-treated distillate, (2) the TIMES raw distillate, (3) the TIMES brine, and (4) the Sabatier product water. Also the TIMES post-treated distillate and raw distillate were sampled for microbial analysis. In addition, gas samples were collected from each of the following: (1) the SFES oxygen and hydrogen output streams, (2) the Sabatier product gas vent, and (3) the 4BMS CO<sub>2</sub> product stream. The results of each contractor's water and gas analysis are listed in Tables 3 through 8.

### **6.2 Quality Control**

In order to provide in-house quality control for the water and gas analysis, each laboratory ran a duplicate, blank, known standard, and spiked sample each day for the instrument in use. Precision for each instrument is reported to be  $\pm 5$  percent for all analytical equipment used. Accuracy is  $\pm 10$  percent for all gas and water results listed in Tables 3 through 6.

TABLE 3. RESULTS OF TIMES PRODUCT WATER

Sample date 6/11/87

MM - Martin Marietta Corp.

B - Boeing Aerospace Comp.

Physical	TIMES (Post-Treated)		TIMES RAW	
	Distillate		Distillate	
	MM	B	MM	B
ph	4.6	4.965	3.5	3.321
Cond. (umho/cm)	46	70.3	94	94.9
Total Solids (ppm)	14	35	4	3
Total Sus. Sol. (ppm)	2	0	0	0
Tot. Dis. Sol. (ppm)	12	45	4	15
Turbidity (NTU)	0.26	.01	0.19	.04
Color (Ft/Co)	0	0	5	2
TOC (ppm)	5.3	6.87	32.0	580
TOA (ppm)	< 200	< 10	< 200	37.3
Ammonia (ppm)	< 0.25	.0305	< 0.25	1.45
Ethanol (ppm)	< 1.4	XXX (3)	< 1.4	XXX (3)
Cyanide (ppm)	0.17	.1349	0.49	.1791

ANIONS

Cl- (ppm)	11.1	8.16	2.65	13.96
F- (ppm)	< 0.5	< .050	9.3	.972
I- (ppm)	(1) XXX	< .1	(1) XXX	< .1
I (ppm)	< 0.5	< .1	< 0.5	< .1
NO3- (ppm)	< 0.5	< .050	< 0.5	4.33
SO4(-2) (ppm)	< 0.5	.14	< 0.5	2870

METALS

As (ppm)	< 0.005	< .023	< 0.005	< .023
Ba (ppm)	< 0.5	< .026	< 0.5	< .026
Ca (ppm)	0.02	.806	0.02	1.168
Cr (ppm)	< 0.025	.008	< 0.025	.006
Cu (ppm)	< 0.5	.092	< 0.5	.301
Fe (ppm)	< 0.15	.064	< 0.15	.087
Pb (ppm)	< 0.07	.017	< 0.07	.04
Hg (ppm)	< 0.005	<.00005	< 0.005	< .81
Mn (ppm)	< 0.025	.002	< 0.025	.003
Mg (ppm)	0.03	.115	0.04	.229
Ni (ppm)	< 0.025	.013	< 0.025	.014
K (ppm)	< 170	.022	< 170	5.938
Se (ppm)	< 0.005	<.000014	< 0.005	< .0004
Ag (ppm)	< 0.02	.015	< 0.02	.015
Zn (ppm)	< 2.5	.044	< 2.5	.116

TABLE 3. (Concluded)

VOLATILE ORGANICS	TIMES (Post-Treated)		TIMES RAW	
	Distillate		Distillate	
	MM	B (3)	MM	B (3)
Bromodichlormethane (ppb)	< 5	XXXX	< 5	XXXX
Bromoform (ppb)	< 5	XXXX	< 5	XXXX
Bromomethane (ppb)	< 10	XXXX	< 10	XXXX
Carbon tetrachloride (ppb)	< 5	XXXX	< 5	XXXX
Chlorobenzene (ppb)	< 5	XXXX	< 5	XXXX
Chloroethane (ppb)	< 10	XXXX	< 10	XXXX
2-Chloroethylvinyl ether (ppb)	< 10	XXXX	< 10	XXXX
Chloroform (ppb)	< 5	XXXX	470	XXXX
Chloromethane (ppb)	< 5	XXXX	< 5	XXXX
Dibromochloromethane (ppb)	< 5	XXXX	< 5	XXXX
1,2-Dichlorobenzene (ppb)	< 5	XXXX	< 5	XXXX
1,3-Dichlorobenzene (ppb)	< 5	XXXX	< 5	XXXX
1,4-Dichlorobenzene (ppb)	< 5	XXXX	< 5	XXXX
Dichlorodifluoromethane (ppb)	< 10	XXXX	< 10	XXXX
1,1-Dichloroethane (ppb)	< 5	XXXX	< 5	XXXX
1,2-Dichloroethane (ppb)	< 5	XXXX	< 5	XXXX
1,1-Dichloroethene (ppb)	< 5	XXXX	< 5	XXXX
trans-1,2-Dichloroethene (ppb)	< 5	XXXX	< 5	XXXX
1,2-Dichloropropane (ppb)	< 5	XXXX	< 5	XXXX
cis-1,3-Dichloropropene (ppb)	< 5	XXXX	< 5	XXXX
trans-1,3-Dichloropropene (ppb)	< 5	XXXX	< 5	XXXX
Methylene chloride (ppb)	< 5	XXXX	< 5	XXXX
1,1,2,2-Tetrachloroethane (ppb)	< 5	XXXX	< 5	XXXX
Tetrachloroethene (ppb)	< 5	XXXX	< 5	XXXX
1,1,1-Trichloroethane (ppb)	< 5	XXXX	< 5	XXXX
1,1,2-Trichloroethane (ppb)	< 5	XXXX	< 5	XXXX
Trichloroethene (ppb)	< 5	XXXX	< 5	XXXX
Trichlorofluoromethane (ppb)	< 5	XXXX	< 5	XXXX
Vinyl chloride (ppb)	< 10	XXXX	< 10	XXXX

XXXX- Refer to designated footnote at end of section.

TABLE 4. RESULTS OF TIMES BRINE SOLUTION

Sample date 6/11/87

MM - Martin Marietta Corp.

B - Boeing Aerospace Comp.

Physicals

	<u>TIMES</u> <u>BRINE</u>	
	<u>MM</u>	<u>B</u>
pH	2.1	1.913
Cond. (umho/cm)	> 20000	100712
Total Solids (ppm)	213714	168470
Total Sus. Sol. (ppm)	1350	254
Total Dis. Sol. (ppm)	212354	176940
Turbidity (NTU)	9.1	7.24
Color (Pt/Co)	(2) 4250	1375
TOC (ppm)	31821	30200
TOA (ppm)	3030	2696
Ammonia (ppm)	5000	1.016
Ethanol (ppm)	< 1.4	XXX (3)
Cyanide (ppm)	< 0.1	.1527

ANIONS

Cl- (ppm)	26280	19520
F- (ppm)	274	.3192
I- (ppm)	(1) XXX	< .7
I (ppm)	(4) XXX	.7
NO3- (ppm)	223	292.4
SO4(-2) (ppm)	53820	64480

METALS

As (ppm)	< 0.005	3.5
Ba (ppm)	< 0.5	< .026
Ca (ppm)	266	224
Cr (ppm)	4.04	3.19
Cu (ppm)	5.56	5.57
Fe (ppm)	16.69	.01348
Pb (ppm)	6.23	5.9
Hg (ppm)	< 0.005	.0012
Mn (ppm)	0.54	.31
Mg (ppm)	675	652
Ni (ppm)	2.55	2.16
K (ppm)	47000	XXX (3)
Se (ppm)	< 0.005	.0445
Ag (ppm)	0.17	.29
Zn (ppm)	4.97	4.13

TABLE 4. (Concluded)

VOLATILE ORGANICS	BRINE	
	MM	B (3)
Bromodichlormethane (ppb)	< 5	XXXX
Bromoform (ppb)	< 5	XXXX
Bromomethane (ppb)	< 10	XXXX
Carbon tetrachloride (ppb)	< 5	XXXX
Chlorobenzene (ppb)	< 5	XXXX
Chloroethane (ppb)	< 10	XXXX
2-Chloroethylvinyl ether (ppb)	< 10	XXXX
Chloroform (ppb)	210	XXXX
Chloromethane (ppb)	< 5	XXXX
Dibromochloromethane (ppb)	< 5	XXXX
1,2-Dichlorobenzene (ppb)	< 5	XXXX
1,3-Dichlorobenzene (ppb)	< 5	XXXX
1,4-Dichlorobenzene (ppb)	< 5	XXXX
Dichlorodifluoromethane (ppb)	< 10	XXXX
1,1-Dichloroethane (ppb)	< 5	XXXX
1,2-Dichloroethane (ppb)	< 5	XXXX
1,1-Dichloroethene (ppb)	< 5	XXXX
trans-1,2-Dichloroethene (ppb)	< 5	XXXX
1,2-Dichloropropane (ppb)	< 5	XXXX
cis-1,3-Dichloropropene (ppb)	< 5	XXXX
trans-1,3-Dichloropropene (ppb)	< 5	XXXX
Methylene chloride (ppb)	< 5	XXXX
1,1,2,2-Tetrachloroethane (ppb)	< 5	XXXX
Tetrachloroethene (ppb)	< 5	XXXX
1,1,1-Trichloroethane (ppb)	< 5	XXXX
1,1,2-Trichloroethane (ppb)	< 5	XXXX
Trichloroethene (ppb)	< 5	XXXX
Trichlorofluoromethane (ppb)	< 5	XXXX
Vinyl chloride (ppb)	< 10	XXXX

TABLE 5. RESULTS OF SABATIER WATER

Sample date 6/11/87

MM - Martin Marietta Corp.

B - Boeing Aerospace Comp.

<u>Physical</u>	<u>SABATIER</u> <u>WATER</u>	
	<u>MM</u>	<u>B</u>
Ph	8.3	8.632
Conductivity (umho/cm)	440	563
Total Solids (ppm)	30	5
Color (Pt/Co)	5	0
TOC (ppm)	3.7	216
Ammonia (ppm)	103	111.9

METALS

Al (ppm)	0.11	< .45
Cr (ppm)	< 0.025	.013
Cu (ppm)	< 0.5	.068
Fe (ppm)	< 0.15	.068
Pb (ppm)	< 0.07	.012
Hg (ppm)	< 0.005	< .013
Mn (ppm)	< .025	.022
Ni (ppm)	< 0.025	.044
K (ppm)	< 170	< 7.50
Ag (ppm)	< 0.02	.027
Zn (ppm)	< 2.5	1.075
Ru (ppm)	0.07	< .177
Na (ppm)	1.3	XXX (5)

TABLE 6. RESULTS OF GAS ANALYSES

Sample date 6/10/87  
 MM - Martin Marietta Corp.  
 B - Boeing Aerospace Comp.

Sabatier  
(Vent)  
MM B

Carbon dioxide	1.0%	38.3%	.
Oxygen	1.5%	4.10%	.
Nitrogen	8.0%	18.4%	.
Hydrogen	15.5%	4.00%	.
Methane	74.4%	86.6%	.
Water Vapor	0.0%	XXX	(3) .
Carbon monoxide	<0.5%	XXX	(3) .
Ammonia	<1%	XXX	(3) .

4-BMS  
(CO2 stream)  
MM B

Carbon dioxide	(6)	85.1% / 81.8%	55.4%/68.5% .
Oxygen		1.2% / 1.3%	3.36% .
Nitrogen		7.8% / 7.9%	9.93% .

SFES  
(O2 stream)  
MM B

Oxygen	82.8%	88.10%	.
Nitrogen	3.3%	3.20%	.
Hydrogen	NOT REPORTED	.34%	.

SFES  
(H2 stream)  
MM B

Oxygen	SAMPLE LOST	19.5%	.
Nitrogen	SAMPLE LOST	59.4%	.
Hydrogen	SAMPLE LOST	XXX (3)	.

TABLE 7. MICROBIAL ANALYSIS OF TIMES POST-TREATED DISTILLATE

Sample date 6/11/87

MM - Martin Marietta Corp.

B - Boeing Aerospace Comp.

	TIMES	
	(Post-Treated)	
	Distillate	
	MM	B
Total Bacterial Count (CFU/ML)	12,000	XXXX (3)
Total Anerobes (CFU/ML)	4/ML	XXXX (3)
Yeast and Mold (CFU/ML)	<1 / 5ML	<1
Total Gram Positive (CFU/ML)	(3) XXXX	13
Total Gram Negative (CFU/ML)	(3) XXXX	10,200
Coliforms (MFC) (CFU/ML)	(3) XXXX	<1
Heterotrophs (PCA) (CFU/ML)	(3) XXXX	10,400
Heterotrophs (R2A) (CFU/ML)	(3) XXXX	11,200
Heterotrophs (HPC) (CFU/ML)	(3) XXXX	9300
Total Viruses (CFU/ML)	<1	XXXX (3)

Martin Marietta identified the following bacteria present in the post-treated distillate.

Gram-negative rod- yellow colony, Pseudomonas cepacia  
 Gram-negative rod- white colony, Aeromonas salmonicida  
 Gram-positive coccus - Gaffkya anaerobia  
 Gram-positive rod - Clostridium sorellii

Boeing Aerospace Company identified the following bacteria present in the post-treated distillate.

Achromobacter xylosoxidans  
Bacillus species  
Corynebacterium michiganense  
Pseudomonas cepacia  
Pseudomonas pickettii/cepacia  
 unidentified GNNFs



TABLE 8. MICROBIAL ANALYSIS OF TIMES RAW DISTILLATE

Sample date 6/11/87  
 MM - Martin Marietta Corp.  
 B - Boeing Aerospace Comp.

	<u>TIMES</u>	
	<u>Raw</u>	
	<u>Distillate</u>	
	<u>MM</u>	<u>B</u>
Total Bacterial Count (CFU/ML)	<1 / 5ML	XXXX (3)
Total Anerobes (CFU/ML)	<1 / 5ML	XXXX (3)
Yeast and Mold (CFU/ML)	<1 / 5ML	<1
Total Gram Positive (CFU/ML)	(3) XXXX	2
Total Gram Negative (CFU/ML)	(3) XXXX	6
Coliforms (MFC) (CFU/ML)	(3) XXXX	<1
Heterotrophs (PCA) (CFU/ML)	(3) XXXX	10
Heterotrophs (R2A) (CFU/ML)	(3) XXXX	12
Heterotrophs (HPC) (CFU/ML)	(3) XXXX	XXXX (3)
Total Viruses (CFU/ML)	<1	XXXX (3)

Boeing Aerospace Company identified the following bacteria present in the TIMES Raw Distillate.

Pseudomonas cepacia  
Micrococcus species

## FOOTNOTES

Sample Date 6/11/87

1. Unable to perform analysis - equipment backordered.
2. Value reported is apparent color; actual reading using spectrophotometry is 4000 Pt/Co.
3. Not analyzed
4. Color interferences prevented analysis from being performed.
5. Matrix interferences prevented analysis from being performed.
6. Duplicate samples

### 6.3 Sampling Technique

Grab samples were taken by each laboratory for both water and gas samples. For the TIMES, all samples were taken directly from collection tanks, except for the post-treated distillate, which was sampled at the outlet of the post-treatment ion exchange bed. All Sabatier water samples were taken from the product water tank. Depending upon the type analyte to be detected, all water samples were collected in glass or polyethylene containers. The gas samples were collected by five-layer air/gas sampling bags.

### 6.4 Discussion of Results

Results of analysis for the TIMES post-treated distillate demonstrated significant differences in conductivity, total solids, and total dissolved solids. The results reported for total solids and total dissolved solids are approaching their lower limits of detection (10 ppm and 4 ppm, respectively). To improve accuracy, larger grab samples would have to be collected which for this test was impractical.

Results of physical properties reported by Boeing for the TIMES post-treated distillate were consistently larger than the values reported by Martin Marietta. One possible explanation for this is the rate at which post-treated distillate water was collected for each grab sample. The low flow rate at which water was pumped through the ion exchange bed gave extended collection times. If the water was not constant in composition during the sampling time, each sequential grab sample could differ chemically. The accuracy of the total solids analysis is poor for the post-treated distillate because low amounts of solids are present in this water. To get a more accurate result, large volumes of water would have to be collected which for these analyses would be impractical.

Both Martin Marietta and Boeing laboratories reported larger values of physical properties for the post-treated distillate than the raw distillate. Since the post-treated distillate water should be better quality, the reverse would be expected. The large bacterial count found in the post-treated distillate could account for these anomalies.

The TIMES raw distillate varies significantly for Total Organic Carbon (TOC), ammonia, chloride, and fluoride. The TOC reported by Boeing is extremely high for product water, and the result is suspect for random error. Further tests are planned to validate or disprove the results. The differences in results for ammonia, chloride, and fluoride could not be explained by either contractor. Again, if the water in the collection tank is not a homogeneous mixture, constant in composition over time, each sample will differ chemically. Also matrix interferences could present a problem. Some of the chemical components could be reacting together to change their composition with time. In this case, each contractor should analyze samples on the same date to assure that they have comparable samples.

The TOC reported for Sabatier water varied significantly. The TOC reported by Boeing is extremely high for this type water and is suspect for random error.

The volatile organic compounds listed for the TIMES post-treated distillate were not found in large quantities. These organic compounds make up less than 1 percent of the TOC reported by Martin Marietta. This indicates the presences of other organic compounds in the post-treated distillate not presently being analyzed.

Table 8 lists the physical properties and analytes for the TIMES raw distillate which were reported by both contractors to be below the present defined quality requirements for hygiene water.

## **7.0 CONCLUSIONS**

The primary goals of the SIT were to (1) demonstrate proper remote operation of an ECLS system in an open simulator, (2) verify ECLS system and subsystem facility interfaces, and (3) gather preliminary performance data for an integrated ECLS system. Despite several anomalies, the first two goals were met during the course of the SIT. Proper remote operation was demonstrated as over 40 hr of system operation were accumulated at nominal steady-state conditions. Additionally, system to facility interfaces were verified since few problems were encountered using the facility provided data management system, fluids, bottled gases, and electrical power. Both of the first two goals of the test were important from the standpoint of continuing into more advanced closed door and extended duration testing, but perhaps the most important long term outcome of the test is related to the third goal of gathering preliminary performance data from an ECLS system. The knowledge acquired from this test will not only be applied to test programs in the immediate future but also to the design of the space station ECLS system.

One lesson learned in the SIT was the importance of minimizing external leakage into the ECLS system. This was evident in the case of the Molecular Sieve carbon dioxide removal subsystem. Carbon dioxide mixed with air can cause a two-fold problem in a downstream carbon dioxide reduction subsystem such as the Sabatier. First of all, oxygen in great enough quantities mixed with hydrogen from the oxygen generation subsystem can create a potentially explosive mixture. Secondly, the presence of nitrogen can result in ammonia being formed in the product water of a carbon dioxide reduction system. During the SIT, a steadily degrading situation was observed where the oxygen content of the carbon dioxide output stream rose to 2.5 percent by conclusion of the test. The concentration of nitrogen was found to be 9 percent by post test laboratory analysis and was confirmed by the presence of ammonia in the Sabatier product water, also found by laboratory analysis. The problem was isolated to two leaky five-way valves internal to the subsystem. These valves were not designed to withstand the high temperatures inside the Molecular Sieve resulting in their replacement and extensive design modifications. This points to the need for increased awareness of leakage problems in the design of future ECLS systems and subsystems.

An important change to the test configuration was the result of gas sampling performed during the SIT. During the test, a subsystem shutdown was caused by reduced inlet pressure due to a gas sample being taken. The subsystem was restarted immediately once the sample was taken. Flow restrictors have now been added to all sample port lines and periods of sampling for future tests have been moved procedurally to the end of the test so as not to affect the subsystems or the collection of data. The time required to sample process streams will now be greater but the effect on the system will be minimized.

Several anomalies concerning instrumentation occurred during the SIT which will have a direct impact on future test configurations. Several hours into the test, a flow sensor on the Sabatier carbon dioxide reduction system product gas line began to record values much greater than normal. The problem was due to moisture carry over through the product gas line. A 1-g water trap has been installed upstream of the sensor. A similar trap of the same type had been previously used upstream of the oxygen sensor in the molecular sieve carbon dioxide output stream. There also remains a continuing problem with product water tank scales functioning properly with the facility data acquisition computer. These scales will be critical to mass balance calculations in future tests. A post-test improvement was made by adding dry bulb temperature sensors upstream of dewpoint sensors in the hydrogen and oxygen product lines of the SFE. These additions will allow for the direct calculation of relative humidity in the SFE output lines. Additional instrumentation will be required for future tests to help determine the composition of intersubsystem process streams. In several instances facility flow sensors were recording a volumetric flow rate with the user unable to determine the composition of a flow stream.

Important performance data was gathered during the test relating to the molecular sieve carbon dioxide removal subsystem. The Molecular Sieve subsystem is cyclic by nature with two alternately adsorbing and desorbing carbon dioxide sorbent beds. The cyclic nature of the Molecular Sieve was evident in the bulk cabin air measurements as well as those in the downstream Sabatier carbon dioxide reduction subsystem. Many measurements in the air revitalization loop were observed to vary in step with the adsorption/desorption cycle of the molecular sieve. This cyclic behavior was not detrimental to the system for this short test although special considerations will be required when interfacing the molecular sieve with alternate CO<sub>2</sub> reduction technologies, maintaining thermal stability inside a closed simulator volume, or in future extended duration testing.

The SIT was only the first test in a series of planned tests designed to eventually emulate the actual space station ECLSS flight configuration. This evolution to a flight like state will occur in phased increments over several years at the MSFC Core Module Integration Facility. Initially, subsystems will be upgraded from their current state to more prototype versions and finally to qualification and flight configurations. Finally, system level simulations will be incorporated to include many of the interdisciplinary aspects of the ECLSS design. The SIT is an important milestone in the development of an ECLSS for the space station.

## **APPENDIX**

# TESTLOG

DATE	TIME	PERSON	
6/09/87	7:05 AM	SCHUNK	TIMES heaters turned on. Startup of TIMES delayed for 1.5 hours for heater warmup.
"	7:06	"	SCATS is ready
"	7:17	"	All gasses available
"	7:22	"	TCCS on
"	7:24	"	SCATS off to reset time and date.
"	7:27	"	SCATS on
"	7:30	"	Molecular sieve on
"	7:38	"	Start data printout every 10 minutes.
"	7:38	"	SCATS off to reset date. Molecular sieve off with SCATS.
"	7:44	"	SCATS on
"	7:46	"	Molecular sieve on
"	8:10	"	SFE on. Started purge.
"	8:48	"	SFE current = 8.2 amps
"	8:56	"	SFE current = 14.0 amps
"	8:56	"	N2 flow off approx. 3 min.
"	9:07	"	Molecular sieve CO2 flow to vent SV04.
"	9:09	"	Sabatier N2 purge started
"	9:17	"	Sabatier running with H2/CO2.
"	9:19	"	SFE current = 16 amps

6/09/87	9:20 AM	SCHUNK	TIMES turned on
"	9:24	"	F003 (O2 in CO2 line) holding at .8-.9% O2 (8432 ppm)
"	9:44	"	No SFE data to controller or SCATS.
"	10:20	CARRASQUILLO	Manual shutdown of TIMES to investigate high evaporator pressure.
"	10:26	"	TIMES reactivated.
"	11:00	SCHUNK	Shutdown SFE.
"	11:00	"	Facility H2 to Sabatier
"	2:31 PM	"	Start to bring SFE up again N2 purge started LSI changed out board.
"	3:06	"	CO2 inlet flow to molecular sieve dropped off to .8 #/HR.
"	3:08	"	SFE current = 8.2 amps
"	3:17	"	Opened SV9 vent.
"	3:20	"	Sabatier shutdown to unlock screen.
"	3:20	"	Sabatier back on line
"	3:24	"	SFE current = 13.4 amps
"	3:25	"	SV9 closed
"	3:26	"	Flowing H2/CO2 to sabatier
"	3:42	"	TIMES product water 85 Mmho
"	3:50	"	Switched to SFE H2. SFE current = 19 amps.
"	4:10	DAVIS	Briefed by G. Schunk.
"	10:55	WILKES	Relieved R. Davis.
6/10/87	3:00 AM	"	FF03 sabatier vent flow sensor increased to 2.88

			SLPM. FF03 was constant at 1.0 SLPM until 1:00 AM.
6/10/87	4:05 AM	WILKES	FF03 increased to 4.151 SLPM. Other sabatier sensors appear normal.
"	5:02	"	Console fault indicator light activated on sabatier console. FF03 at 7.338 SLPM
"	6:30	SCHUNK	Sabatier scale FS04 reads .56 lbs. probably an anomaly; should read 1.4 lb
"	6:46	"	Sabatier 1.4 lbs. of H2O production seems low. Should probably be double.
"	7:10	"	N2 line to Sabatier turned off. Sabatier vent flow dropped to 7.5 SLPM.
"	7:15	"	Starting to reboot DCC
"	7:51	"	Manual sabatier vent flow measurement 1-2 SLPM; suspect bad FF03 sensor.
"	8:10	"	N2 pressure seems to have no effect on sabatier vent flow; manually adjusted pressure regulator.
"	9:20	"	TIMES low production warning.
"	9:23	"	Samplers are here.
"	9:34	"	TIMES brine dump.
"	9:55	"	Moisture found in sabatier sample lines.
"	11:00	OGLE	Scientific Services here to take samples of sabatier outlet gas.
"	11:20	"	Sabatier alarm/shutdown; H2O/CH4 delta P is out of range.
"	11:30	"	Sabatier restart successful Problem believed to be



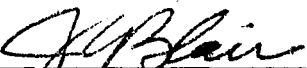
			caused by sampling.
6/10/87	12:28 PM	SCHUNK	N2 bottle low pressure warning.
"	2:35	DAVIS	Briefed by G. Schunk
"	7:15	"	Sabatier CH4 vent line flow rate up; production of H2O appears to be slowing.
"	7:45	"	Notified Ham. Std. rep. of sabatier CH4 vent line flow problem. (now 7.2 SLPM) and was not concerned. Discussed possibility of opening HV13 to relieve condensation buildup. Notified Schunk at home.
"	10:15	"	FF03 at 8.2 SLPM, sabatier H2O production rate OK.
"	11:00	WILKES	Relieved Davis
6/11/87	7:54 AM	SCHUNK	SFE high voltage warning (1.75 V)
"	10:00	"	TIMES in standby (off)
"	10:03	"	Sabatier off; open SV9 and SV3.
"	10:06	"	Open SV3; SFE off.
"	10:07	"	Shutdown TCCS
"	10:08	"	Simulator alarm FG01 (real)
"	10:16	"	Molecular sieve shutdown.

## APPROVAL

### SPACE STATION ECLSS SIMPLIFIED INTEGRATED TEST FINAL REPORT

By Richard G. Schunk, Robert M. Bagdigian, Robyn L. Carrasquillo,  
Kathryn Y. Ogle, and Paul O. Wieland

The information in this report has been reviewed for technical content. Review of any information concerning Department of Defense or nuclear energy activities or programs has been made by the MSFC Security Classification Officer. This report, in its entirety, has been determined to be unclassified.

  
\_\_\_\_\_  
JAMES C. BLAIR

Director, Structures and Dynamics Laboratory